Proteomic and metabolomic insights into the liver and heart in the absence of growth hormone (GH) action - Lessons from a GH receptor deficient pig model

von
Evamaria O. Riedel

Ludwig-Maximilians-Universität München
Fakultät für Medizin

Im Jahr 2022

Aus der Medizinischen Klinik und Poliklinik IV

Klinik der Ludwig-Maximilians-Universität München

Vorstand: Prof. Dr. med. Martin Reincke

Proteomic and metabolomic insights into the liver and heart in the absence of growth hormone (GH) action - Lessons from a GH receptor deficient pig model

Dissertation

zum Erwerb des Doktorgrades der Medizin

an der Medizinischen Fakultät der

Ludwig-Maximilians-Universität zu München

vorgelegt von

Evamaria Olga Riedel

aus

München

im Jahr

2022

Mit Genehmigung der Medizinischen Fakultät

der Universität München

Berichterstatter:	Prof. Dr. Jochen Schopohl
Mitberichterstatter:	PD Dr. Sebastian Pratschke
	Prof. Dr. Susanne Bechtold-Dalla Pozza
	PD Dr. Josefine Römmler-Zehrer
Mitbetreuung durch die promovierten Mitarbeiter:	Prof. Dr. Eckhard Wolf
	Dr. Thomas Fröhlich
	Dr. Martin Bidlingmaier
Dekan:	Prof. Dr. Thomas Gudermann
Tag der mündlichen Prüfung:	30.11.2022

Award of the Carl-Gustav Groth Xeno Prize of the International Xenotransplantation Society (IXA):

For the paper *Growth hormone receptor knockout to reduce the size of donor pigs for preclinical xenotransplantation studies,* which is part of this inaugural dissertation, the Carl-Gustav Groth Xeno Prize 2020 was awarded.

The prize of US $7,000 is jointly sponsored by the International Xenotransplantation Association (IXA) and the publisher of *Xenotransplantation* (Wiley) and is awarded to the first author(s) of the best paper published in the journal Xenotransplantation each calendar year. The Prize is named after the past-Editor-in-Chief, Dr. Carl-Gustav Groth, who initiated the idea of the prize and was also the Founding President of IXA.

The judging of published articles is carried out by a Prize Committee convened specifically for this purpose, composed by the President of IXA, the President-Elect, the Immediate Past-President, the Chief Editor, and 5 members of the IXA council.

The Prize was presented at the Joint IXA-CTRMS Virtual Congress on September 23-25, 2021.

During the preparation of this thesis the following papers have been published:

Riedel E O, Hinrichs A, Kemter E, Dahlhoff M, Backman M, Rathkolb B, Prehn C, Adamski J, Renner S, Blutke A, Hrabě de Angelis M, Bidlingmaier M, Schopohl J, Arnold G J, Fröhlich T°, Wolf E°. Functional changes of the liver in the absence of growth hormone (GH) action – proteomic and metabolomic insights from a GH receptor deficient pig model, Molecular Metabolism, 2020. https://doi.org/10.1016/j.molmet.2020.100978.

Zettler S, Renner S, Kemter E, Hinrichs A, Klymiuk N, Backman M, Riedel E O, Fehlings C, Streckel E, Braun-Reichhart C, Martins A S, Kurome M, Kessler B, Zakhartchenko V, Flenkenthaler F, Arnold G J, Fröhlich T, Blum H, Blutke A, Wanke R, Wolf E. A decade of experience with genetically tailored pig models for diabetes and metabolic research, Animal Reproduction, 2020. http://dx.doi.org/10.1590/1984-3143-ar2020-0064.

Hinrichs A*, Riedel E O*, Klymiuk N, Blutke A, Kemter E, Längin M, Dahlhoff M, Keßler B, Kurome M, Zakhartchenko V, Jemiller E, Ayares D, Bidlingmaier M, Flenkenthaler F, Hrabě de Angelis M, Arnold G J, Reichart B, Fröhlich T°, Wolf E°. Growth hormone receptor knockout to reduce the size of donor pigs for preclinical xenotransplantation studies. Xenotransplantation, 2020. https://doi.org/10.1111/xen.12664.

* Arne Hinrichs and Evamaria O. Riedel equal first author contribution

° Thomas Fröhlich and Eckhard Wolf equal last author contribution

At the following conferences I could present parts of this study:

May 2021	Gene Center Seminar Series PhD/Postdoc Seminar, LMU Munich, Germany
July 2020	2020 International Meeting on GH/IGF: actions in the shadow of COVID19, New York University, USA
May 2019	Gene Center Retreat, Frauenchiemsee, Germany

Affidavit

Eidesstattliche Versicherung

Riedel, Evamaria Olga

_____

Name, Vorname

Ich erkläre hiermit an Eides statt, dass ich die vorliegende Dissertation mit dem Titel:

Proteomic and metabolomic insights into the liver and heart in the absence of growth hormone (GH) action - Lessons from a GH receptor deficient pig model

selbständig verfasst, mich außer der angegebenen keiner weiteren Hilfsmittel bedient und alle Erkenntnisse, die aus dem Schrifttum ganz oder annähernd übernommen sind, als solche kenntlich gemacht und nach ihrer Herkunft unter Bezeichnung der Fundstelle einzeln nachgewiesen habe.

Ich erkläre des Weiteren, dass die hier vorgelegte Dissertation nicht in gleicher oder in ähnlicher Form bei einer anderen Stelle zur Erlangung eines akademischen Grades eingereicht wurde.

München, den 01.12.2022 Evamaria Olga Riedel

_____ _____

Ort, Datum Unterschrift Doktorandin bzw. Doktorand

Table of contents

Table of abbreviations

1GM	Single-modified
4GM	Quadruple-modified
ANOVA	Analysis of variance
B4GALNT2	β1,4-N-acetylgalactosyltransferase
C18	Octadecylsilane
CD	Clusters of differentiation
CMAH	Cytidine monophosphate-N-acetylneuraminic acid hydroxylase
CPT1	Carnitine palmitoyltransferase 1A
CRISPR/Cas	Clustered Regularly Interspaced Short Palindromic Repeats/CRISPR-associated
DAVID	Database for Annotation, Visualization and Integrated Discovery
EPCR	Endothelial protein C receptor
ERK	Extracellular signal-regulated kinase
e.g.	Exempli gratia
FDR	False discovery rate
GGTA1	α1,3-galactosyltransferas
GH	Growth hormone
GHIH	Growth hormone-inhibiting hormone
GHR	Growth hormone receptor
GHRH	Growth hormone-releasing hormone
GO	Gene Ontology
GSEA	Gene set enrichment analysis
hCD46	Human cluster of differentiation 46
HMGCS2	3-hydroxy-3-methylglutaryl-CoA synthase 2
HO1	Heme oxygenase 1
HPA	Hypothalamic-pituitary-adrenal
hTHBD	Human thrombomodulin
IGF	Insulin-like growth factor
IGFBP	IGF binding protein
IXA	International Xenotransplantation Association
JAK2	Janus kinase 2
kDa	Kilodalton
KO	Knockout
LC-MS/MS	Liquid chromatography tandem mass spectrometry

LFQ	Label free quantification
LS	Laron syndrome
LVEF	Left ventricular ejection fraction
min	Minute
miRNA	MicroRNA
MS	Mass spectrometry
MS/MS	Tandem mass spectrometry
m/z	Mass-to-charge ratio
NAFLD	Non-alcoholic fatty liver disease
NEFA	Non-esterified fatty acid
nL	Nanoliter
OMIM	Online Mendelian Inheritance in Man
p	P-value
PCA	Principal component analysis
PEP	Posterior error probability
RNA-Seq	RNA Sequencing
SILAC	Stable isotope labeling by/with amino acids in cell culture
Src	Proto-oncogene tyrosine-protein kinase Src
STAT5	Signal transducer and activator of transcription 5
TCA	Tricarboxylic acid
THBD	Thrombomodulin
TRPV4	Transient receptor potential cation channel subfamily V member 4
µm	Micrometer

List of publications

The following papers are part of this inaugural dissertation:

Riedel E O, Hinrichs A, Kemter E, Dahlhoff M, Backman M, Rathkolb B, Prehn C, Adamski J, Renner S, Blutke A, Hrabě de Angelis M, Bidlingmaier M, Schopohl J, Arnold G J, Fröhlich T°, Wolf E°. Functional changes of the liver in the absence of growth hormone (GH) action – proteomic and metabolomic insights from a GH receptor deficient pig model, Molecular Metabolism, 2020. https://doi.org/10.1016/j.molmet.2020.100978.

° Thomas Fröhlich and Eckhard Wolf equal last author contribution

Hinrichs A*, Riedel E O*, Klymiuk N, Blutke A, Kemter E, Längin M, Dahlhoff M, Keßler B, Kurome M, Zakhartchenko V, Jemiller E, Ayares D, Bidlingmaier M, Flenkenthaler F, Hrabě de Angelis M, Arnold G J, Reichart B, Fröhlich T°, Wolf E°. Growth hormone receptor knockout to reduce the size of donor pigs for preclinical xenotransplantation studies. Xenotransplantation, 2020. https://doi.org/10.1111/xen.12664.

* Arne Hinrichs and Evamaria O. Riedel equal first author contribution

° Thomas Fröhlich and Eckhard Wolf equal last author contribution

1. Contribution to the publications

1.1 Contribution to Paper I

I am first author of the paper *Functional changes of the liver in the absence of growth hormone (GH) action - Proteomic and metabolomic insights from a GH receptor deficient pig model*, which was published in the journal Molecular Metabolism. For the paper, I conceived the experiments and conducted and analyzed the proteomics measurements. I created almost all figures and tables and wrote and revised the manuscript. I am also a guarantor of this work and, as such, had full access to all the data in the study and take responsibility for the integrity of the data and the accuracy of the data analysis.

1.2 Contribution to Paper II

For the paper *Growth hormone receptor knockout to reduce the size of donor pigs for preclinical xenotransplantation studies*, which was published in Xenotransplantation, I conceptualized the proteomics experiments. I also conducted the proteomics experiments, analyzed them statistically and interpreted them. Also, I have written parts of the manuscript, created several figures and have revised the manuscript.

In this case I share the first authorship with Dr. Arne Hinrichs, who developed the animal model, performed sampling and revised the manuscript. The shared first authorship for this paper is reasonable, as both of our contributions – the development of the animal model and collection of heart muscle samples as well as the screening of the samples on a molecular level - are substantial parts of the paper and are mutually dependent for the significance of the paper.

I also share with Dr. Arne Hinrichs the Carl-Gustav Groth Xeno Prize 2020 of the International Xenotransplantation Association (IXA) for this paper, which was awarded to us as the first authors of the best paper published in the journal Xenotransplantation in the calendar year 2020.

2. Introduction

2.1 Laron Syndrome (LS)

Laron syndrome (Growth Hormone Receptor Deficiency, OMIM reference 262500) is a rare autosomal recessive genetic disorder, which is caused by homozygous or compound heterozygous mutation of the growth hormone receptor (GHR) located on the short arm of chromosome 5 (5p13-p12). Only some hundred cases of LS patients are described worldwide (Rosenfeld et al., 1994). Most of these patients occur in Israel and Ecuador. Patients of the Israeli Cohort were the first patients with GHR deficiency described by Zvi Laron (Laron et al., 1968), exhibiting a diverse set of mutations and a diverse phenotype (Shevah and Laron, 2011). The Ecuadorian cohort which was first described by Jaime Guevara-Aguirre (Guevara-Aguirre et al., 1993) exhibits a more homogenous population, in which most patients carry the same splice mutation in the GHR Gene (Rosenbloom and Guevara-Aguirre, 1998).

Laron syndrome patients are defined by a marked short stature, decreased growth velocity and delayed bone age that arises from the failure to generate insulin-like growth factor I (IGF1) in response to normal or increased growth hormone (GH) levels due to dysfunction of the growth hormone receptor (GHR). Patients with Growth Hormone Receptor Deficiency may also exhibit additional features like hypoglycemia in infancy, obesity, a high pitched voice, and characteristic facial features as a small head circumference, protuberance of the forehead, sunken bridge of the nose, blue sclerae, and a downward gaze of the eyes ((Laron and Kauli, 2011), reviewed in (Laron, 2004)). Interestingly, patients with LS seem to be protected from malignancies (Laron et al., 2017; Shevah and Laron, 2007; Steuerman et al., 2011) and patients from the Ecuadorian cohort – despite of severe obesity - also of type 2 diabetes (Guevara-Aguirre et al., 2011). Treatment of LS is possible by long-term application of recombinant IGF1, which increases growth velocity and improves adult height (Backeljauw et al., 2013; Chernausek et al., 2007; Laron, 2011a).

2.1.1 The endocrine growth axis

The endocrine growth axis comprises of GH, which is secreted by the pituitary gland under control of several feedback mechanisms and promotes growth mostly via the stimulation of IGF1 production, but also by other factors. GH action functions via interaction with the growth hormone receptor (GHR), which is required to maintain GH actions.

Growth hormone (GH, Somatotropin) is a peptide hormone of 22 kDa size that is produced by acidophilic cells in the in the pituitary gland (adenohypophysis). GH secretion is regulated by several feedback mechanisms involving circulating factors and the hypothalamus. In the hypothalamus, growth hormone-releasing hormone (GHRH) stimulates GH secretion, whereas the growth hormone-inhibiting hormone (GHIH, Somatostatin) inhibits GH secretion. Additionally, ghrelin, amino acids, physiological cortisol levels, thyroid hormones, estrogens as well as testosterone, noradrenaline, low blood sugar and physical activity are stimuli for GH secretion. Adrenaline, high blood glucose levels, free fatty acids, prolonged elevated levels of cortisol and circulating growth factors (via negative feedback regulation) inhibit GH secretion. Secretion of GH occurs in a pulsatile pattern influenced by the circadian rhythm with a nocturnal maximum of GH secretion (Honda et al., 1969) and is also influenced by age and sex (reviewed in (Jansson et al.,

1985)). The effects of GH on the target organs are either mediated by GH itself or via so-called somatomedins, among them especially IGF1.

While IGF2 mainly stimulates intrauterine growth and is not dependent to GH, IGF1 – where production depends on GH - is an effective growth factor during postnatal development (Baker et al., 1993). IGF binding proteins (IGFBPs) bind IGFs in the circulation, with most of the IGF1 bound to a complex with IGFBP3. There are six different high-affinity IGFBPs: IGFBP3 provides a reservoir of IGF in circulation; IGFBP1, 2 and 4 transport IGFs to peripheral tissues; IGFBP2, 4 and 6 can inhibit IGF-IGF receptor interactions (reviewed in (Cohick and Clemmons, 1993)).

The Growth Hormone Receptor (GHR) finally mediates GH actions indirectly by induction of insulin-like growth factor 1 (IGF1) and directly by tyrosine kinase activation (reviewed in (Brooks and Waters, 2010)). Downstream signaling includes activation of JAK2-STAT5 signaling and the Src/ERK pathway (reviewed in (Brooks et al., 2008)).

Insensitivity or lack of growth hormone can lead to dwarfism. There are diverse causes for this condition, among them hypopituitarism where GH levels are diminished, or GHR-deficiency where GH levels are normal or even elevated. Excess of GH production (e.g. caused by a tumor in the pituitary gland) in childhood age leads to gigantism with excess longitudinal growth (Beckers et al., 2018) and in adult age to a condition called acromegaly, which results in appositional growth of bones, on cartilage and soft tissues especially at the extremities and enlargement of inner organs as well as to an increase of blood glucose levels (Vilar et al., 2017).

2.1.2 Animal models for Laron syndrome

GHR deficiency is crucial to study the endocrine growth axis and in particular GH actions in growth and metabolism, but populations of humans with GHR deficiency with only a few hundred cases over the world are very limited. As also certain investigations in humans, like e.g. biopsies of inner organs are not practicable, well suited animal models are mandatory.

A first animal model for Laron Syndrome was the Laron mouse/*Ghr*-KO mouse (Zhou et al., 1997), which has so far been widely used to study Laron syndrome and GH-related effects (List et al., 2011). Despite the significance of the *Ghr*-KO mouse model, there are - due to the small size, short life expectancy and physiological differences - several limitations of mice regarding the representation of the human phenotype in general. And also with regard to the endocrine growth axis there is a special limitation of mouse models: in contrast to humans, which already have a fully mature hypothalamic-pituitary-adrenal axis (HPA axis) axis at birth, the maturation of the HPA axis of rodents occurs not until the postnatal period (Symonds et al., 2009). The pig as a large animal model can be useful to overcome the gap to the human organism.

Existing pig models are the Wuzhishan minipig with dominant-negative GHR (Li et al., 2015), the GHR deficient miniature pig (Cui et al., 2015) and the GHR modified Diannan miniature pig (Yu et al., 2018). Even though miniature pigs are a highly suggested animal model in research, this background may be questioned for generating a *GHR*-KO model since it has been speculated that the selection of the dwarf phenotype leads to an accumulation of alleles downregulating the GH/IGF pathway (Gärke et al., 2014).

Hinrichs et al. used the background of the German landrace pig in order to maintain a pig population with undisturbed IGF1 function (Hinrichs et al., 2018). *GHR*-Knockout (*GHR*-KO) pigs were generated using CRISPR/Cas9 technology to mutate exon 3 of the *GHR* gene. Heterozygous *GHR*-mutant and wild-type pigs did not significantly differ in any parameter investigated - including

body and organ growth, body composition, endocrine and clinical-chemical parameters, as well as signaling studies in liver tissue. *GHR*-KO pigs resembled the pathophysiology of human LS: With a normal body weight, growth retardation became significant at the age of five weeks; and at an age of 6 months, the body weight of *GHR*-KO pigs was 60% reduced in comparison to the GHR expressing control group. Besides, organ weights were reduced, most of them proportionally to body weight, but the weights of liver, kidneys, and heart were disproportionately more reduced, whereas relative brain weight was almost doubled. *GHR*-KO pigs also had a markedly increased percentage of total body fat and displayed transient juvenile hypoglycemia together with decreased serum cholesterol and triglyceride levels. Serum insulin-like growth factor 1 (IGF1) levels were markedly reduced along with reduced IGF-binding protein 3 (IGFBP3) activity but increased IGFBP2 levels, and serum GH concentrations were significantly higher compared with control pigs.

2.2 The liver in GHR-deficiency

The liver as central hub of metabolism is of pivotal interest when studying GH-actions. GH in the liver has manifold effects as it plays – amongst other functions - an important role in hepatic lipid metabolism by stimulating uptake, storage and secretion of triglycerides (reviewed in (Vijayakumar et al., 2010)) or stimulation of hepatic glucose production (Vijayakumar et al., 2011).

Patients with adult GH deficiency show an increased prevalence of non-alcoholic fatty liver disease, which improves upon GH treatment (reviewed in (Takahashi, 2017)). In a proportion of patients with GHR deficiency (Laron syndrome), steatosis was observed (Laron, 2011b; Laron et al., 2008).

Serum liver enzyme levels in patients with GHR-deficiency are variably normal with no effect of IGF1 treatment on levels of liver enzymes. GHR-deficient patients with NAFLD had slightly elevated levels of liver enzymes (Laron and Karmon, 2011).

Despite the central role of GH in energy homeostasis and metabolism (reviewed in (Ranke and Wit, 2018; Vijayakumar et al., 2011)) and of many studies addressing GH effects on specific metabolic pathways in the liver, a holistic approach towards analyzing GH actions in the liver has so far been missing. Therefore, we performed an integrated proteomics/metabolomics study to identify effects in the liver in GHR-deficiency. This approach should not only lead to a dataset of interest for future meta-analyses with other species like humans or mice and to the identification of a spectrum of biological pathways that are significantly altered in the absence of GH action, but would also provide a basis for answering upcoming questions related to the endocrine growth axis.

2.3 Relevance of GHR-deficiency to xenotransplantation

One question of high social and medical interest is, what would happen to a GHR-deficient organ when xenotransplanted into an organism with normal IGF1 levels. A study of liver-specific *Igf1* knockout mice suggests local IGF1 levels - which would be low in a *GHR*-KO organ – to be of higher significance for organ growth than circulating IGF1 which is mostly derived from the liver (Yakar et al., 1999).

This question is especially relevant in the context of xenotransplantation to overcome shortage of organs for transplantation (Eurotransplant, 2021). Transplantation is often the only cure for patients with end-stage heart and organ failure, but there is an immense discrepancy between organ donations and organs needed (Eurotransplant, 2021; Lund et al., 2017; Rossano et al., 2017).

Pig organs are for diverse reasons proposed to be the most likely donors for xenotransplantation of cells, tissues and organs (reviewed in (Kemter et al., 2020)). Pigs show physiological and anatomical similarities with humans, exhibit the possibility of precise and efficient genetic engineering and can be maintained under pathogen-free conditions.

By consistent long-term survival of orthotopic pig-xenografts in baboons (Längin et al., 2018), xenotransplantation of genetically modified pig hearts attained a landmark in a study in which baboons with orthotopic xenotransplanted hearts from genetically modified pigs could survive up to 195 days. Genetic modifications included α1,3-galactosyltransferase (GGTA1)-deficiency, as αGal carbohydrate antigens on the surface of pig cells can trigger hyperacute graft rejection. Pigs were additionally expressing the human cluster of differentiation 46 (hCD46) and human thrombomodulin (hTHBD), of which the one counteracts graft rejection by inhibiting activation of the complement system and the other prevents blood clotting in the transplanted xeno-heart. As continued xeno-organ growth after transplantation into baboons has been observed (Iwase et al., 2021; Iwase et al., 2017; Iwase et al., 2015; Tanabe et al., 2017), xenograft growth is an important factor limiting recipient survival (Längin et al., 2018); and since pigs grow much faster than non-human primates, we looked for a way to reduce organ size by gene editing of xeno-organ donor pigs. A *GRH*-KO seemed to be a suitable and feasible strategy.

Goerlich et al. could show using echocardiography >6 months after transplantation, that GHR-knockout-xenografts, which were xenotransplanted into baboons, exhibited reduced xenograft growth post transplantation without the use of adjuncts to prevent intrinsic graft growth after transplantation (Goerlich et al., 2021). On January 07, 2022 the first human – David Bennett, 57 - received a genetically-modified (knockouts of *GGTA1*, *CMAH*, *B4GALNT2*, and *GHR*; transgenic for human *CD46*, *CD55*, *THBD*, *EPCR*, *HO1* and *CD47*) pig heart in Baltimore, USA.

2.4 The heart in GHR-deficiency

IGF1 - which is low in GHR-deficiency - plays a pivotal role in postnatal growth (Baker et al., 1993) and also in pre- as well as postnatal maturation and growth of the heart. IGF1 is produced by myocytes in the heart (Montessuit et al., 2006) and expressed in smooth muscle cells of the coronary artery, suggesting a role in myocardial perfusion by controlling vascular tone (Chisalita and Arnqvist, 2005). IGF1 excess seems to be linked to hypertrophy of cardiac myocytes (Laustsen et al., 2007), whereas defects in IGF1 signaling are associated with functional abnormalities of the heart, which could in part be reversed by IGF treatment (Santini et al., 2007).

The ability of the heart to adjust cardiomyocyte growth in order to adapt to hypertension is shown to be utterly dependent on local IGF1 produced by resident cardiac macrophages (Zaman et al., 2021). Resident cardiac macrophages are found to sense cardiomyocyte stress by TRPV4 calcium channels and subsequently upregulating IGF1 expression to promote beneficial cardiac remodeling and affect coronary angiogenesis (De Ponti and Scott, 2021; Wong et al., 2021).

Ghr-KO mice do not present major cardiovascular abnormalities, their overall cardiovascular risk even seems diminished (Cruz-Topete and Kopchick, 2011). Baseline and post-dobutamine stress test echocardiography as well as longitudinal blood pressure measurements of 4-month-old mice

with a cardiac-specific inducible knockout of *Ghr* revealed not to influence heart function (Jara et al., 2016). Patients with GHR-deficiency exhibited reduced cardiac dimensions and out-put but normal left ventricular ejection fraction (LVEF) at rest as well as left ventricular contractile reserve following stress (Feinberg et al., 2000). IGF1-deficiency in GHR-deficient patients even seems – despite the obesity of these patients - to exert a protective mechanism on vascular endothelial function (Scheinowitz et al., 2011).

As xeno-organ growth has been demonstrated to be significant for xenograft and recipient survival (Goerlich et al., 2021; Längin et al., 2018) and as patients with GHR-deficiency have small hearts, which do not seem to have major functional aberrations (Scheinowitz et al., 2011), reduction of heart size for xenotransplantation by *GHR*-knockout seems a worthwhile strategy. However, it was necessary to further quantify effects of *GHR*-KO on cardiac growth parameters and to screen *GHR*-KO hearts for molecular alterations by proteomics of myocardium.

2.5 Quantitative Proteomics to investigate GHR-deficiency in the liver and heart

Proteome profiling of tissue samples from a clinically relevant GHR-deficient large animal model (Hinrichs et al., 2018) and suitable controls has the potential to attain systematic insights into molecular consequences of missing GH action. Proteomics analyses are of particular relevance, as proteins are functionally active products of genes and their abundance can not be gathered from other techniques, like RNA-Seq, due to several layers of regulation between transcription and translation, e.g. by regulatory miRNA. Therefore, measurements at the level of proteins are crucial to understand a biological system.

2.5.1 Mass spectrometry-based quantitative proteomics

MS-based proteomics allows for a comprehensive, unbiased and quantitative analysis of proteins in manifold tissue types and body fluids in large-scale investigations (Cox and Mann, 2011; Mallick and Kuster, 2010). Proteomic strategies can be divided into targeted and discovery (shotgun) approaches. While targeted approaches address the accurate and sensitive quantification of a set of predetermined protein candidates, shotgun approaches allow to identify and quantify as many proteins as possible without prior knowledge about the composition of the analyzed proteome. For protein identification and quantification, mass spectrometry is the method of choice. Electrospray instruments coupled to a nano-liquid chromatography system equipped with a C18 reversed phase column are used frequently. Nano LC-MS/MS is characterized by a very small inner-diameter of the separation column of typically 75 µm, which leads to a flow rate of 20-200 nL/min. In combination with small C18 particle sizes of ≤3 µm, higher analyte concentrations of the separated analytes at the mass spectrometer orifice are facilitated. Resulting sharp narrow analyte peaks at the detector lead to a higher signal to noise ratio for a given amount of analyte and result in sensitivities between the mid attomole and the low femtomole range.

Since the analysis of intact proteins is less efficient and sensitive, protein identification is performed at the level of peptides after proteolytic cleavage of the proteins. During LC-MS/MS, m/z values of all peptide ions eluting from the chromatography system are determined with the mass spectrometer in very short time intervals. The mass spectrometer consecutively selects peptide ions for fragmentation by collision with gas molecules. Masses of the resulting fragments are

determined by the instrument. This process is continued through the entire chromatographic separation of the protein lysate and yields up to 10^4 MS spectra and up to 10^5 MS/MS spectra. In order to identify the underlying peptides, the acquired mass spectra are compared to theoretical spectra, calculated from sequence databases of all known proteins of an organism using bioinformatic algorithms like e.g. MASCOT (Perkins et al., 1999). Peptides are then assigned to their corresponding proteins and scored according to the probability that the observed match is correct.

For MS-based protein quantification, there are two main strategies, either using spectral counting or precursor ion intensity measurements in a label-free approach or based on the incorporation of stable isotope labels (reviewed in (Ong and Mann, 2005; Walther and Mann, 2010)). Since metabolic labeling, like stable isotope labeling by/with amino acids in cell culture (SILAC) (Cox et al., 2014), is not applicable for large animal models like the pig, we chose a label-free quantification (LFQ) LC-MS/MS proteomics approach. Label-free quantitation methods are due to simpler and more economical handling and their excellent scalability an attractive alternative to strategies based on stable isotope labeling.

2.5.2 Proteome data interpretation and pathway analysis

The size of the resulting dataset, which consists of thousands of proteins and their quantitative values, makes it necessary to use powerful bioinformatics tools to interpret the data.

To visualize and estimate differences between proteome profiles, quantitative data are frequently subjected to unsupervised hierarchical clustering and principal component analysis, which can be performed in statistical software packages for instance in R (Team, 2022), or the Perseus (Tyanova et al., 2016) module of MaxQuant. Hierarchical clustering analysis is a method of cluster analysis which seeks to build a hierarchy of the samples by the similarity of all proteins in a sample and can assign the specimens to clusters. Principal component analysis (PCA) is a technique for reducing the dimensionality of large and complex datasets like a proteomics dataset. It replaces the original variables by a smaller number of derived variables - the principal components, which are linear combinations of the original variables, retaining most of their variability (reviewed in (Jolliffe and Cadima, 2016) (Ringnér, 2008)).

After statistical evaluation of the quantitative data, several bioinformatic tools can be used to assign the differently abundant proteins to molecular functions, related biochemical pathways and biological processes. Commonly used tools for functional annotation clustering are the DAVID online platform (Huang da et al., 2009) and the ClueGO (Bindea et al., 2009) and CluePedia (Bindea et al., 2013) plugins in Cytoscape (Shannon et al., 2003). A further method for interpreting transcriptomics and proteomics datasets is the Gene Set Enrichment Analysis (GSEA), focusing on groups of genes/proteins that share common biological function, chromosomal location, or regulation – so-called gene sets (Subramanian et al., 2005).

A combination of different tools and algorithms can be even advantageous for a comprehensive analysis of large-scale experiments.

3. Abstract

Growth hormone (GH) plays a crucial role for an organism by regulating postnatal growth and affecting manifold biochemical pathways. The liver is a central target organ of GH, where its action accounts for the majority of insulin-like growth factor 1 (IGF1) in the circulation, stimulates - inter alia - hepatic glucose production and plays an important role in hepatic lipid metabolism. Despite of the significant role of GH in the liver, no holistic multi-omics analysis of hepatic GH actions had been performed so far. We analyzed liver samples of 6-month-old GHR-deficient (*GHR*-KO) pigs in a shotgun proteomics and targeted metabolomics approach, not only taking the effect of the *GHR*-KO, but also the sex-specific differences in metabolism and energy homeostasis and the interaction of both factors into account (Riedel et al., 2020).

Body and liver weights, and also the relative liver weight of *GHR*-KO pigs were significantly reduced compared to controls. 32,169 peptides (PEP-value < 0.05) could be identified from liver tissue, which could be assigned to 3,231 protein groups at an FDR < 0.01. The *GHR*-KO liver proteome differed significantly from the control. Statistical analysis of the proteome data using a two-way ANOVA (group x sex) identified 87 protein groups significantly ($p < 0.05$) altered in abundance by group, of which 53 protein groups were more and 34 protein groups were less abundant in the *GHR*-KO liver proteome. The sex of the animals significantly altered the abundance of 16 proteins, with 13 proteins more abundant in male animals and three proteins more abundant in female animals. Eight proteins were significantly influenced by the interaction group x sex. In order to complement the proteome findings on the metabolite level and for a comprehensive physiological interpretation, we incorporated data from targeted metabolomics out of liver and serum and from clinical-chemical analyses in serum. With this integrated proteomics/targeted metabolomics approach we identified a spectrum of biological pathways which were significantly altered in the absence of GH action (Riedel et al., 2020).

Most prominent were significantly increased levels of multiple proteins involved in amino acid metabolism, especially degradation of amino acids. We detected significantly increased concentrations of enzymes involved in transamination and the urea cycle in *GHR*-KO samples. As an estimate for the activity of these enzymes, we compared the concentrations of the resulting metabolites, which could underline the increased activity of the urea cycle. Several enzymes of the TCA cycle, which metabolizes the remaining carbon part from transamination of amino acids, were increased in abundance in the *GHR*-KO liver proteome. The key enzyme of ketogenesis - 3-hydroxy-3-methylglutaryl-CoA synthase 2 (HMGCS2) - was 48.5 times more abundant in *GHR*-KO than in control liver. Interestingly, in spite of the marked up-regulation of the key ketogenic enzyme, there was no evidence for stimulated ketogenesis. In the context of a reduced CPT1-ratio as metabolic indicator of the carnitine shuttle and reduced serum levels of non-esterified fatty acids (NEFAs) as well as reduced mitochondrial import of long-chain fatty acids, increased short-chain acylcarnitine levels may result from an impairment of beta-oxidation of short-chain fatty acids. The concentration of mono-unsaturated fatty acids was significantly increased in the liver of *GHR*-KO pigs without morphological signs of steatosis, although the abundances of several proteins functionally linked to non-alcoholic fatty liver disease were increased (Riedel et al., 2020).

In summary, this study gave new insights to manifold central pathways that were altered by missing GH action on a molecular level and into the role of GH in the specification of sex-related

liver functions. Furthermore, the dataset provides a resource for future meta-analyses for translational research and will help to investigate arising questions, one of them what would happen to a GHR-deficient organ if it is xenotransplanted into a host with normal IGF1 levels.

Xenotransplantation of genetically modified pig hearts attained a breakthrough by consistent long-term survival of orthotopic pig-xenografts in baboons, demonstrating that post-transplantation growth control of the xenotransplant is essential (Längin et al., 2018). As pigs grow much faster than non-human primates, we looked for a way to reduce the size by gene editing of xeno-organ donor pigs in one step. The generation of GHR-deficient (*GHR*-KO) pigs, which exhibit low plasma insulin-like growth factor 1 (IGF1) levels and significantly reduced postnatal body and organ growth, but normal fertility, seemed to be a worthwhile strategy. In order to screen the hearts from our *GHR*-KO deficient pigs, we quantified effects of *GHR*-KO on cardiac growth parameters and performed screening for molecular alterations by holistic label-free proteomics of myocardium (Hinrichs et al., 2021).

GHR-KO pigs at the age of 6 months showed to have a 61% reduced body and a 63% reduced heart weight without reduction of the relative heart weight when compared to control animals. Morphometric studies of cardiomyocytes showed a 28% reduction of the mean minimal diameter of cardiomyocytes in *GHR*-KO versus control animals. Proteomics of myocardium samples could identify 1,642 protein groups at a false discovery rate (FDR) < 0.01. Comparison of the quantitative proteome profiles of myocardium samples from *GHR*-KO and control pigs indicated no major aberration in the myocardium proteome as a consequence of GHR deficiency. Statistical analysis of the proteome data using a two-way ANOVA (group × sex) identified no significantly ($p < 0.05$) altered protein groups influenced by the factors group, sex or by the interaction of the factors group and sex. A less strict statistical volcano plot analysis that analyzed data without taking the sex into consideration, identified one protein with reduced abundance and 5 proteins with increased abundance in the *GHR*-KO myocardium proteome, but none of these proteins is specifically expressed in myocardium, directly involved in heart contraction, nor known to be directly regulated by or involved in GH/IGF1 pathways in the heart (Hinrichs et al., 2021).

These results suggest the knockout of the GHR as a practicable strategy to reduce the size of pigs as organ donors for preclinical xenotransplantation studies. Subsequently, 4 GM pigs with *GGTA1*-KO*,* expressing *hCD46/hTHBD* and a knockout for the *GHR* gene could be generated and exhibited the characteristic phenotype of GHR deficiency and reduced serum IGF1 levels comparable to *GHR*-KO 1GM pigs (Hinrichs et al., 2021).

4. Zusammenfassung (Deutsch)

Das Wachstumshormon (Growth Hormone, GH) ist ein Hormon mit großer Bedeutung für einen Organismus, da es wichtige Mechanismen wie postnatales Wachstum und verschiedene biochemische Stoffwechselwege reguliert. Die Leber ist zentrales Zielorgan von GH, wo es unter anderem die Synthese und Sekretion von Insulin-like growth factor 1 (IGF1) stimuliert und somit für den Großteil des IGF1 im Blutkreislauf verantwortlich ist, die Produktion von Glukose stimuliert, und eine wichtige Rolle im hepatischen Fettstoffwechsel spielt. Trotz der bedeutenden Rolle, die das Wachstumshormon in der Leber spielt, gab es bisher noch keine holistische Multi-Omics-Studie von GH-Wirkungen in der Leber. Deswegen haben wir Leberproben von 6 Monate alten Wachstumshormonrezeptor-defizienten (*GHR*-KO) Schweinen mittels holistischer Proteom- und gezielter Metabolom-Analysen untersucht. Hierbei haben wir uns nicht nur auf die Effekte des *GHR*-Knockouts beschränkt, sondern auch die geschlechtsspezifischen Unterschiede von Metabolismus und Energiehomöostase sowie die Interaktion beider Faktoren untersucht (Riedel et al., 2020).

Das Körpergewicht sowie das Lebergewicht, inklusive des relativen Lebergewichts der GHR-defizienten Schweine war im Vergleich zu Kontrolltieren signifikant reduziert. Wir konnten 32.169 Peptide (PEP-Value < 0.05) aus Lebergewebe identifizieren, die wir 3.231 Proteingruppen zuordnen konnten (False Discovery rate (FDR) < 0.01). Im *GHR*-KO Leber-Proteom zeigten sich signifikante Unterschiede zum Kontroll-Proteom. Statistische Analysen der Proteomdaten mittels einer two-way ANOVA (group x sex) konnte 87 Proteine detektieren, die sich durch den *GHR*-Knockout in ihrer Abundanz signifikant ($p < 0.05$) verändert zeigten. Davon waren im *GHR*-KO Leber-Proteom 53 Proteine höher und 34 Proteine weniger abundant. 16 Proteine waren signifikant durch das Geschlecht der Tiere beeinflusst, wobei 13 Proteine in männlichen Tieren, und 3 Proteine in weiblichen Tieren höher abundant waren. 8 Proteine zeigten sich durch die Interaktion der Faktoren Genotyp und Geschlecht beeinflusst. Um die Ergebnisse der Proteom-Analysen für eine umfassende physiologische Interpretation auch auf der Ebene der Metaboliten nachzuweisen, konnten wir gezielte Metabolomics-Analysen aus Lebergewebe und Serum sowie klinisch-chemische Analysen aus Serumproben ergänzen. So konnten wir mit diesem integrierten Proteomics/Metabolomics-Ansatz ein Spektrum an biologischen Stoffwechselwegen identifizieren, die sich bei Ausbleiben von GH-Wirkungen signifikant verändert zeigten (Riedel et al., 2020).

Am auffälligsten waren signifikant erhöhte Level multipler Proteine, die im Metabolismus von Aminosäuren - besonders beim Aminosäure-Abbau - eine Rolle spielen. Hier konnten wir beispielsweise im *GHR*-KO Proteom signifikant erhöhte Konzentrationen von Enzymen der Transaminierung und des Harnstoffzyklus feststellen. Um die Aktivität dieser Enzyme einordnen zu können, haben wir die Konzentrationen der aus den Reaktionen resultierenden Metaboliten verglichen, die eine erhöhte Aktivität des Harnstoffzyklus unterstreichen konnten. Mehrere Enzyme des Zitratzyklus, der den aus der Transaminierung der Aminosäuren resultierende Kohlenstoff-Anteil abbaut, waren in ihrer Abundanz im *GHR*-KO Leber-Proteom erhöht. 3-Hydroxy-3-Methylglutaryl-CoA Synthase 2 (HMGCS2), das Schlüsselenzym der Ketogenese, war im *GHR*-KO-Leberproteom 48,5-mal mehr abundant als in der Kontrolle. Interessanterweise zeigte sich trotz dieser deutlichen Abundanz-Erhöhung des Schlüsselenzyms der Ketogenese keine Evidenz für eine stimulierte Ketogenese. Im Kontext einer verminderten CPT1-Ratio als metabolischem Indikator des Carnitin-Shuttles und verminderten Serum-Spiegeln unveresterter Fettsäuren (NEFAs), sowie einem reduzierten Import langkettiger Fettsäuren, könnten die erhöhten Spiegel kurzkettiger Acylcarnitine aus einer Verminderung der beta-Oxidation langkettiger Fettsäuren resultieren. Die Konzentration einfach ungesättigter Fettsäuren war in der Leber von *GHR*-KO Schweinen ohne

morphologische Zeichen einer Steatose signifikant erhöht, obwohl sich signifikant erhöhte Abundanzen von Proteinen zeigten, die funktionell mit der nicht-alkoholischen Fettlebererkrankung in Zusammenhang stehen (Riedel et al., 2020).

Zusammengefasst konnte unsere Studie zentrale Stoffwechselwege detektieren, die sich bei fehlenden GH-Wirkungen verändert zeigten und Einblicke in die molekulare Ebene dieser Stoffwechselwege gewähren. Außerdem konnte sie neue Einblicke in die Rolle von GH auf die Spezifizierung geschlechtsabhängiger Leberfunktionen geben und stellt einen Datensatz dar, der als Ressource zukünftiger Metaanalysen mit murinen und humanen Datensätzen dienen wird, um interessante aufkommende Fragen zu beantworten. Eine dieser Fragen ist, was mit einem GHR-defizienten Organ passiert, wenn es in einen Empfänger mit normalen IGF1-Spiegeln xenotransplantiert wird.

In der Xenotransplantation genetisch modifizierter Schweineherzen konnte durch Langzeit-Überleben orthotoper Schweine-Xenografts in Pavianen ein Meilenstein erreicht werden (Längin et al., 2018). Da sich gezeigt hat, dass die Wachstumskontrolle des Xenotransplantats nach der Transplantation wesentlich für das Transplantatüberleben ist und Schweine viel schneller als nichthumane Primaten wachsen, haben wir nach einer Möglichkeit gesucht, die Organgrößen durch Gene Editing von Xeno-Organ-Spendertieren in einem Schritt zu reduzieren. Die Erzeugung GHR-defizienter (*GHR*-KO) Schweine, die niedrige Spiegel von Insulin-like growth factor 1 (IGF1) im Serum aufweisen und postnatal ein signifikant reduziertes Körper- und Organwachstum bei normaler Fertilität zeigen, schien eine umsetzbare Strategie zu sein. Um die Herzen der GHR-defizienten Schweine zu untersuchen, haben wir die Effekte des *GHR* Knockouts auf kardiale Wachstumsparameter quantifiziert und ein Screening auf molekulare Veränderungen mittels einer holistischen labelfreien Proteomanalyse von Myokardgewebe durchgeführt (Hinrichs et al., 2021).

GRH-KO Schweine im Alter von 6 Monaten wiesen im Vergleich zu Kontrolltieren ein um 61% geringeres Körpergewicht und ein um 63% geringeres Herzgewicht – ohne eine Reduktion des relativen Herzgewichts – auf. Morphometrische Analysen von Kardiomyozyten zeigten, dass der mittlere kleinste Durchmesser der Kardiomyozyten in *GHR*-KO im Vergleich zu Kontrolltieren um 28% reduziert war. Proteomics von Myokardgewebe konnte 1.642 Proteingruppen bei einer Falscherkennungsrate (FDR) < 0.01 identifizieren. Ein Vergleich der quantitativen Proteomprofile von Myokardproben von *GHR*-KO und Kontrolltieren zeigten keine großen Abweichungen im Myokard-Proteom als Folge der GHR-Defizienz. Statistische Analysen der Proteomdaten mittels Zweiweg-Varianzanalyse (group × sex) konnte keine signifikant veränderten ($P < 0.05$) Proteingruppen identifizieren, die durch den GHR-Knockout, das Geschlecht der Tiere oder die Interaktion beider Faktoren beeinflusst waren. Eine weniger stringente statistische Volcano Plot Analyse, die die Daten ohne das Geschlecht zu berücksichtigen analysiert, hat ein Protein mit verminderter Abundanz und 5 Proteine mit erhöhter Abundanz im *GHR*-KO Herz-Proteom identifiziert, wobei keines dieser Proteine spezifisch im Myokard exprimiert wird, direkt in der Herzkontraktion involviert ist oder in GH/IGF1-Pathways im Herzen direkt reguliert oder involviert ist (Hinrichs et al., 2021).

Diese Ergebnisse legen den Knockout des GHR als realisierbare Strategie nahe, um die Größe von Schweinen als Organspender für präklinische Xenotransplantations-Studien zu reduzieren. In der Folge konnten 4 GM Schweine mit einem *GGTA1*-KO, Expression von *hCD46/hTHBD* und einem Knockout für das *GHR* Gen erzeugt werden und wiesen den charakteristischen Phenotyp der GHR Defizienz sowie reduzierte IGF1 Spiegel vergleichbar mit denen von 1GM *GHR*-KO-Schweinen auf (Hinrichs et al., 2021).

5. Paper I

Mol Metab. 2020 Jun;36:100978. doi: 10.1016/j.molmet.2020.100978. Epub 2020 Mar 18.

Functional changes of the liver in the absence of growth hormone (GH) action - Proteomic and metabolomic insights from a GH receptor deficient pig model

Evamaria O Riedel [1], Arne Hinrichs [2], Elisabeth Kemter [3], Maik Dahlhoff [2], Mattias Backman [4], Birgit Rathkolb [5], Cornelia Prehn [6], Jerzy Adamski [7], Simone Renner [3], Andreas Blutke [8], Martin Hrabě de Angelis [9], Martin Bidlingmaier [10], Jochen Schopohl [10], Georg J Arnold [4], Thomas Fröhlich [4, °], Eckhard Wolf [11, °]

Affiliations

[1] Laboratory for Functional Genome Analysis, (LAFUGA), Gene Center, LMU Munich, 81377 Munich, Germany; Medizinische Klinik und Poliklinik IV, Klinikum der LMU München, 80336 Munich, Germany. [2] Institute of Molecular Animal Breeding and Biotechnology, Gene Center and Department of Veterinary Sciences, LMU Munich, 81377 Munich, Germany. [3] Institute of Molecular Animal Breeding and Biotechnology, Gene Center and Department of Veterinary Sciences, LMU Munich, 81377 Munich, Germany; German Center for Diabetes Research (DZD), 85764 Neuherberg, Germany. [4] Laboratory for Functional Genome Analysis, (LAFUGA), Gene Center, LMU Munich, 81377 Munich, Germany. [5] Institute of Molecular Animal Breeding and Biotechnology, Gene Center and Department of Veterinary Sciences, LMU Munich, 81377 Munich, Germany; German Mouse Clinic (GMC), Institute of Experimental Genetics, Helmholtz Zentrum München, 85764 Neuherberg, Germany. [6] Research Unit Molecular Endocrinology and Metabolism (MEM), Helmholtz Zentrum München, 85764 Neuherberg, Germany. [7] Research Unit Molecular Endocrinology and Metabolism (MEM), Helmholtz Zentrum München, 85764 Neuherberg, Germany; Chair of Experimental Genetics, School of Life Science Weihenstephan, Technische Universität München, 85354 Freising, Germany; Department of Biochemistry, Yong Loo Lin School of Medicine, National University of Singapore, Singapore. [8] Research Unit Analytical Pathology, Helmholtz Zentrum München, 85764 Neuherberg, Germany. [9] German Center for Diabetes Research (DZD), 85764 Neuherberg, Germany; German Mouse Clinic (GMC), Institute of Experimental Genetics, Helmholtz Zentrum München, 85764 Neuherberg, Germany; Chair of Experimental Genetics, School of Life Science Weihenstephan, Technische Universität München, 85354 Freising, Germany. [10] Medizinische Klinik und Poliklinik IV, Klinikum der LMU München, 80336 Munich, Germany. [11] Laboratory for Functional Genome Analysis, (LAFUGA), Gene Center, LMU Munich, 81377 Munich, Germany; Institute of Molecular Animal Breeding and Biotechnology, Gene Center and Department of Veterinary Sciences, LMU Munich, 81377 Munich, Germany; German Center for Diabetes Research (DZD), 85764 Neuherberg, Germany. Electronic address: ewolf@genzentrum.lmu.de.

° Thomas Fröhlich and Eckhard Wolf equal last author contribution

PMID: 32277923 PMCID: PMC7184181 DOI: 10.1016/j.molmet.2020.100978

Free PMC article

Abstract

Objective: The liver is a central target organ of growth hormone (GH), which stimulates the synthesis of insulin-like growth factor 1 (IGF1) and affects multiple biochemical pathways. A systematic multi-omics analysis of GH effects in the liver has not been performed. GH receptor (GHR) deficiency is a unique model for studying the consequences of lacking GH action. In this study, we used molecular profiling techniques to capture a broad spectrum of these effects in the liver of a clinically relevant large animal model for Laron syndrome.

Methods: We performed holistic proteome and targeted metabolome analyses of liver samples from 6-month-old GHR-deficient (*GHR*-KO) pigs and GHR-expressing controls (four males, four females per group).

Results: GHR deficiency resulted in an increased abundance of enzymes involved in amino acid degradation, in the urea cycle, and in the tricarboxylic acid cycle. A decreased ratio of long-chain acylcarnitines to free carnitine suggested reduced activity of carnitine palmitoyltransferase 1A and thus reduced mitochondrial import of fatty acids for beta-oxidation. Increased levels of short-chain acylcarnitines in the liver and in the circulation of *GHR*-KO pigs may result from impaired beta-oxidation of short-chain fatty acids or from increased degradation of specific amino acids. The concentration of mono-unsaturated glycerophosphocholines was significantly increased in the liver of *GHR*-KO pigs without morphological signs of steatosis, although the abundances of several proteins functionally linked to non-alcoholic fatty liver disease (fetuin B, retinol binding protein 4, several mitochondrial proteins) were increased. Moreover, GHR-deficient liver samples revealed distinct changes in the methionine and glutathione metabolic pathways, in particular, a significantly increased level of glycine N-methyltransferase and increased levels of total and free glutathione. Several proteins revealed a sex-related abundance difference in the control group but not in the *GHR*-KO group.

Conclusions: Our integrated proteomics/targeted metabolomics study of GHR-deficient and control liver samples from a clinically relevant large animal model identified a spectrum of biological pathways that are significantly altered in the absence of GH action. Moreover, new insights into the role of GH in the sex-related specification of liver functions were provided.

Keywords: Growth hormone; Laron syndrome; Liver; Metabolomics; Pig model; Proteomics.

Original Article

MOLECULAR METABOLISM

Functional changes of the liver in the absence of growth hormone (GH) action – Proteomic and metabolomic insights from a GH receptor deficient pig model

Evamaria O. Riedel [1,2], Arne Hinrichs [3], Elisabeth Kemter [3,4], Maik Dahlhoff [3], Mattias Backman [1], Birgit Rathkolb [3,5], Cornelia Prehn [6], Jerzy Adamski [6,7,8], Simone Renner [3,4], Andreas Blutke [9], Martin Hrabě de Angelis [4,5,7], Martin Bidlingmaier [2], Jochen Schopohl [2], Georg J. Arnold [1], Thomas Fröhlich [1,10], Eckhard Wolf [1,3,4,*,10]

ABSTRACT

Objective: The liver is a central target organ of growth hormone (GH), which stimulates the synthesis of insulin-like growth factor 1 (IGF1) and affects multiple biochemical pathways. A systematic multi-omics analysis of GH effects in the liver has not been performed. GH receptor (GHR) deficiency is a unique model for studying the consequences of lacking GH action. In this study, we used molecular profiling techniques to capture a broad spectrum of these effects in the liver of a clinically relevant large animal model for Laron syndrome.
Methods: We performed holistic proteome and targeted metabolome analyses of liver samples from 6-month-old GHR-deficient (*GHR*-KO) pigs and GHR-expressing controls (four males, four females per group).
Results: GHR deficiency resulted in an increased abundance of enzymes involved in amino acid degradation, in the urea cycle, and in the tricarboxylic acid cycle. A decreased ratio of long-chain acylcarnitines to free carnitine suggested reduced activity of carnitine palmitoyltransferase 1A and thus reduced mitochondrial import of fatty acids for beta-oxidation. Increased levels of short-chain acylcarnitines in the liver and in the circulation of *GHR*-KO pigs may result from impaired beta-oxidation of short-chain fatty acids or from increased degradation of specific amino acids. The concentration of mono-unsaturated glycerophosphocholines was significantly increased in the liver of *GHR*-KO pigs without morphological signs of steatosis, although the abundances of several proteins functionally linked to non-alcoholic fatty liver disease (fetuin B, retinol binding protein 4, several mitochondrial proteins) were increased. Moreover, GHR-deficient liver samples revealed distinct changes in the methionine and glutathione metabolic pathways, in particular, a significantly increased level of glycine N-methyltransferase and increased levels of total and free glutathione. Several proteins revealed a sex-related abundance difference in the control group but not in the *GHR*-KO group.
Conclusions: Our integrated proteomics/targeted metabolomics study of GHR-deficient and control liver samples from a clinically relevant large animal model identified a spectrum of biological pathways that are significantly altered in the absence of GH action. Moreover, new insights into the role of GH in the sex-related specification of liver functions were provided.

Keywords Liver; Growth hormone; Laron syndrome; Pig model; Proteomics; Metabolomics

1. INTRODUCTION

Growth hormone (GH) is an important regulator of postnatal growth and has profound effects on metabolism and energy homeostasis (reviewed in [1,2]). In the liver, GH stimulates the synthesis and secretion of insulin-like growth factor 1 (IGF1), accounting for the majority of IGF1 in the circulation [3]. In addition, GH stimulates hepatic glucose production, but the relative contributions of gluconeogenesis

[1]Laboratory for Functional Genome Analysis, (LAFUGA), Gene Center, LMU Munich, 81377 Munich, Germany [2]Medizinische Klinik und Poliklinik IV, Klinikum der LMU München, 80336 Munich, Germany [3]Institute of Molecular Animal Breeding and Biotechnology, Gene Center and Department of Veterinary Sciences, LMU Munich, 81377 Munich, Germany [4]German Center for Diabetes Research (DZD), 85764 Neuherberg, Germany [5]German Mouse Clinic (GMC), Institute of Experimental Genetics, Helmholtz Zentrum München, 85764 Neuherberg, Germany [6]Research Unit Molecular Endocrinology and Metabolism (MEM), Helmholtz Zentrum München, 85764 Neuherberg, Germany [7]Chair of Experimental Genetics, School of Life Science Weihenstephan, Technische Universität München, 85354 Freising, Germany [8]Department of Biochemistry, Yong Loo Lin School of Medicine, National University of Singapore, Singapore [9]Research Unit Analytical Pathology, Helmholtz Zentrum München, 85764 Neuherberg, Germany

[10] Contributed equally.

*Corresponding author. Gene Center, LMU Munich, Feodor-Lynen-Str. 25, 81377 Munich, Germany. E-mail: ewolf@genzentrum.lmu.de (E. Wolf).

Received February 22, 2020 • Revision received March 7, 2020 • Accepted March 10, 2020 • Available online 18 March 2020

https://doi.org/10.1016/j.molmet.2020.100978

and glycogenolysis are still a matter of discussion (reviewed in [1]). GH also plays a major role in hepatic lipid metabolism, including stimulation of uptake and storage, but also secretion of triglycerides (reviewed in [4]). Patients with adult GH deficiency show an increased prevalence of non-alcoholic fatty liver disease (NAFLD), which improves upon GH treatment (reviewed in [5]). Steatosis was also observed in a proportion of patients with growth hormone receptor (GHR) deficiency (Laron syndrome; OMIM reference 262500) [6] and in mice with a liver-specific deletion of the GHR [7]. To clarify whether this was due to deficient GH action or low IGF1 levels, Liu and coworkers [8] restored IGF1 in liver-specific GHR-deficient mice by a liver-specific *Igf1* transgene. The increase in IGF1 did not prevent steatosis, suggesting that this was a direct consequence of the lack of GH action. Interestingly, global GHR deficiency in mice was not associated with steatosis [9].

In spite of numerous studies addressing GH effects on specific metabolic pathways in the liver, a holistic multi-omics analysis of hepatic GH actions has not been performed. We therefore analyzed liver samples of 6-month-old GHR-deficient (*GHR*-KO) pigs [10] and of littermate controls with intact *GHR* alleles ($GHR^{+/-}$ or $GHR^{+/+}$) by shotgun proteomics and targeted metabolomics. Samples from male and female pigs were analyzed to take sex-specific differences in metabolism and energy homeostasis (reviewed in [11]) into account.

2. MATERIALS AND METHODS

2.1. Animal model, collection of blood and liver samples

GHR-KO pigs were generated and maintained as described previously [10]. *GHR*-KO pigs ($GHR^{-/-}$; four males, four females) and control animals ($GHR^{+/-}$, $GHR^{+/+}$; two males, two females of each genotype) were euthanized at an age of 6 months after overnight fasting. Since several studies demonstrated circadian oscillations of the liver proteome profile [12–14], necropsies and tissue sampling were always performed at the same time of the day (between 9.00 and 11.00 a.m.). Blood was collected from the jugular vein. After clotting for 30 min at room temperature, serum was separated by centrifugation (1,200 ×g) for 20 min at 6 °C and stored at −80 °C until analysis. Liver samples (100 mg) were taken according to a standardized protocol [15,16], shock frozen on dry ice, and stored at −80 °C until further analysis. The experimental design is summarized in Figure 1A.

2.2. Determination of body weight, liver weight and relative body weight

Body and liver weights were determined the same day when pigs were euthanized (at the age of 6 months). Relative liver weight was calculated by dividing liver weight by body weight.

2.3. Clinical chemistry

Clinical-chemical parameters in serum were determined using an AU480 autoanalyzer (Beckman–Coulter). For determination of non-esterified fatty acids (NEFA), the NEFA HR kit (Wako Chemicals) was used, and glycerol levels were measured using the test kit GY105 (Randox). Beta hydroxybutyrate was measured by Alomed (Radolfzell-Böhringen, Germany) using a validated and accredited photometric method. For determination of all other parameters, we used adapted reagents from Beckman–Coulter. Kits and methods have been described in detail by Rathkolb et al. [17].

2.4. Proteomics

Sample preparation: For sample processing, 15 µl of 8 M urea/0.4 M NH_4HCO_3 per mg frozen tissue was added. Tissues were lysed using a homogenizer (ART-MicraD8, ART Prozess- & Labortechnik) twice at a speed of 23,500 rpm for 30 s and centrifuged through QIA-Shredder devices (Qiagen). Protein concentrations were determined by a 660 nm protein assay (Thermo Scientific Pierce) [18] and adjusted with 8 M urea/0.4 M NH_4HCO_3 to a concentration of 2 mg/ml. One hundred µg protein was reduced with DTE/TCEP at a concentration of 4.5 mM DTE/2 mM TCEP for 30 min. Cysteine

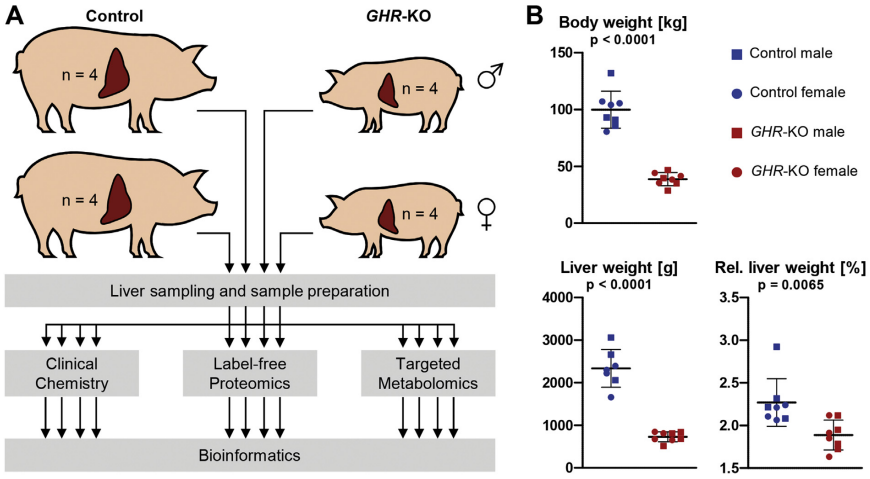

Figure 1: Study outline, body and liver weights. *A:* Serum and liver samples from male and female six-month-old *GHR*-KO and control pigs were analyzed for clinical-chemical parameters, proteins and metabolites affected by group, sex and the interaction group × sex. *B:* Body and liver weights as well as relative liver weights of *GHR*-KO and control pigs.

MOLECULAR METABOLISM

residues were blocked with iodoacetamide (final concentration 8.3 mM) for 30 min in the dark. After adding DTT stock solution to a final concentration of 10 mM, 1:50 (enzyme:substrate) lysyl endopeptidase (Fujifilm Wako) was added to the sample and incubated for 4 h at 37 °C. After dilution with water to a concentration of 1 M urea, 1:50 (enzyme:substrate) porcine trypsin (Promega) was added to the sample and incubated for 18 h at 37 °C.

Mass spectrometry: LC-MS/MS was performed on an UltiMate3000 RSLCnano chromatography system (Thermo Scientific) coupled to a Q Exactive HF-X mass spectrometer (Thermo Scientific). One μg of peptides diluted in 0.1% formic acid (FA) was transferred to a trap column (2 cm; Acclaim® PepMap 100, 75 μm × 2 cm, nanoViper C18, 3 μm, 100 Å, Thermo Scientific) and separated at a flow rate of 250 nL/min (Column: 50 cm; PepMap® RSLC, 75 μm × 50 cm, nanoViper C18, 2 μm, 100 Å, Thermo Scientific). LC gradients were consecutive linear gradients from 3% to 25% solvent B (0.1% formic acid, 100% ACN) in 160 min, from 25% to 40% solvent B in 10 min, and from 40% to 85% solvent B in 10 min. For data acquisition, cycles consisted of one full MS scan at a resolution of 60,000 and 15 data-dependent HCD (higher collision dissociation) MS/MS scans at a resolution of 15,000 and a collision energy of 28. Resulting data were evaluated using Thermo Xcalibur Qual Browser. The mass spectrometry proteomics data have been deposited to the ProteomeXchange Consortium via the PRIDE [19] partner repository with the dataset identifier PXD017671.

Bioinformatics: For label-free quantification (LFQ) [20], MS data were processed using MaxQuant V1.6.2.10 and the Sus scrofa subset of the NCBI database (NCBI RefSeq Sus scrofa Annotation Release 106 Scrofa 11.1, available at: www.ncbi.nlm.nih.gov/assembly/GCF_000003025.6/). For identification, the following parameters were used: i) Enzyme: Trypsin; ii) Mass tolerance precursor: 10 ppm; iii) Mass tolerance MS/MS: 0.02 Da; iv) Fixed modification: Carbamidomethylation of cysteine; v) Variable modifications: oxidized methionine. FDRs at the peptide and protein level were set to 1%. In case proteins were detected in all replicates of one group but in no replicate of the other group, the MaxQuant imputation feature was used to allow statistical evaluation. Hierarchical clustering was performed in R, a principal component analysis was done with with the Perseus module V1.6.2.2 of MaxQuant. For the DAVID analysis as well as for the discussion, we exclusively used proteins with a p-value < 0.05. To facilitate a meta-analysis addressing also less prominent abundance alterations, the quantitative values (LFQ) of all identified proteins are listed in Supplementary Table 1A. For functional annotation clustering, the DAVID online platform [21] as well as the GlueGO and CluePedia plugins in Cytoscape were used. Furthermore, Gene Set Enrichment Analysis (GSEA) [22] was performed.

2.5. Metabolomics

The targeted metabolomics approach was performed using liquid chromatography-electrospray ionization-tandem mass spectrometry (LC-ESI-MS/MS) and flow injection analysis-electrospray ionization tandem mass spectrometry (FIA-ESI-MS/MS) using the AbsoluteIDQ™ p180 Kit (Biocrates Life Sciences AG), which allows for the quantification of 188 metabolites out of 10 μL plasma and liver tissue homogenate [23]. For a list of the 188 quantified metabolites see Supplementary Table 2. Liver tissue samples were processed, extracted, and quantified as described previously [24]. Per mg of frozen liver tissue 3 μL of a dry ice cooled mixture of ethanol/phosphate buffer (85/15 v/v) were added. Sample handling was performed by a Hamilton Microlab STAR™ robot (Hamilton Bonaduz AG) and an Ultravap nitrogen evaporator (Porvair Sciences). An API 4000 triple quadrupole system (Sciex Deutschland GmbH) equipped with a 1200 Series HPLC (Agilent Technologies Deutschland GmbH) and an HTC PAL auto sampler (CTC Analytics) controlled by the software Analyst 1.6.2. were used for mass spectrometric analyses. MultiQuant 3.0.1 (Sciex) and the MetIDQ™ software package were used for data evaluation for the quantification of metabolite concentrations and quality assessment. As reference for the calculation of metabolite concentrations, internal standards were used. Metabolite concentrations in tissue homogenate are given in μM. The LOD (limit of detection) was set to three times the values of the zero samples (PBS). Metabolites were log transformed and Pareto scaled to model them for two-way ANOVA.

2.6. Determination of liver glutathione

Total liver glutathione (GSH) and oxidized glutathione (GSSG) concentrations were determined using a Glutathione Colorimetric Detection Kit (EIAGSHC, Invitrogen). Twenty mg of frozen liver tissue was homogenized with a rod homogenizer (Polytron® PT 2500 E) in ice-cold 1 x phosphate-buffered saline (PBS) and immediately centrifuged (14,000 rpm, 10 min, 4 °C). After protein quantification using the Coomassie Plus (Bradford) Assay Kit (Thermo Scientific), the supernatant was deproteinized with 5% 5-sulfo-salicylic acid dihydrate solution (SSA). For GSSG determination, free GSH and other thiols in the samples were blocked with 2-vinylpyridine (2VP). After adding colorimetric detection reagent and reaction mixture provided with the kit, colorimetric reaction was detected at a wavelength of 405 nm using a Tecan Infinite M 200 pro plate reader. Free glutathione concentration was calculated by subtracting GSSG from GSH. Glutathione levels were normalized for protein content and expressed as μmol/g protein.

2.7. Immunoblot analyses

Protein samples were separated on 5% stacking/12% separation polyacrylamide gels with a Mini-Protean Tetra Cell (BioRad). Separated proteins were transferred onto polyvinylidene fluoride (PVDF) membranes (0.45 μm, IPVH00010, Millipore) for 30 min at 1.0 A/25 V. Equal loading was assessed by Ponceau S staining. Blots were blocked (5% non-fat dry milk in Tris-buffered saline with 0.1% Tween 20) for 1 h and incubated overnight at 4 °C with the primary antibody (PGC-1α antibody ab54481, GAPDH antibody #2118, Cell Signaling). Detection was performed with horseradish peroxidase-conjugated polyclonal goat anti-rabbit antibody (1:2500, no. 7074, Cell Signaling; for 1 h at RT) and SuperSignal™ West Dura chemiluminescence substrate (Thermo Scientific). Fluorescence imaging was performed using Intas ECL Chemostar. Western blot band intensities were quantitatively analyzed by Adobe Photoshop CS6. Normalized signal intensities of *GHR*-KO and control samples were compared using the Mann—Whitney *U*-test.

2.8. Immunohistochemistry

Fixation of liver samples with 4% formalin or methacarn, paraffin embedding and sectioning and histological analyses of liver samples were performed as described previously [25]. Immunohistochemistry on formalin-fixed tissue slices after heat-induced antigen retrieval in citrate buffer (pH 6) was performed using the following primary antibodies: rabbit polyclonal antibody against ARG1 (1:1200, no. 16001-1-AP, proteintech) and rabbit polyclonal antibody against ACADL (1:400, no. 17526-1-AP, proteintech). As secondary antibody, a horseradish peroxidase-conjugated polyclonal goat anti-rabbit antibody (1:200, no. P0448, Dako) was used. Immunohistochemistry on methacarn-fixed tissue slices was performed using rabbit polyclonal antibody against

villin-1 (1:100, no. 2369, Cell Signaling) and horseradish peroxidase-conjugated polyclonal goat anti-rabbit antibody (SignalStain Boost IHC Detection Reagent, no. 8114, Cell Signaling). Immunoreactivity was visualized using 3,3-diaminobenzidine tetrahydrochloride dihydrate (DAB) (brown color). Nuclear counterstaining was done with hemalum (blue color).

2.9. Statistical analysis

Statistical analyses were performed using R [26] with the qvalue package and SAS (SAS Institute) as well as GraphPad Prism (GraphPad Software). Visualizations were performed using R with the ggplot2 [27] and pheatmap packages and GraphPad Prism. Effects of group (*GHR*-KO, control), sex, and the interaction group $\times$ sex were evaluated using two-way ANOVA. If individual clinical-chemical and metabolomics parameters were addressed in a hypothesis-driven manner, student *t*-tests were used.

FDR for the proteomics and metabolomics ANOVA was calculated with the Benjamini-Hochberg procedure using the qvalue package. Values were considered significant at FDR <0.05. Additionally, 2D principal component analysis was performed using the algorithms implemented in Perseus [28]. All figures have a consistent color code (red = *GHR*-KO, blue = control). Protein abundance differences are given as log2 fold change (l2fc).

3. RESULTS

3.1. Body and liver weights

Body and liver weights of *GHR*-KO pigs were significantly ($p < 0.0001$) lower than those of controls. In addition, the relative liver weight (liver weight/body weight) was significantly ($p = 0.0065$) lower in *GHR*-KO vs. control pigs. No sex-related differences were observed for any of these parameters (Figure 1B).

3.2. Clinical-chemical and metabolomic findings in serum

Clinical-chemical analysis of serum samples revealed significantly increased activities of alanine transaminase (ALT; $p = 0.0001$) and alkaline phosphatase (AP; $p = 0.0138$) and a higher urea concentration ($p = 0.0004$) in *GHR*-KO compared to control pigs. The serum levels of creatinine ($p = 0.0050$) and glycerol ($p = 0.0305$) were significantly, and those of non-esterified fatty acids (NEFA; $p = 0.0813$) as a trend lower in *GHR*-KO vs. control samples (Figure 2A). Sex-related differences were observed for the serum concentrations of glycerol ($p = 0.0305$), triglycerides ($p = 0.0225$), lactate ($p = 0.0158$) (Figure 2B) and beta hydroxybutyrate ($p = 0.0357$), with significantly higher levels in female than in male pigs. The complete set of clinical-chemical data is shown in Supplementary Table 3.

The concentrations of propionylcarnitine, butyrylcarnitine and carnitine were significantly increased in serum samples of *GHR*-KO vs. control pigs. In addition, acetylcarnitine levels were higher (143% of control) in serum samples of *GHR*-KO pigs (Supplementary Figure 1). While not significant by ANOVA, the concentrations of alpha-aminoadipic acid (32% of control), carnosine (74% of control), creatinine (73% of control), spermidine (20% of control), and spermine (11% of control) were reduced in the *GHR*-KO samples (all significant by *t*-test at the $p < 0.05$ level except for spermidine and spermine due to high variability in the control group).

No sex-related differences were observed for any metabolite concentration in serum, nor was any parameter affected by the interaction group $\times$ sex (Supplementary Table 4).

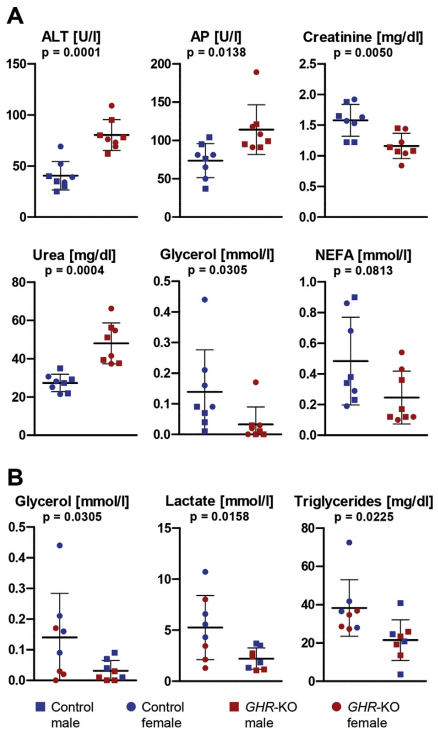

Figure 2: Clinical-chemical parameters in serum. *A:* Parameters affected by group. *B:* Parameters affected by sex. Horizontal lines represent mean and SD. ALT = alanine aminotransaminase, AP = alkaline phosphatase, NEFA = non-esterified fatty acids.

3.3. Proteome findings in liver

In total, 32,169 peptides could be identified (PEP-value < 0.05), which could be assigned to 3,231 protein groups at an FDR < 0.01. All 3,231 identified protein groups are — together with a GO analysis via pantherdb.org (Supplementary Figure 2) — listed in Supplementary Table 1A. Only protein groups that were detected in at least five animals of one group ($n = 1{,}913$) were selected for further analyses.

$GHR^{+/-}$ and $GHR^{+/+}$ animals were pooled as a control group, since they were phenotypically not different [10] and also did not show significant differences in the liver proteome profiles (all q-values = 1; Supplementary Table 1B).

A two-dimensional principal component analysis (2D-PCA) clearly separated *GHR*-KO from control pigs (Figure 3A).

Statistical analysis of the proteome data set using a two-way ANOVA (group $\times$ sex) identified 87 protein groups that were significantly ($p < 0.05$) altered in abundance by group, with 53 protein groups (25 with a $l2fc > 0.6$) being more abundant and 34 protein groups (9 with a $l2fc < -0.6$) being less abundant in *GHR*-KO vs. control animals (Supplementary Table 5A). A corresponding volcano plot and a heat map are shown in Figure 3B,C.

MOLECULAR METABOLISM

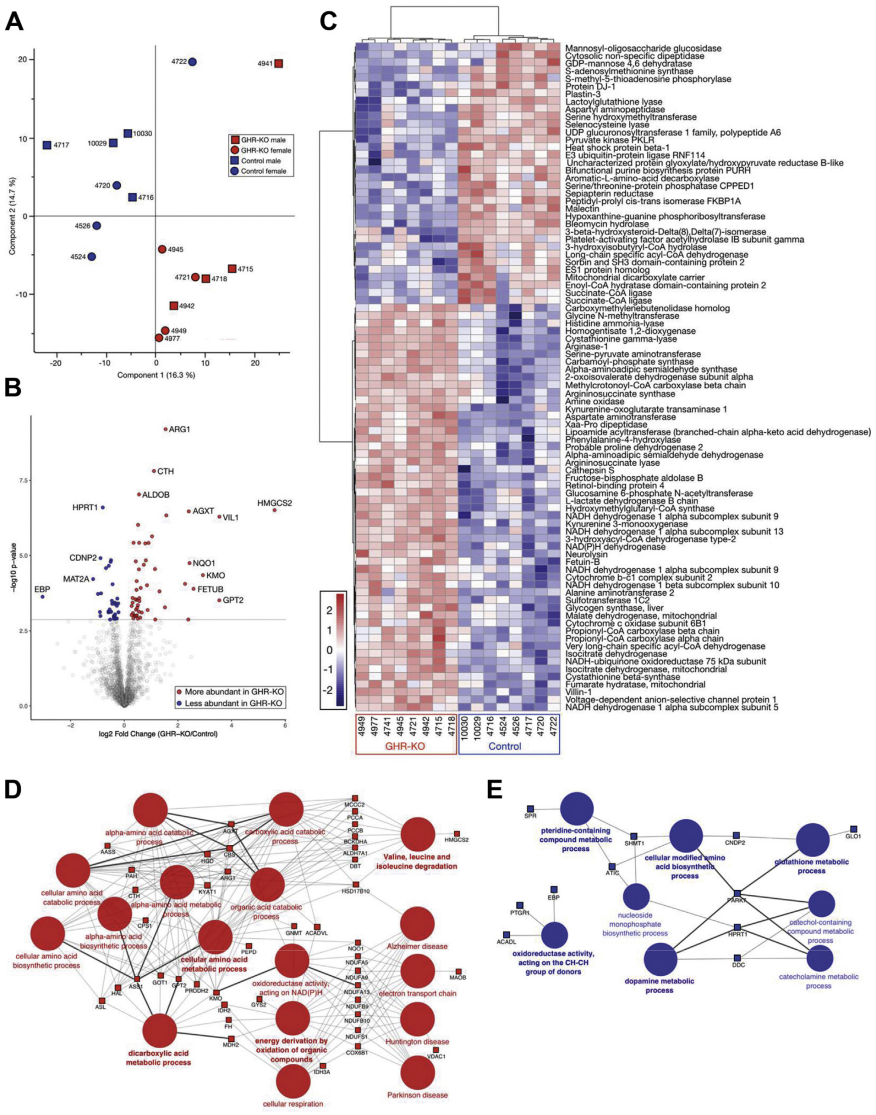

Figure 3: Proteome differences between liver samples from *GHR*-KO and control pigs. *A:* Principal component analysis (PCA) clearly separates proteomes from *GHR*-KO and control samples. *B:* Volcano plot of log2 fold changes (*GHR*-KO/control). Differentially abundant proteins ($p < 0.05$) are highlighted. *C:* Heat map of the differentially abundant proteins. *D, E:* ClueGO functional enrichment analysis for proteins significantly increased (*D*) or decreased (*E*) in abundance in *GHR*-KO vs. control liver samples. The analysis used the term GO Biological Process and KEGG pathways (min. 8 genes/cluster in *D* and min. 3 genes/cluster in *E*). The size of the circles indicates the significance of enrichment.

DAVID analysis of the 53 protein groups with increased abundance in *GHR*-KO pigs revealed three enriched functional clusters, which were related to protein biosynthesis (10 proteins, enrichment score: 6.5), carbon metabolism (especially TCA cycle; 10 proteins, enrichment score: 5.2), and mitochondrial respiration (eight proteins, enrichment score: 4.2).
DAVID analysis of the 34 protein families with decreased abundance in *GHR*-KO pigs showed no enriched functional clusters; most of these proteins are related to metabolism, especially carbohydrate, lipid and amino acid metabolism and to the complement and coagulation cascades. The results of the DAVID analysis are listed in Supplementary Table 5B.
A ClueGO functional enrichment analysis for the significantly more abundant protein groups in the liver of *GHR*-KO vs. control animals in GO Biological Process and KEGG pathways revealed amino acid metabolism, especially amino acid catabolism, dicarboxylic acid metabolism, cellular respiration and electron transport chain as overrepresented (Figure 3D), whereas proteins related to oxidoreductase activity acting on the CH−CH group donors, pteridine-containing compound metabolic process, glutathione metabolic process, dopamine metabolic process, and cellular modified amino acid biosynthetic process were enriched in the set of less abundant proteins (Figure 3E).
In addition, Gene Set Enrichment Analysis (GSEA) [22] was performed using the entire data set of quantified proteins, revealing 206 gene sets significantly enriched in *GHR*-KO pigs and 324 gene sets enriched in control pigs (FDR < 0.25). Gene sets related to mitochondria and the respiratory chain, amino acid metabolism, carbohydrate metabolism, lipid metabolism, oxidoreductase activity, nucleotide/nucleoside metabolism, RNA metabolism, and ribosome were overrepresented in *GHR*-KO pigs, whereas gene sets related to complement and coagulation, immune response and inflammation, protein maturation, modification and localization, regulation of canonical WNT signaling and MAPK pathways, cell structure and regulation of cell death were enriched in control pigs (Supplementary Table 5C).
In addition to genotype-related effects, 16 proteins were significantly altered in abundance by the sex of the animals; 13 proteins were more abundant in male animals, and three proteins were more abundant in female animals. The proteins with the highest sex-related abundance difference were glycine N-phenylacetyltransferase (LOC100517803; 79% homologous to human GLYAT; l2fc 0.85 in males vs. females, $p = 0.0033$) and dimethylaniline monooxygenase (FMO5; l2fc 1.01 in females vs. males, $p = 0.0393$). All proteins affected by sex are listed in Supplementary Table 5D.
The abundance of eight proteins was significantly influenced by the interaction group $\times$ sex (Supplementary Table 5E). In the control group, the hepatic concentrations of carnosine dipeptidase 2 (CNDP2), proteasome subunit beta 1 (PSMB1), proteasome subunit alpha 4 (PSMA4), aldehyde oxidase 1 (AOX1), flavin containing dimethylaniline monooxygenase 5 (FMO5), and aldehyde dehydrogenase 9 family member A1 (ALDH9A1) were significantly higher in female than in male pigs, whereas the abundance of LOC100517803 (79% homologous to human glycine-N-acyltransferase) was significantly higher in male vs. female pigs. No sex-related difference for the abundance of these proteins was observed in the *GHR*-KO group. Conversely, the level of platelet-activating factor acetylhydrolase 1b catalytic subunit 3 (PAFAH1B3) was significantly higher in female than male *GHR*-KO pigs, whereas no sex-related difference was noted in the control group.
Since the abundance of multiple mitochondrial proteins was increased in liver samples from *GHR*-KO pigs and increased transcript levels of *Ppargc1a* (coding the mitochondrial biogenesis factor PPARG coactivator 1 alpha) were reported in skeletal muscle and kidney tissue from GHR-deficient mice [29], we performed Western blot analyses of PGC-1α (PPARGC1A) in liver extracts from *GHR*-KO and control pigs. Significantly increased levels were detected in both male and female *GHR*-KO pigs compared with sex-matched controls (Figure 4).
In addition, we performed localization studies by immunohistochemistry of proteins with major abundance differences between *GHR*-KO and control liver samples and characteristic known expression profiles in different liver zones or cell types. The urea cycle enzyme arginase 1 (ARG1) is predominantly expressed in the periphery of liver lobules [30]. Accordingly, ARG1 staining in control liver samples was stronger in the periphery than in the center of liver lobules. In *GHR*-KO liver samples, which revealed a significantly increased ARG1 concentration (l2fc 1.54; $p = 0.26 \times 10^{-5}$), staining was more intensive, but the zonation of the liver lobule was maintained (Figure 5A).
The abundance of acyl-CoA dehydrogenase long chain (ACADL), an enzyme involved in the beta-oxidation of fatty acids, was significantly reduced in *GHR*-KO vs. control liver samples (l2fc −0.91, $p = 0.0393$). In both groups, centrolobular localization of ACADL was revealed (Figure 5B).
The abundance of villin 1 (VIL1) was markedly increased in the *GHR*-KO liver samples (l2fc 3.55, $p = 0.0003$). VIL1 staining was revealed at the luminal membrane of bile duct epithelium. In *GHR*-KO samples, some bile canaliculi proximal to the bile ducts were additionally stained (Figure 5C), explaining — at least in part — the higher overall abundance of VIL1 in *GHR*-KO vs. control liver samples.

3.4. Liver metabolomics

ANOVA of the liver metabolomics data revealed that the concentrations of five glycerophospholipids (PC aa C32:1, PC aa C32:2, PC aa C34:1, PC ae C34:1, and PC aa C40:4) and of two sphingolipids (SM (OH) C24:1 and SM (OH) C14:1) were significantly higher in *GHR*-KO compared with control liver samples. The same was true for the levels of carnitine (C0), hydroxyvalerylcarnitine (C5−OH/C3-DC-M), and

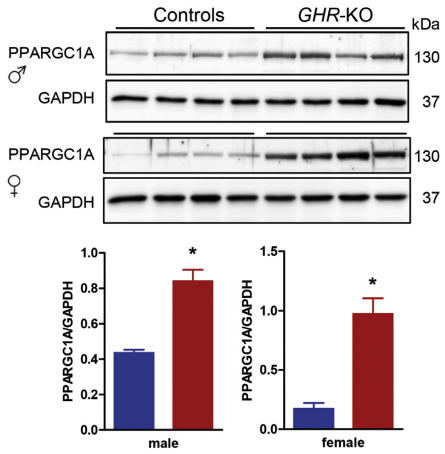

Figure 4: Western blot analysis of PPARGC1A in liver extracts from *GHR*-KO and control pigs. GAPDH was used as reference protein. Corresponding densitometrical analysis illustrating a significantly increased expression of PPARGC1A in liver of *GHR*-KO pigs compared to controls. Data were analyzed by Mann Whitney *U*-test and are presented as means ± SEM ($n = 4$/group), *$p < 0.05$.

MOLECULAR METABOLISM

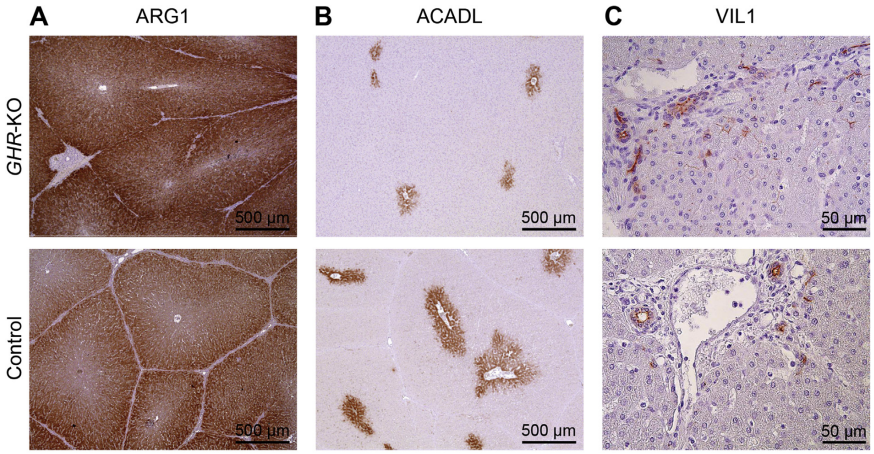

Figure 5: Immunohistochemical localization of arginase 1 (ARG1; *A*), acyl-CoA dehydrogenase long chain (ACADL; *B*), and villin 1 (VIL1; *C*) in liver sections from *GHR*-KO and control pigs.

glutarylcarnitine/hydroxyhexanoylcarnitine (C5-DC/C6−OH). While not significant by ANOVA, increased levels of short-chain acylcarnitines, for example, acetylcarnitine (C2; 145% of control), propionylcarnitine (C3; 229% of control), butyrylcarnitine (C4; 176% of control), and valerylcarnitine (C5; 226% of control) were found in the *GHR*-KO liver samples. These differences were all significant ($p < 0.05$) when testing them individually with student *t*-tests.

The concentration of mono-unsaturated glycerophosphocholines (MUFA (PC)) and the ratio of mono-unsaturated to saturated glycerophosphocholines (MUFA (PC)/SFA (PC)) were significantly higher, while the ratio of poly-unsaturated to mono-unsaturated glycerophosphocholines (PUFA (PC)/MUFA (PC)) was significantly lower in liver samples of *GHR*-KO vs. control pigs. In addition, the concentration of taurine and the ratio of tyrosine to phenylalanine were significantly increased in the *GHR*-KO samples, whereas the concentrations of creatinine and aspartate were significantly decreased. Furthermore, reduced (*t*-test: $p < 0.05$) concentrations of the biogenic amines, carnosine (76% of control) and spermine (65% of control), were observed (Figure 6A, Supplementary Figure 3, Supplementary Table 6A).

While no consistent sex-related difference was observed for any metabolite concentration in liver, phenylethylamine, two glycerophospholipids (PC aa C40:4 and PC ae C40:4) and two sphingolipids (SM (OH) C24:1, SM C24:1) were affected by the interaction group × sex (Supplementary Table 6B). In the control group, values for these metabolites were higher in females than in males. In *GHR*-KO pigs, there were no sex-related differences except for phenylethylamine, with higher levels in males than in females.

The complete targeted metabolomics data for liver tissue are shown in Supplementary Table 6C.

In addition, we determined the concentrations of glutathione (GSH) in liver samples from *GHR*-KO and control pigs. The levels of total and free GSH were significantly increased in the *GHR*-KO samples, while the levels of oxidized glutathione (GSSG) were not different between the two groups (Figure 6B, Supplementary Table 6D).

4. DISCUSSION

4.1. General aspects

Proteome and metabolome profiling of liver tissue from a clinically relevant GHR-deficient large animal model [10] and appropriate controls holds the potential to gain systematic insights into molecular consequences of missing GH action in this central hub of metabolic homeostasis. *GHR*-KO pigs resemble the clinical hallmarks of human Laron syndrome and can be maintained under standardized conditions, thus minimizing variance induced by confounding factors. Moreover, samples can be taken in sufficient amounts according to standardized operating procedures [15], ensuring a sample quality that would be difficult to achieve with human samples. Our experimental design used male and female pigs to comply with the fact that a large proportion of mammalian traits are influenced by sex [31]. Since heterozygous *GHR* mutant ($GHR^{+/-}$) pigs were phenotypically and in the liver proteome not different from wild-type ($GHR^{+/+}$) animals [10], these two genotypes were pooled as the control group.

Previous proteome studies of GHR-deficient humans or mouse models investigated serum/plasma or white adipose tissue (mouse only) but not liver tissue. Moreover, these studies relied on 2D gel electrophoresis and identification of differentially abundant protein spots by mass spectrometry and revealed only a small number of differentially abundant proteins (reviewed in [32]).

We chose a label-free quantification (LFQ) LC-MS/MS proteomics approach since metabolic labeling, like stable isotope labeling by/with amino acids in cell culture (SILAC) [20], is not applicable for large animal models like the pig. In order to diminish under-sampling, we used long chromatographic gradients (170 min) combined with long separation columns (50 cm, 2 µm beads) instead of pre-fractionation steps, which bear the risk of preventing reliable LFQ-based protein quantification. Retention time stability was controlled thoroughly between each run to ensure the reproducibility of our label-free quantification experiments.

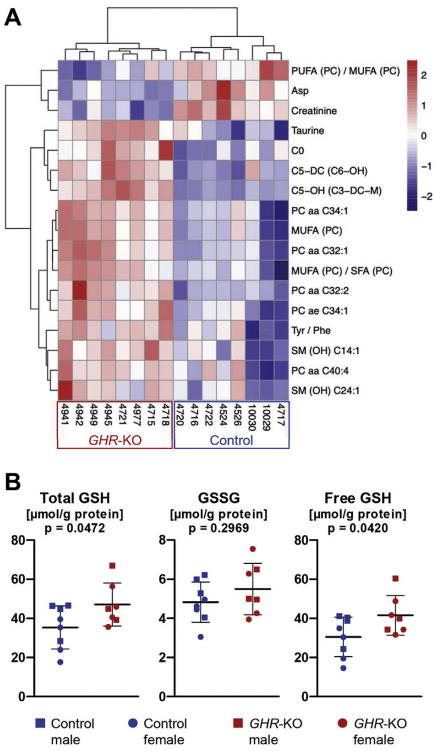

Figure 6: Metabolome differences between liver samples from *GHR*-KO and control pigs. *A:* Heatmap of metabolites significantly affected by group. *B:* Concentrations of total glutathione (GSH), oxidized glutathione (GSSG) and free GSH.

Proteomics of liver tissue is particularly challenging due to the high abundance of several proteins like, for example, plasma proteins; nonetheless we were able to identify 3,231 protein groups at an FDR <1%. A comparison of individual protein abundances in $GHR^{+/-}$ and $GHR^{+/+}$ pigs using student *t*-tests revealed no protein groups that differed significantly in abundance (q-value of 1, Supplementary Table 1B), indicating that no significant differences between these genotypes were detectable and justifying that they were pooled as control group.

Proteome data were analyzed by ANOVA, taking the effects of group, sex, and the interaction group × sex into account. Liver proteome profiles were mostly influenced by group. Accordingly, a 2D-PCA clearly separated *GHR*-KO and control samples (Figure 3A).

In order to facilitate a comprehensive physiological interpretation of proteome changes in the liver, clinical-chemical analyses of serum and targeted metabolomics of serum and liver tissue were additionally performed.

4.2. Increased degradation of amino acids

DAVID GO analysis revealed an annotation cluster including amino acid metabolism and urea cycle as significantly enriched in the *GHR*-KO samples (Supplementary Table 5B), and the gene set enrichment analysis identified many gene sets related to amino acid metabolism as overrepresented (Supplementary Table 5C).

The proteome profile of *GHR*-KO liver samples was characterized by significantly increased levels of multiple proteins involved in amino acid metabolism, especially amino acid catabolism. These enzymes and their respective amino acid substrates are illustrated in Figure 7A.

In the liver metabolome of *GHR*-KO pigs, the ratio of tyrosine to phenylalanine (Tyr/Phe) was significantly increased (0.78 vs. 0.65 in controls; $p = 0.0460$), indicating an increased activity of phenylalanine hydroxylase (PAH), the rate-limiting enzyme of the metabolic pathway that degrades excess phenylalanine.

In addition, significantly increased concentrations of glutamic-pyruvic transaminase 2 alias alanine aminotransferase 2 (GPT2; l2fc 3.54, $p = 0.0252$) and glutamic-oxaloacetic transaminase 1 alias aspartate aminotransferase 1 (GOT1; l2fc 1.14, $p = 0.0044$) were detected in *GHR*-KO compared to control liver samples. Transamination is an important step in the degradation of amino acids, as it removes their α-amino group and transfers it to α-ketoglutarate. The resulting glutamate undergoes oxidative deamination, releasing ammonia that is detoxified via the urea cycle. The remaining carbon part can be further metabolized in the tricarboxylic acid (TCA) cycle (reviewed in [33]).

All enzymes of the urea cycle, except for ornithine carbamoyltransferase (OTC), were significantly more abundant in *GHR*-KO than in control samples: carbamoyl-phosphate synthase (CPS1; l2fc 0.80, $p = 0.0033$), argininosuccinate synthase 1 (ASS1; l2fc 0.65, $p = 0.0393$), argininosuccinate lyase (ASL; l2fc 0.56, $p = 0.0232$), and arginase 1 (ARG1; l2fc 1.54, $p = 0.26 \times 10^{-5}$) (Figure 7B). As an estimate for the activity of these enzymes, we compared the concentrations of citrulline, aspartate, arginine, ornithine, and their ratios (Figure 7C). A significantly reduced concentration of aspartate in *GHR*-KO liver samples may reflect an increased activity of ASS1, using it for the synthesis of argininosuccinate. Another potential explanation is the lower abundance of aspartyl aminopeptidase (DNPEP; l2fc −0.98, $p = 0.0180$), which releases an N-terminal aspartate or glutamate from peptides, with a preference for aspartate (reviewed in [34]). The trend of lower arginine concentrations in *GHR*-KO samples may be related to reduced synthesis limited by the availability of aspartate or by increased hydrolysis by ARG1. A significantly ($p = 0.0127$) increased ratio of citrulline to ornithine in the liver metabolome of *GHR*-KO pigs indicates an increased activity of OTC. Significantly increased urea levels in the serum of *GHR*-KO pigs (Figure 2A) underline the increased activity of the urea cycle.

4.3. Increased activity of the TCA cycle

The carbon part of degraded amino acids is further metabolized, mainly to intermediates of the TCA cycle. The abundance of three TCA cycle enzymes was significantly increased in the *GHR*-KO liver proteome (Figure 8A): isocitrate dehydrogenase (IDH2; l2fc 0.35, $p = 0.0012$ and IDH3A; l2fc 0.46, $p = 0.0446$), fumarase (FH; l2fc 0.55, $p = 0.0393$), and malate dehydrogenase (MDH2; l2fc 0.32, $p = 0.046$). In addition, a protein cluster related to the TCA cycle and carbon metabolism was identified in the DAVID GO analysis (Supplementary Table 5B), and GSEA revealed 27 proteins related to the KEGG pathway TCA cycle as enriched in the *GHR*-KO samples (Supplementary Table 5C).

Pyruvate or any of the TCA cycle intermediates of glucogenic amino acids can serve as substrates for gluconeogenesis. While GSEA revealed 35 proteins related to the KEGG pathway glycolysis/gluconeogenesis as enriched in the *GHR*-KO samples (Supplementary

MOLECULAR METABOLISM

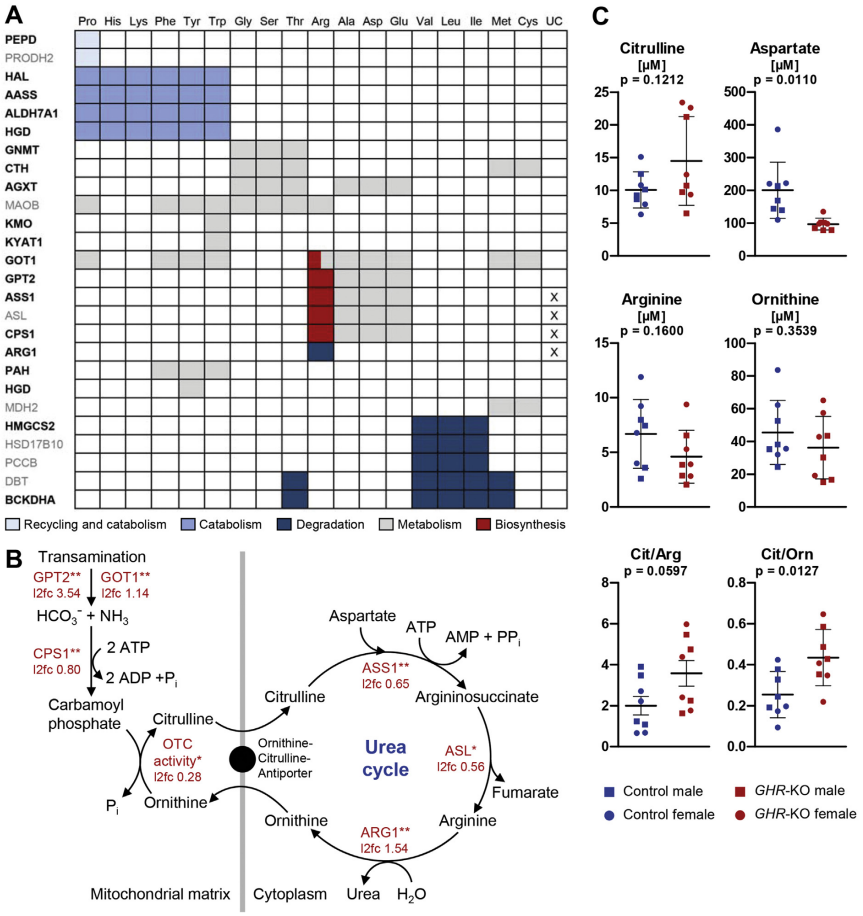

Figure 7: Evidence for increased amino acid degradation in *GHR*-KO vs. control liver samples. *A:* Proteins of amino acid metabolism with significantly ($p < 0.05$) increased abundance in the *GHR*-KO samples. Black bold font: l2fc > 0.6; grey standard font: l2fc < 0.6. The functions of the enzymes are indicated by color code, X indicates involvement in the urea cycle (UC). *B:* Increased abundance/activity of urea cycle enzymes in *GHR*-KO liver samples. Significant differences are indicated by asterisks: *$p < 0.05$; **$p < 0.01$. *C:* Concentrations and ratios of urea cycle substrates. Differences between groups were tested for significance using student *t*-tests. Abbreviations: AASS, alpha-aminoadipic semialdehyde synthase; AGXT, serine-pyruvate aminotransferase; ALDH7A1, alpha-aminoadipic semialdehyde dehydrogenase; ASL, argininosuccinate lyase; ASS1, argininosuccinate synthase 1; ARG1, arginase 1; BCKDHA, 2-oxoisovalerate dehydrogenase subunit alpha; CPS1, carbamoyl-phosphate synthase 1; CTH, cystathionine gamma-lyase; DBT, lipoamide acyltransferase component of branched-chain alpha-keto acid dehydrogenase complex; GNMT, glycine N-methyltransferase; GOT1, aspartate aminotransferase 1; GPT2, alanine aminotransferase 2; HAL, histidine ammonia-lyase; HGD, homogentisate 1,2-dioxygenase; HMGCS2, hydroxymethylglutaryl-CoA synthase; HSD17B10, 3-hydroxyacyl-CoA dehydrogenase type-2; KMO, kynurenine 3-monooxygenase; KYAT1, kynurenine-oxoglutarate transaminase 1; MAOB, amine oxidase; MDH2, malate dehydrogenase; OTC, ornithine carbamoyltransferase; PAH, phenylalanine-4-hydroxylase; PCCB, propionyl-CoA carboxylase beta chain; PEPD, xaa-Pro dipeptidase; PRODH2, probable proline dehydrogenase 2.

Table 5C), none of the enzymes involved in gluconeogenesis were significantly altered in abundance in *GHR*-KO vs. control liver samples. However, pyruvate kinase (PKLR, liver and red blood cell isoform), the enzyme catalyzing the last of the three rate-limiting steps of glycolysis, was significantly less abundant in the *GHR*-KO pigs (l2fc −0.89, $p = 0.0033$). Reduced levels of PKLR may be a mechanism to maintain gluconeogenesis in the absence of GH action by reducing the conversion of phosphoenolpyruvate (PEP) into pyruvate and thus

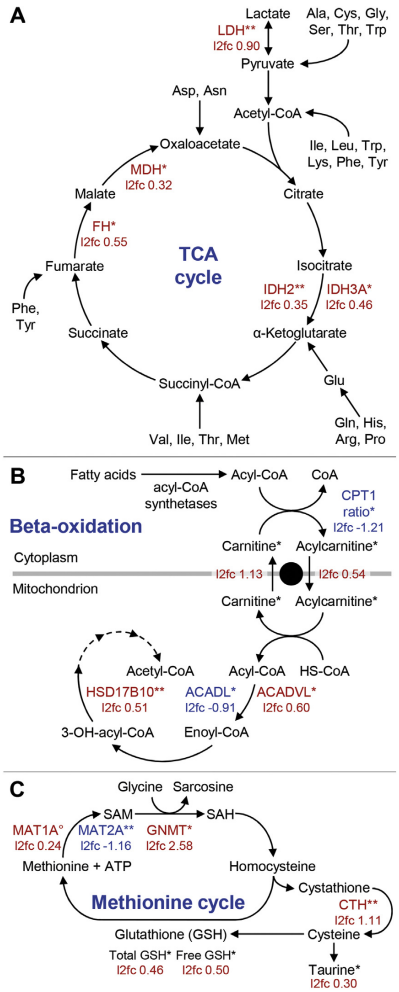

Figure 8: Proteome and metabolome alterations in specific metabolic pathways. Red indicates increased abundance, blue decreased abundance in *GHR*-KO vs. control liver samples. Significant differences are indicated by asterisks: *p < 0.05; **p < 0.01. *A:* Tricarboxylic acid (TCA) cycle. Abbreviations: LDH, lactate dehydrogenase; IDH, isocitrate dehydrogenase; FH, fumarate hydratase; MDH, malate dehydrogenase. *B:* Fatty acid beta-oxidation. Abbreviations: ACAD(V)L, acyl-CoA dehydrogenase (very)long chain; HSD17B10, 3-hydroxyacyl-CoA dehydrogenase type 2; CPT1A, carnitine palmitoyltransferase 1A. CPT1A activity was calculated as ratio of long-chain acylcarnitines to free carnitine. Differences in these parameters were tested for significance using student *t*-tests. *C:* Methionine cycle. Abbreviations: SAM, S-adenosyl-methionine; SAH, S-adenosyl-L-homocysteine; MAT, methionine adenosyltransferases; GNMT, glycine N-methyltransferase; CTH, cystathionine gamma-lyase; ATP, adenosine triphosphate; GSH, glutathione. °p < 0.07.

preserving PEP as the basic substrate for gluconeogenesis. A characteristic consequence of GHR deficiency in humans is juvenile hypoglycemia, but glucose levels normalize when the patients become adults [35,36]. Similarly, young (3 months old) *GHR*-KO pigs showed fasting hypoglycemia, whereas normal glucose levels were measured at age 6 months [10]. A common explanation for juvenile hypoglycemia in GHR deficiency is the lack of stimulatory GH effects on hepatic glucose production by glycogenolysis and gluconeogenesis (reviewed in [4]). Different mechanisms, including changes in insulin secretion and insulin sensitivity or increased gluconeogenesis, may account for the normalization of glucose levels during puberty. Future studies determining the rates of gluconeogenesis in young and mature *GHR*-KO pigs along with the levels of gluconeogenic enzymes and potential regulatory proteins in the liver will clarify, if the reduction of PKLR levels in 6-month-old *GHR*-KO pigs indeed has an effect on gluconeogenesis.

The B subunit of lactate dehydrogenase (LDHB) was significantly more abundant in *GHR*-KO vs. control liver tissue (l2fc 0.90, $p = 0.0012$). LDH, a tetrameric enzyme, catalyzes the interconversion of lactate and pyruvate. Recent studies indicate that lactate can be used as carbon source for the TCA cycle both in tumors and normal tissues (reviewed in [37]). A study of rat liver showed that the LDH isoforms $LDHA_4$ (LDH5) and $LDHA_3B$ (LDH4) are both present in the cytosol and the peroxisomal matrix of hepatocytes, with peroxisomes comprising relatively more LDH-A3B than the cytosol [38]. Intraperoxisomal (and intramitochondrial) LDH may be involved in the re-oxidation of NADH generated by the beta-oxidation pathway (reviewed in [39]).

4.4. Marked up-regulation of 3-hydroxy-3-methylglutaryl-CoA synthase 2

The protein with the highest abundance increase in *GHR*-KO vs. control liver tissue was 3-hydroxy-3-methylglutaryl-CoA synthase 2 (HMGCS2; l2fc 5.60, $p = 0.0002$), the key enzyme of ketogenesis (reviewed in [40]). The expression of HMGCS2 is subject to complex regulation, involving hormones, nutrient-responsive pathways, and post-translational modifications (reviewed in [40–42]).

For instance, insulin suppresses *HMGCS2* expression via activation of the PI3K-AKT pathway leading to inactivation by phosphorylation and nuclear export of the forkhead box transcription factor FOXA2 (reviewed in [40]). Consequently, high levels of HMGCS2 have been observed in the liver of a genetically engineered pig model for insulin-deficient diabetes mellitus [43]. A direct role of GH in the regulation of HMGCS2 has not, to our knowledge, been described so far. A potential link between deficient GH action and highly upregulated HMGCS2 are increased levels of peroxisome proliferator-activated receptor-gamma (PPARG), which were previously described in the liver of *GHR*-KO pigs [10]. A stimulatory role of PPARG on HMGCS2 expression has been observed, for example, in a mouse model of diabetic cardiomyopathy [44] and in intestinal tumor cell lines and normal intestinal organoids [45]. Increased levels of PPARG in the *GHR*-KO liver samples may also be responsible for the higher abundance of glycogen synthase 2 (GYS2; l2fc 1.16, $p = 0.0497$), the rate limiting enzyme in the storage of glycogen in liver and adipose tissue [46].

In spite of the marked up-regulation of the key ketogenic enzyme HMGCS2 in *GHR*-KO liver, there was no evidence for stimulated ketogenesis. First, the levels of beta hydroxybutyrate in serum were not different between *GHR*-KO and control pigs. Second, the concentrations of ketogenic amino acids in the circulation and in the liver were not different between *GHR*-KO and control pigs. Third, the serum levels of non-esterified fatty acids, the main substrate of ketogenesis, were, as a trend, reduced in *GHR*-KO pigs, reflecting the missing lipolytic

MOLECULAR METABOLISM

action of GH that also resulted in significantly reduced serum levels of glycerol.

4.5. Reduced mitochondrial uptake of fatty acids for beta-oxidation

After cellular uptake of fatty acids via different mechanisms, they are converted to acyl-CoA by acyl-CoA synthetases (reviewed in [47]). Several isoforms of acyl-CoA synthetases were detected in our proteome study, but their abundances were not significantly different between *GHR*-KO and control liver samples. Since the mitochondrial membrane is impermeable for acyl-CoAs, they are converted into acylcarnitines by carnitine palmitoyltransferase 1A (CPT1A). A proxy for the activity of this carnitine shuttle is the ratio of long-chain acylcarnitines (C16 + C18) to free carnitine (C0) (CPT1 ratio). This ratio was lower in *GHR*-KO compared to control animals both in the liver (0.0060 ± 0.0041 vs. 0.0139 ± 0.0071; $p = 0.0197$) and in the serum (0.0045 ± 0.0025 vs. 0.0079 ± 0.0016; $p = 0.0078$), indicating a reduced mitochondrial uptake of fatty acids for beta-oxidation. In contrast, the concentration of C0 was significantly higher in the *GHR*-KO than in the control liver samples. In humans, 75% of carnitine is obtained from the diet, whereas the remaining proportion is synthetized from the essential amino acids lysine and methionine in liver, kidney and brain (reviewed in [48]). Since *GHR*-KO and control pigs received the same standardized diet, the higher C0 levels in *GHR*-KO pigs are most likely due to increased endogenous C0 synthesis, probably associated with the generally increased amino acid metabolism (see above).

The abundances of several enzymes involved in fatty acid beta-oxidation were significantly different between *GHR*-KO and control pigs. While acyl-CoA dehydrogenase long chain (ACADL; l2fc −0.91, $p = 0.0393$) was less abundant in the *GHR*-KO samples, acyl-CoA dehydrogenase very long chain (ACADVL; l2fc 0.60, $p = 0.0483$) and 3-hydroxyacyl-CoA dehydrogenase type 2 (HSD17B10; l2fc 0.51, $p = 0.0004$) were more abundant (Figure 8B). Interestingly, increased concentrations of short-chain acylcarnitines were found in liver (C2, C3, C4, C5, C5−OH/C3-DC-M, C5-DC/C6−OH) and serum (C2, C3, C4) of *GHR*-KO pigs. In the context of reduced serum levels of non-esterified fatty acids and reduced mitochondrial up-take of long-chain fatty acids (reduced activity of CPT1A, see above), increased short-chain acylcarnitine levels may result from an impairment of beta-oxidation of short-chain fatty acids. In addition, the degradation of lysine, tryptophan, valine, leucine, and isoleucine can yield short-chain acylcarnitines (C3 and C5 and other carnitines) (reviewed in [49]). We observed an increased amino acid degradation (see above). Increased concentrations of short-chain acylcarnitines were reported to have positive effects in terms of reversing age-dependent deficits in cellular function by improving energy balance (reviewed in [50]).

4.6. Increased synthesis of mono-unsaturated fatty acids and other changes in lipid metabolism

In the liver of *GHR*-KO pigs, the concentration of mono-unsaturated glycerophosphocholines (MUFA (PC)) was significantly increased, whereas the concentrations of saturated (SFA (PC)) and poly-unsaturated (PUFA (PC)) glycerophosphocholines were not different from control samples. Consequently, the ratio MUFA (PC)/SFA (PC) was significantly ($p = 0.0290$) increased, whereas the ratio PUFA (PC)/MUFA (PC) was significantly ($p = 0.0353$) decreased in the *GHR*-KO samples. MUFA can either be obtained from the diet, or be synthesized by elongase and desaturase enzymes from SFA (reviewed in [51]). Since *GHR*-KO and control pigs received the same standard diet as controls, increased synthesis is the most likely cause of significantly increased MUFA (PC) concentrations in GHR-deficient liver samples. The enzyme catalyzing the critical committed step in the *de novo* synthesis of MUFA is stearoyl-coenzyme A desaturase (SCD). Our holistic proteome analysis did not detect SCD in control liver samples (0/8), but in 3/8 samples from *GHR*-KO pigs. A direct effect of GH on the expression of SCD has been demonstrated in an immunodeficient, liver-damaged mouse model whose liver was almost completely repopulated with human hepatocytes. Since human hepatocytes do not respond to rodent GH, they were in a GH-deficient state. Upon treatment of the mice with human GH, the human *SCD* transcript level was significantly reduced compared to the GH-deficient state [52].

SCD requires NADH, the flavoprotein cytochrome b5 reductase, and the electron acceptor cytochrome b5 as well as molecular oxygen to introduce a single double bond in a spectrum of methylene-interrupted fatty acyl-CoA substrates. NADH is provided by the TCA cycle, which appears to be more active in *GHR*-KO than in control liver (see above). The preferred substrates of SCD are palmitoyl- and stearoyl-CoA, which are then converted into palmitoleoyl- and oleoyl-CoA, respectively. These products are the most abundant MUFA and serve as substrates for the synthesis of phospholipids, triglycerides, cholesteryl esters, and alkyldiacylglycerols (reviewed in [53]). While steatosis has been described in some patients with Laron syndrome [6] and in male mice with liver-specific GHR deficiency [7,54], this was not observed in mice with global GHR deficiency [9] nor in our *GHR*-KO pig model. Nevertheless, the abundances of fetuin B (FETUB; l2fc 2.39, $p = 0.0497$), a hepatokine increased in patients with liver steatosis [55], of retinol binding protein 4 (RBP4; l2fc 0.73, $p = 0.0038$) that stimulates hepatic lipogenesis [56], and of several mitochondrial proteins (see below), which DAVID functional annotation clustering links to NAFLD, were significantly increased in the *GHR*-KO liver samples. It is worth noting that pigs have a natural resistance to steatosis, even in morbid obesity [57].

Interestingly, the abundance of solute carrier family 25 member 10 (SLC25A10), a mitochondrial dicarboxylate carrier that plays an important role in supplying malate for citrate transport required for fatty acid synthesis [58], was significantly decreased in the *GHR*-KO liver samples (l2fc −0.49, $p = 0.0393$). Furthermore, 3-beta-hydroxysteroid-delta(8),delta(7)-isomerase alias EBP cholestenol delta-isomerase (EBP), an endoplasmic reticulum membrane protein that catalyzes the conversion of delta(8)-sterols into delta(7)-sterols and is involved in cholesterol biosynthesis [59], was markedly decreased in abundance in *GHR*-KO vs. control liver tissue (l2fc −3.05, $p = 0.0218$).

4.7. Increased abundance of multiple mitochondrial proteins

Several subunits of the mitochondrial membrane respiratory chain NADH dehydrogenase (Complex I) were more abundant in the liver of *GHR*-KO animals: the core subunit S1 (NDUFS1; l2fc 0.43, $p = 0.0033$), the alpha subcomplex subunits A5 (NDUFA5; l2fc 0.44, $p = 0.0373$), A9 (NDUFA9; l2fc 0.40, $p = 0.0446$) and A13 (NDUFA13; l2fc 0.55, $p = 0.0044$), and the beta subcomplex subunits B9 (NDUFB9; l2fc 0.42, $p = 0.0241$) and B10 (NDUFB10; l2fc 0.34, $p = 0.0497$). In addition, DAVID GO analysis found the cellular component (CC) term mitochondrial respiratory chain complex I as enriched in the *GHR*-KO samples (Supplementary Table 5B), and GSEA analysis revealed several terms related to the mitochondrial respiratory chain as enriched. Furthermore, the abundances of cytochrome c oxidase subunit 6B (COX6B, Complex IV; l2fc = 0.48, $p = 0.0340$) and of cytochrome b-c1 complex subunit 2 (LOC100524613, 94% homologous to human UQCRC2; l2fc 0.27, $p = 0.0309$) were significantly increased in the liver of *GHR*-KO pigs.

In addition to proteins of the respiratory chain complexes, many other mitochondrial proteins were more abundant in the *GHR*-KO than in the control liver samples, including HMGCS2, GPT2 and GOT1, isocitrate dehydrogenase ($NADP(^+)$) 2, mitochondrial (IDH2) and IDH3A, kynurenine 3-monooxygenase (KMO), aminoadipate-semialdehyde synthase (AASS), ACADVL, proline dehydrogenase 2 (PRODH2), fumarate hydratase (FH), hydroxysteroid 17-beta dehydrogenase 10 (HSD17B10), monoamine oxidase B (MAOB), dihydrolipoamide branched chain transacylase E2 (DBT), neurolysin (NLN), and voltage-dependent anion-selective channel protein 1 (VDAC1).

Gesing et al. [29] investigated transcript levels of genes known to be involved in mitochondrial biogenesis in several tissues of GHR-deficient and control mice. The authors reported increased transcript levels of *Ppargc1a* (coding PPARG coactivator 1 alpha, PPARGC1A) in skeletal muscle, of *Prkaa* (coding AMP-activated protein kinase), *Sirt1* (coding sirtuin 1), *Sirt3*, *Nos3* (coding endothelial nitric oxide synthase) and *Mfn2* (coding mitofusin 2) in heart, and of *Ppargc1a*, *Prkaa*, *Sirt3*, *Nos3* and *Mfn2* in kidney of GHR-deficient mice. In our holistic proteome study of liver samples, only SIRT3 and MFN2 were detected at the protein level; however, the signal intensities were too low to allow a reliable quantification of these proteins. Western blot analysis revealed significantly increased concentrations of PPARGC1A in the *GHR*-KO liver samples ($p = 0.0286$ for both males and females). Nicotinamide phosphoribosyltransferase (NAMPT), a rate-limiting enzyme in mammalian nicotinamide adenine dinucleotide $(NAD)^+$ biosynthesis and regulator of SIRT1 that activates PPARGC1A through deacetylation at specific lysine residues (reviewed in [29]), was also more abundant in *GHR*-KO liver samples, although the difference was not statistically significant (l2fc 0.90, $p = 0.2575$).

4.8. Altered methionine and glutathione metabolism

Proteomics of *GHR*-KO and control liver samples revealed abundance alterations of enzymes of the methionine cycle (Figure 8C), which plays a critical role in the regulation of concentrations of S-adenosylmethionine (SAM), the major biological methyl group donor. SAM is synthesized from methionine and adenosine triphosphate (ATP) by methionine adenosyltransferases (MAT). The abundance of MAT1A, the major enzyme responsible for SAM synthesis in adult liver [60], was slightly higher in *GHR*-KO vs. control samples, whereas MAT2A that is expressed in non-parenchymal cells of the liver (hepatic stellate and Kupffer cells) and extrahepatic tissues (reviewed in [61]) was less abundant (l2fc −1.16, $p = 0.0080$). In contrast, the major hepatic SAM utilizing enzyme, glycine N-methyltransferase (GNMT), that converts SAM (along with glycine) to S-adenosyl-L-homocysteine and sarcosine, was significantly more abundant in the *GHR*-KO samples (l2fc 2.58, $p = 0.0134$). Notably, GH-deficient Ames dwarf mice revealed significantly increased MAT and GNMT levels [62] that were reduced upon GH treatment [63].

Increased GNMT levels in *GHR*-KO liver may decrease the availability of SAM and increase downstream products of the methionine cycle, such as homocysteine, cystathionine, and glutathione (reviewed in [64,65]). Cystathionine gamma-lyase (CTH), which converts cystathionine into cysteine, the amino acid limiting glutathione synthesis, was more abundant in the *GHR*-KO samples (l2fc 1.11, $p < 0.0001$). Indeed, increased levels of free and total glutathione were revealed in the *GHR*-KO liver samples. Cysteine is also a precursor of taurine, which was more abundant in the *GHR*-KO vs. control liver samples. Lactoylglutathione lyase alias glyoxalase I (GLO1) that catalyzes the conversion of hemimercaptal, formed from methylglyoxal and glutathione, to S-lactoylglutathione was reduced (l2fc −0.28; $p = 0.0309$).

4.9. Additional proteome alterations associated with GHR deficiency

The abundance of villin 1 (VIL1) was markedly increased in the *GHR*-KO liver samples (l2fc 3.55, $p = 0.0003$). Expression of VIL1 in adult pig liver [66] and in normal human liver [67] was described to be restricted to bile canaliculi. Our immunohistochemical analysis detected VIL1 in the luminal membrane of bile duct epithelium in liver samples of both groups. In *GHR*-KO samples, some bile canaliculi proximal to the bile ducts were additionally stained. The markedly increased level of VIL1 in the *GHR*-KO liver samples suggests that GH directly or indirectly suppresses the expression of VIL1 in the bile canaliculi.

Another protein with increased abundance in *GHR*-KO liver samples was sulfotransferase 1C2 (SULT1C2; l2fc 1.52, $p = 0.0333$). Sulfotransferase enzymes catalyze the sulfate conjugation of hormones, drugs, and xenobiotic compounds, making them more hydrophilic such that they are readily excreted in the urine or bile (reviewed in [68]). The role of GH in the regulation of SULT1C2 has not been described as of yet.

The abundances of hypoxanthine-guanine phosphoribosyltransferase (HPRT; l2fc −0.80, $p = 0.0002$) and of malectin (MLEC; l2fc −0.68, $p = 0.0043$) were significantly reduced in the *GHR*-KO samples. HRPT catalyzes the conversion of hypoxanthine to inosine monophosphate and of guanine to guanosine monophosphate, thus playing a central role in the generation of purine nucleotides through the purine salvage pathway [69]. MLEC is a membrane-anchored ER protein that preferentially binds misfolded proteins and directs them to the ER-associated degradation (ERAD) pathway (reviewed in [70]). Neither HPRT nor MLEC has as yet been shown to be affected by alterations in the GH/IGF1 system.

4.10. GHR deficiency partially ameliorates sex-related protein abundance differences in the liver

ANOVA revealed that the abundances of eight proteins were significantly influenced by the interaction group × sex (Supplementary Table 5E), that is, they were influenced by sex in one group but not in the other. Seven proteins showed a sex-related abundance difference in the control group but not in *GHR*-KO pigs. In the latter, only one protein was different in abundance between males and females without a sex-related difference in the control group. These findings point to sex-related GH effects on the abundances of specific proteins, which are eliminated in the absence of the GHR.

A sexual dimorphism in the GH secretion pattern has been described in rodents: in male rats, GH secretion is pulsatile, whereas in female rats it is more continuous (reviewed in [71]). Elimination of GH by hypophysectomy abolished the sex specificity of approximately 90% of 1032 genes that were found to be expressed in a sex-dependent manner in rat liver, demonstrating a dominant role of GH in regulating liver sexual dimorphism [72]. Permanent overexpression of GH in male transgenic mice or continuous infusion of GH by mini-pumps into male mice resulted in a "feminization" of liver functions in terms of reducing the synthesis of major urinary proteins (MUPs), which are normally much more abundant in male than in female mice [73].

Sex-dependent differences in GH secretion have also been described in humans. Adult women have more uniform GH pulses throughout the day, while men have a large nocturnal pulse and relatively low GH output over the rest of the day [74]. A more recent study dissecting factors affecting GH secretion found that women younger than 50 years had a 2-fold higher basal, pulsatile, and total GH secretion compared with men in the same age range, but the sex differences for pulsatile and total GH secretion were no longer significant in subjects older than 50 years [75].

MOLECULAR METABOLISM

In pigs, a comprehensive characterization of the sex-specific patterns of GH secretion has not, to our knowledge, been conducted. Our observation that significant abundance differences in several proteins in the porcine liver were eliminated by ablation of GHR suggests sex-related differences in GH secretion influencing liver functions also in this species.

5. CONCLUSIONS

Our integrated proteomics/targeted metabolomics study of GHR-deficient and control liver samples from a clinically relevant large animal model identified a spectrum of biological pathways that are significantly altered in the absence of GH action. In particular, enzymes involved in amino acid degradation, in the urea cycle, and in the tricarboxylic acid cycle were increased in abundance. A decreased ratio of long-chain acylcarnitines to free carnitine suggested reduced mitochondrial import of fatty acids for beta-oxidation. The concentration of mono-unsaturated glycerophosphocholines was significantly increased without morphological signs of steatosis. Distinct abundance changes of enzymes in the methionine and glutathione metabolic pathways were associated with increased levels of total and free glutathione. Moreover, new insights into the role of GH in the specification of sex-related liver functions were provided.

The data set generated in this study is an interesting resource for meta-analyses with human and murine data sets that aim, for example, to investigate why GHR-deficient humans and rodents develop steatosis while pigs don't. Another interesting topic are age-related changes in the function of the GH/GHR system, in particular the question of why GHR deficiency leads to juvenile hypoglycemia that normalizes during puberty. Finally, it will be interesting to see to what extent altered liver functions in GHR deficiency are corrected by IGF1 treatment or somatic *GHR* gene therapy.

FUNDING

This study was supported in part by a grant from the German Federal Ministry of Education and Research (BMBF) to the German Center for Diabetes Research (DZD) and — in part — by the Deutsche Forschungsgemeinschaft (TRR127).

AUTHOR CONTRIBUTIONS

E.O.R., T.F. and E.W. conceived the experiments. E.O.R. and E.W. wrote the manuscript. T.F, G.J.A., M.Bi. and J.S. revised the manuscript. All authors contributed to the manuscript and read and approved the final version.

A.H., M.D., and E.W. developed the animal model, A.H. and A.B. collected the samples, E.O.R. and T.F. conducted and analyzed the proteomics measurements. C.P. and J.A. performed the targeted metabolomics analyses, M.Ba. performed bioinformatics analyses on the metabolomics measurements. E.K. performed immunohistochemical studies, S.R. glutathione measurements, B.R. and M.H.d.A. the clinical-chemical measurements, and M.D. the Western blot analysis.

E.O.R., T.F. and E.W. are the guarantors of this work and, as such, had full access to all the data in the study and take responsibility for the integrity of the data and the accuracy of the data analysis.

ACKNOWLEDGEMENTS

The authors thank Tatjana Schröter, Christina Blechinger and Franziska Kress for excellent technical assistance. We thank Julia Scarpa and Silke Becker for metabolomics measurements performed at the Helmholtz Zentrum München, Genome Analysis Center, Metabolomics Core Facility, and Lisa Pichl for histological analyses.

CONFLICT OF INTEREST

No potential conflicts of interest relevant to this article are reported.

APPENDIX A. SUPPLEMENTARY DATA

Supplementary data to this article can be found online at https://doi.org/10.1016/j.molmet.2020.100978.

REFERENCES

[1] Vijayakumar, A., Yakar, S., Leroith, D., 2011. The intricate role of growth hormone in metabolism. Frontiers in Endocrinology (Lausanne) 2:32.
[2] Ranke, M.B., Wit, J.M., 2018. Growth hormone - past, present and future. Nature Reviews Endocrinology 14(5):285—300.
[3] Yakar, S., Liu, J.L., Stannard, B., Butler, A., Accili, D., Sauer, B., et al., 1999. Normal growth and development in the absence of hepatic insulin-like growth factor I. Proceedings of the National Academy of Sciences of the U S A 96(13): 7324—7329.
[4] Vijayakumar, A., Novosyadlyy, R., Wu, Y., Yakar, S., LeRoith, D., 2010. Biological effects of growth hormone on carbohydrate and lipid metabolism. Growth Hormone & IGF Research 20(1):1—7.
[5] Takahashi, Y., 2017. The role of growth hormone and insulin-like growth factor-I in the liver. International Journal of Molecular Sciences 18(7):1447.
[6] Laron, Z., Ginsberg, S., Webb, M., 2008. Nonalcoholic fatty liver in patients with Laron syndrome and GH gene deletion - preliminary report. Growth Hormone & IGF Research 18(5):434—438.
[7] Fan, Y., Menon, R.K., Cohen, P., Hwang, D., Clemens, T., DiGirolamo, D.J., et al., 2009. Liver-specific deletion of the growth hormone receptor reveals essential role of growth hormone signaling in hepatic lipid metabolism. Journal of Biological Chemistry 284(30):19937—19944.
[8] Liu, Z., Cordoba-Chacon, J., Kineman, R.D., Cronstein, B.N., Muzumdar, R., Gong, Z., et al., 2016. Growth hormone control of hepatic lipid metabolism. Diabetes 65(12):3598—3609.
[9] Piotrowska, K., Borkowska, S.J., Wiszniewska, B., Laszczyńska, M., Słuczanowska-Głabowska, S., Havens, A.M., et al., 2013. The effect of low and high plasma levels of insulin-like growth factor-1 (IGF-1) on the morphology of major organs: studies of Laron dwarf and bovine growth hormone transgenic (bGHTg) mice. Histology & Histopathology 28(10):1325.
[10] Hinrichs, A., Kessler, B., Kurome, M., Blutke, A., Kemter, E., Bernau, M., et al., 2018. Growth hormone receptor-deficient pigs resemble the pathophysiology of human Laron syndrome and reveal altered activation of signaling cascades in the liver. Molecular Metabolism 11(5):113—128.
[11] Wang, C., Xu, Y., 2019. Mechanisms for sex differences in energy homeostasis. Journal of Molecular Endocrinology 62(2):R129—R143.
[12] Robles, M.S., Cox, J., Mann, M., 2014. In-vivo quantitative proteomics reveals a key contribution of post-transcriptional mechanisms to the circadian regulation of liver metabolism. PLoS Genetics 10(1):e1004047.
[13] Mauvoisin, D., Wang, J., Jouffe, C., Martin, E., Atger, F., Waridel, P., et al., 2014. Circadian clock-dependent and -independent rhythmic proteomes implement distinct diurnal functions in mouse liver. Proceedings of the National Academy of Sciences of the U S A 111(1):167—172.
[14] Wang, J., Mauvoisin, D., Martin, E., Atger, F., Galindo, A.N., Dayon, L., et al., 2017. Nuclear proteomics uncovers diurnal regulatory landscapes in mouse liver. Cell Metabolism 25(1):102—117.

[15] Albl, B., Haesner, S., Braun-Reichhart, C., Streckel, E., Renner, S., Seeliger, F., et al., 2016. Tissue sampling guides for porcine biomedical models. Toxicologic Pathology 44(3):414—420.

[16] Blutke, A., Renner, S., Flenkenthaler, F., Backman, M., Haesner, S., Kemter, E., et al., 2017. The Munich MIDY Pig Biobank - a unique resource for studying organ crosstalk in diabetes. Molecular Metabolism 6(8): 931—940.

[17] Rathkolb, B., Hans, W., Prehn, C., Fuchs, H., Gailus-Durner, V., Aigner, B., et al., 2013. Clinical chemistry and other laboratory tests on mouse plasma or serum. Current Protocol Mouse Biology 3(2):69—100.

[18] Antharavally, B.S., Mallia, K.A., Rangaraj, P., Haney, P., Bell, P.A., 2009. Quantitation of proteins using a dye-metal-based colorimetric protein assay. Analytical Biochemistry 385(2):342—345.

[19] Perez-Riverol, Y., Csordas, A., Bai, J., Bernal-Llinares, M., Hewapathirana, S., Kundu, D.J., et al., 2019. The PRIDE database and related tools and resources in 2019: improving support for quantification data. Nucleic Acids Research 47(D1):D442—D450.

[20] Cox, J., Hein, M.Y., Luber, C.A., Paron, I., Nagaraj, N., Mann, M., 2014. Accurate proteome-wide label-free quantification by delayed normalization and maximal peptide ratio extraction, termed MaxLFQ. Molecular & Cellular Proteomics 13(9):2513—2526.

[21] Huang da, W., Sherman, B.T., Lempicki, R.A., 2009. Systematic and integrative analysis of large gene lists using DAVID bioinformatics resources. Nature Protocols 4(1):44—57.

[22] Subramanian, A., Tamayo, P., Mootha, V.K., Mukherjee, S., Ebert, B.L., Gillette, M.A., et al., 2005. Gene set enrichment analysis: a knowledge-based approach for interpreting genome-wide expression profiles. Proceedings of the National Academy of Sciences of the U S A 102(43):15545—15550.

[23] Zukunft, S., Sorgenfrei, M., Prehn, C., Möller, G., Adamski, J., 2013. Targeted metabolomics of dried blood spot extracts. Chromatographia 76(19):1295—1305.

[24] Zukunft, S., Prehn, C., Rohring, C., Moller, G., Hrabe de Angelis, M., Adamski, J., et al., 2018. High-throughput extraction and quantification method for targeted metabolomics in murine tissues. Metabolomics 14(1):18.

[25] Kemter, E., Frohlich, T., Arnold, G.J., Wolf, E., Wanke, R., 2017. Mitochondrial dysregulation secondary to endoplasmic reticulum stress in autosomal dominant tubulointerstitial kidney disease - UMOD (ADTKD-UMOD). Scientific Reports 7:42970.

[26] Team, R.C., 2018. R: A language and environment for statistical computing. Vienna: R Foundation for Statistical Computing.

[27] Wickham, H., 2016. ggplot2: elegant graphics for data analysis, 2 ed. Springer International Publishing.

[28] Tyanova, S., Temu, T., Sinitcyn, P., Carlson, A., Hein, M.Y., Geiger, T., et al., 2016. The Perseus computational platform for comprehensive analysis of (prote)omics data. Nature Methods 13(9):731—740.

[29] Gesing, A., Masternak, M.M., Wang, F., Joseph, A.M., Leeuwenburgh, C., Westbrook, R., et al., 2011. Expression of key regulators of mitochondrial biogenesis in growth hormone receptor knockout (GHRKO) mice is enhanced but is not further improved by other potential life-extending interventions. J Gerontol A Biology Science Medicine Science 66(10):1062—1076.

[30] Colnot, S., Perret, C., 2011. Liver zonation. In: Monga, S.P.S. (Ed.), Molecular pathology of liver diseases. Boston, MA: Springer US. p. 7—16.

[31] Karp, N.A., Mason, J., Beaudet, A.L., Benjamini, Y., Bower, L., Braun, R.E., et al., 2017. Prevalence of sexual dimorphism in mammalian phenotypic traits. Nature Communications 8:15475.

[32] Duran-Ortiz, S., Brittain, A.L., Kopchick, J.J., 2017. The impact of growth hormone on proteomic profiles: a review of mouse and adult human studies. Clinical Proteomics 14:24.

[33] Litwack, G., 2018. Metabolism of amino acids. In: Litwack, G. (Ed.), Human biochemistry. Academic Press. p. 359—94.

[34] Sanderink, G.J., Artur, Y., Siest, G., 1988. Human aminopeptidases: a review of the literature. Journal of Clinical Chemistry & Clinical Biochemistry 26(12): 795—807.

[35] Laron, Z., 2004. Laron syndrome (primary growth hormone resistance or insensitivity): the personal experience 1958-2003. Journal of Clinical Endocrinology & Metabolism 89(3):1031—1044.

[36] Laron, Z., Avitzur, Y., Klinger, B., 1995. Carbohydrate metabolism in primary growth hormone resistance (Laron syndrome) before and during insulin-like growth factor-I treatment. Metabolism 44(10 Suppl 4):113—118.

[37] Martinez-Reyes, I., Chandel, N.S., 2017. Waste not, want not: lactate oxidation fuels the TCA cycle. Cell Metabolism 26(6):803—804.

[38] Baumgart, E., Fahimi, H.D., Stich, A., Volkl, A., 1996. L-lactate dehydrogenase A4- and A3B isoforms are bona fide peroxisomal enzymes in rat liver. Evidence for involvement in intraperoxisomal NADH reoxidation. Journal of Biological Chemistry 271(7):3846—3855.

[39] Gladden, L.B., 2004. Lactate metabolism: a new paradigm for the third millennium. Journal of Physiology 558(Pt 1):5—30.

[40] Newman, J.C., Verdin, E., 2014. Ketone bodies as signaling metabolites. Trends in Endocrinology and Metabolism 25(1):42—52.

[41] Rescigno, T., Capasso, A., Tecce, M.F., 2018. Involvement of nutrients and nutritional mediators in mitochondrial 3-hydroxy-3-methylglutaryl-CoA synthase gene expression. Journal of Cellular Physiology 233(4):3306—3314.

[42] Grabacka, M., Pierzchalska, M., Dean, M., Reiss, K., 2016. Regulation of ketone body metabolism and the role of PPARalpha. International Journal of Molecular Sciences 17(12):2093.

[43] Backman, M., Flenkenthaler, F., Blutke, A., Dahlhoff, M., Landstrom, E., Renner, S., et al., 2019. Multi-omics insights into functional alterations of the liver in insulin-deficient diabetes mellitus. Molecular Metabolism 26(8):30—44.

[44] Sikder, K., Shukla, S.K., Patel, N., Singh, H., Rafiq, K., 2018. High fat diet upregulates fatty acid oxidation and ketogenesis via intervention of PPAR-gamma. Cellular Physiology and Biochemistry 48(3):1317—1331.

[45] Kim, J.T., Li, C., Weiss, H.L., Zhou, Y., Liu, C., Wang, Q., et al., 2019. Regulation of ketogenic enzyme HMGCS2 by wnt/beta-catenin/PPARgamma pathway in intestinal cells. Cells 8(9):1106.

[46] Mandard, S., Stienstra, R., Escher, P., Tan, N.S., Kim, I., Gonzalez, F.J., et al., 2007. Glycogen synthase 2 is a novel target gene of peroxisome proliferator-activated receptors. Cellular and Molecular Life Sciences : CMLS 64(9):1145—1157.

[47] Longo, N., Frigeni, M., Pasquali, M., 2016. Carnitine transport and fatty acid oxidation. Biochimica et Biophysica Acta 1863(10):2422—2435.

[48] Flanagan, J.L., Simmons, P.A., Vehige, J., Willcox, M.D., Garrett, Q., 2010. Role of carnitine in disease. Nutrition and Metabolism (Lond) 7:30.

[49] Schooneman, M.G., Vaz, F.M., Houten, S.M., Soeters, M.R., 2013. Acylcarnitines: reflecting or inflicting insulin resistance? Diabetes 62(1):1—8.

[50] Reuter, S.E., Evans, A.M., 2012. Carnitine and acylcarnitines: pharmacokinetic, pharmacological and clinical aspects. Clinical Pharmacokinetics 51(9): 553—572.

[51] Piccinin, E., Cariello, M., De Santis, S., Ducheix, S., Sabba, C., Ntambi, J.M., et al., 2019. Role of oleic acid in the gut-liver Axis: from diet to the regulation of its synthesis via stearoyl-CoA desaturase 1 (SCD1). Nutrients 11(10):2283.

[52] Tateno, C., Kataoka, M., Utoh, R., Tachibana, A., Itamoto, T., Asahara, T., et al., 2011. Growth hormone-dependent pathogenesis of human hepatic steatosis in a novel mouse model bearing a human hepatocyte-repopulated liver. Endocrinology 152(4):1479—1491.

[53] Paton, C.M., Ntambi, J.M., 2009. Biochemical and physiological function of stearoyl-CoA desaturase. American Journal of Physiology. Endocrinology and Metabolism 297(1):E28—E37.

[54] List, E.O., Berryman, D.E., Funk, K., Jara, A., Kelder, B., Wang, F., et al., 2014. Liver-specific GH receptor gene-disrupted (LiGHRKO) mice have decreased

MOLECULAR METABOLISM

endocrine IGF-I, increased local IGF-I, and altered body size, body composition, and adipokine profiles. Endocrinology 155(5):1793–1805.

[55] Meex, R.C., Hoy, A.J., Morris, A., Brown, R.D., Lo, J.C., Burke, M., et al., 2015. Fetuin B is a secreted hepatocyte factor linking steatosis to impaired glucose metabolism. Cell Metabolism 22(6):1078–1089.

[56] Xia, M., Liu, Y., Guo, H., Wang, D., Wang, Y., Ling, W., 2013. Retinol binding protein 4 stimulates hepatic sterol regulatory element-binding protein 1 and increases lipogenesis through the peroxisome proliferator-activated receptor-gamma coactivator 1beta-dependent pathway. Hepatology 58(2):564–575.

[57] Renner, S., Blutke, A., Dobenecker, B., Dhom, G., Müller, T.D., Finan, B., et al., 2018. Metabolic syndrome and extensive adipose tissue inflammation in morbidly obese Göttingen minipigs. Molecular Metabolism 16:180–190.

[58] Mizuarai, S., Miki, S., Araki, H., Takahashi, K., Kotani, H., 2005. Identification of dicarboxylate carrier Slc25a10 as malate transporter in de novo fatty acid synthesis. Journal of Biological Chemistry 280(37):32434–32441.

[59] Long, T., Hassan, A., Thompson, B.M., McDonald, J.G., Wang, J., Li, X., 2019. Structural basis for human sterol isomerase in cholesterol biosynthesis and multidrug recognition. Nature Communications 10(1):2452.

[60] Ji, Y., Nordgren, K.K., Chai, Y., Hebbring, S.J., Jenkins, G.D., Abo, R.P., et al., 2012. Human liver methionine cycle: MAT1A and GNMT gene resequencing, functional genomics, and hepatic genotype-phenotype correlation. Drug Metabolism & Disposition 40(10):1984–1992.

[61] Ramani, K., Lu, S.C., 2017. Methionine adenosyltransferases in liver health and diseases. Liver Research 1(2):103–111.

[62] Uthus, E.O., Brown-Borg, H.M., 2003. Altered methionine metabolism in long living Ames dwarf mice. Experimental Gerontology 38(5):491–498.

[63] Brown-Borg, H.M., Rakoczy, S.G., Uthus, E.O., 2005. Growth hormone alters methionine and glutathione metabolism in Ames dwarf mice. Mechanism of Ageing and Development 126(3):389–398.

[64] Lu, S.C., 2013. Glutathione synthesis. Biochimica et Biophysica Acta 1830(5): 3143–3153.

[65] Mosharov, E., Cranford, M.R., Banerjee, R., 2000. The quantitatively important relationship between homocysteine metabolism and glutathione synthesis by the transsulfuration pathway and its regulation by redox changes. Biochemistry 39(42):13005–13011.

[66] Maunoury, R., Robine, S., Pringault, E., Leonard, N., Gaillard, J.A., Louvard, D., 1992. Developmental regulation of villin gene expression in the epithelial cell lineages of mouse digestive and urogenital tracts. Development 115(3):717–728.

[67] Bacchi, C.E., Gown, A.M., 1991. Distribution and pattern of expression of villin, a gastrointestinal-associated cytoskeletal protein, in human carcinomas: a study employing paraffin-embedded tissue. Laboratory Investigation 64(3): 418–424.

[68] Rondini, E.A., Pant, A., Kocarek, T.A., 2015. Transcriptional regulation of cytosolic sulfotransferase 1C2 by intermediates of the cholesterol biosynthetic pathway in primary cultured rat hepatocytes. Journal of Pharmacology and Experimental Therapeutics 355(3):429–441.

[69] Berg, J.M., Tymoczko, J.L., Stryer, L., 2002. Purine bases can Be synthesized de Novo or recycled by salvage pathways. Biochemistry, 5th ed. W. H. Freeman: New York, p. Available from: https://www.ncbi.nlm.nih.gov/books/NBK22385/.

[70] Ferris, S.P., Kodali, V.K., Kaufman, R.J., 2014. Glycoprotein folding and quality-control mechanisms in protein-folding diseases. Disease Model Mechcanical 7(3):331–341.

[71] Jansson, J.O., Eden, S., Isaksson, O., 1985. Sexual dimorphism in the control of growth hormone secretion. Endocrine Reviews 6(2):128–150.

[72] Wauthier, V., Waxman, D.J., 2008. Sex-specific early growth hormone response genes in rat liver. Molecular Endocrinology 22(8):1962–1974.

[73] Norstedt, G., Palmiter, R., 1984. Secretory rhythm of growth hormone regulates sexual differentiation of mouse liver. Cell 36(4):805–812.

[74] Jaffe, C.A., Ocampo-Lim, B., Guo, W., Krueger, K., Sugahara, I., DeMott-Friberg, R., et al., 1998. Regulatory mechanisms of growth hormone secretion are sexually dimorphic. Journal of Clinical Investigation 102(1): 153–164.

[75] Roelfsema, F., Veldhuis, J.D., 2016. Growth hormone dynamics in healthy adults are related to age and sex and strongly dependent on body mass index. Neuroendocrinology 103(3–4):335–344.

5.1 Supplementary data

Supplementary data to this article can be found online at *https://doi.org/10.1016/j.molmet.2020.100978.*

The supplementary data to this article consists of:

Supplementary Table 1

Supplementary Table 2

Supplementary Table 3

Supplementary Table 4

Supplementary Table 5

Supplementary Table 6

Supplementary Figure 1

Supplementary Figure 2

Supplementary Figure 3

Due to the size of the Supplementary Tables, only Supplementary Table 2 and the Supplementary Figures are included in this version. The Supplementary Tables 1,3,4,5 and 6 can be accessed via the link above.

Supplementary Table 2: Addition to Supplementary Figures 1 and 2. List of metabolites measured with the Absolute*IDQ*® p180 Kit GAC.

Acylcarnitines (40)			
C0	Carnitine	C10:1	Decenoylcarnitine
C2	Acetylcarnitine	C10:2	Decadienylcarnitine
C3	Propionylcarnitine	C12	Dodecanoylcarnitine
C3:1	Propenoylcarnitine	C12:1	Dodecenoylcarnitine
C3-OH	Hydroxypropionylcarnitine	C12-DC	Dodecanedioylcarnitine
C4	Butyrylcarnitine	C14	Tetradecanoylcarnitine
C4:1	Butenoylcarnitine	C14:1	Tetradecenoylcarnitine
C4-OH (C3-DC)	Hydroxybutyrylcarnitine	C14:1-OH	Hydroxytetradecenoylcarnitine
C5	Valerylcarnitine	C14:2	Tetradecadienylcarnitine
C5:1	Tiglylcarnitine	C14:2-OH	Hydroxytetradecadienylcarnitine
C5:1-DC	Glutaconylcarnitine	C16	Hexadecanoylcarnitine
C5-DC (C6-OH)	Glutarylcarnitine (Hydroxyhexanoylcarnitine)	C16:1	Hexadecenoylcarnitine
C5-M-DC	Methylglutarylcarnitine	C16:1-OH	Hydroxyhexadecenoylcarnitine
C5-OH (C3-DC-M)	Hydroxyvalerylcarnitine (Methylmalonylcarnitine)	C16:2	Hexadecadienylcarnitine
C6 (C4:1-DC)	Hexanoylcarnitine (Fumarylcarnitine)	C16:2-OH	Hydroxyhexadecadienylcarnitine
C6:1	Hexenoylcarnitine	C16-OH	Hydroxyhexadecanoylcarnitine
C7-DC	Pimelylcarnitine	C18	Octadecanoylcarnitine
C8	Octanoylcarnitine	C18:1	Octadecenoylcarnitine
C9	Nonanoylcarnitine	C18:1-OH	Hydroxyoctadecenoylcarnitine
C10	Decanoylcarnitine	C18:2	Octadecadienylcarnitine
Amino Acids (21)			
Ala	Alanine	Lys	Lysine
Arg	Arginine	Met	Methionine
Asn	Asparagine	Orn	Ornithine
Asp	Aspartate	Phe	Phenylalanine
Cit	Citrulline	Pro	Proline
Gln	Glutamine	Ser	Serine
Glu	Glutamate	Thr	Threonine
Gly	Glycine	Trp	Tryptophan
His	Histidine	Tyr	Tyrosine
Ile	Isoleucine	Val	Valine
Leu	Leucine		
Monosaccharides (1)			
Sum of Hexoses (including Glucose)			
Glycerophospholipids (90)			
lysoPC a C14:0	PC aa C34:1	PC aa C42:0	PC ae C38:2
lysoPC a C16:0	PC aa C34:2	PC aa C42:1	PC ae C38:3

lysoPC a C16:1	PC aa C34:3	PC aa C42:2	PC ae C38:4
lysoPC a C17:0	PC aa C34:4	PC aa C42:4	PC ae C38:5
lysoPC a C18:0	PC aa C36:0	PC aa C42:5	PC ae C38:6
lysoPC a C18:1	PC aa C36:1	PC aa C42:6	PC ae C40:1
lysoPC a C18:2	PC aa C36:2	PC ae C30:0	PC ae C40:2
lysoPC a C20:3	PC aa C36:3	PC ae C30:1	PC ae C40:3
lysoPC a C20:4	PC aa C36:4	PC ae C30:2	PC ae C40:4
lysoPC a C24:0	PC aa C36:5	PC ae C32:1	PC ae C40:5
lysoPC a C26:0	PC aa C36:6	PC ae C32:2	PC ae C40:6
lysoPC a C26:1	PC aa C38:0	PC ae C34:0	PC ae C42:0
lysoPC a C28:0	PC aa C38:1	PC ae C34:1	PC ae C42:1
lysoPC a C28:1	PC aa C38:3	PC ae C34:2	PC ae C42:2
PC aa C24:0	PC aa C38:4	PC ae C34:3	PC ae C42:3
PC aa C26:0	PC aa C38:5	PC ae C36:0	PC ae C42:4
PC aa C28:1	PC aa C38:6	PC ae C36:1	PC ae C42:5
PC aa C30:0	PC aa C40:1	PC ae C36:2	PC ae C44:3
PC aa C30:2	PC aa C40:2	PC ae C36:3	PC ae C44:4
PC aa C32:0	PC aa C40:3	PC ae C36:4	PC ae C44:5
PC aa C32:1	PC aa C40:4	PC ae C36:5	PC ae C44:6
PC aa C32:2	PC aa C40:5	PC ae C38:0	
PC aa C32:3	PC aa C40:6	PC ae C38:1	
Sphingolipids (15)			
SM (OH) C14:1	SM C18:0	SM (OH) C22:1	SM (OH) C24:1
SM C16:0	SM C18:1	SM (OH) C22:2	SM C26:0
SM C16:1	SM C20:2	SM C24:0	SM C26:1
SM (OH) C16:1	SM C22:3	SM C24:1	
Biogenic Amines (21)			
Ac-Orn	Acetylornithine	PEA	Phenylethylamine
ADMA	Asymmetric dimethylarginine	*cis*-OH-Pro	*cis*-4-Hydroxyproline
alpha-AAA	alpha-Aminoadipic acid	*trans*-OH-Pro	*trans*-4-Hydroxyproline
Carnosine	Carnosine	Putrescine	Putrescine
Creatinine	Creatinine	SDMA	Symmetric dimethylarginine
DOPA	DOPA	Serotonin	Serotonin
Dopamine	Dopamine	Spermidine	Spermidine
Histamine	Histamine	Spermine	Spermine
Kynurenine	Kynurenine	Taurine	Taurine
Met-SO	Methionine sulfoxide	total DMA	Total dimethylarginine
Nitro-Tyr	Nitrotyrosine		

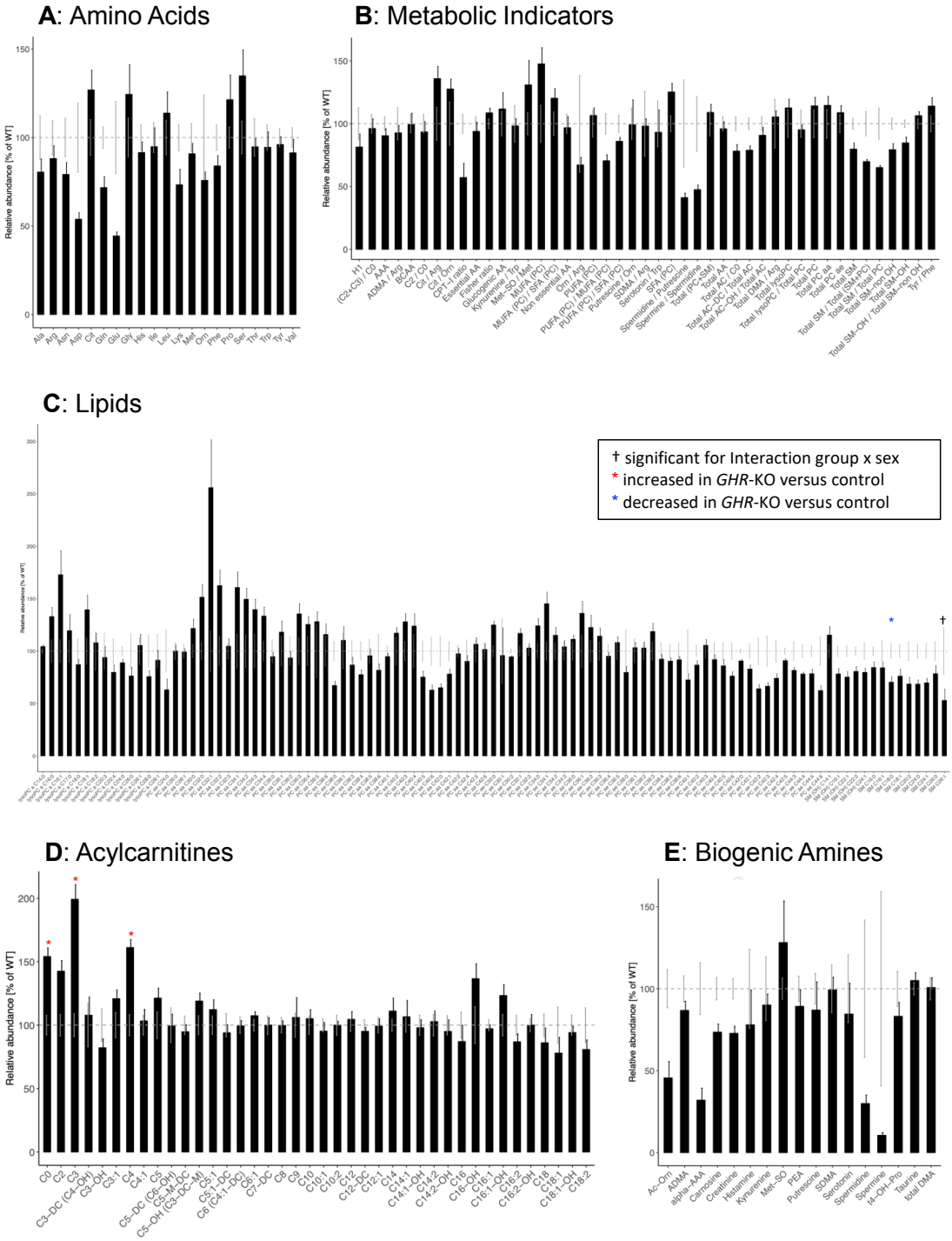

Supplementary Figure 1: Relative abundance changes of metabolites in *GHR*-KO and control serum samples. Graphs show the relative abundances of amino acids (A), metabolic indicators (B), lipids (C), acylcarnitines (D), and biogenic amines (E) determined by targeted metabolomics. The dashed line indicates the mean abundance of the control samples, bars show the mean relative abundance in *GHR*-KO samples. Error bars represent the standard error of the mean (SEM).

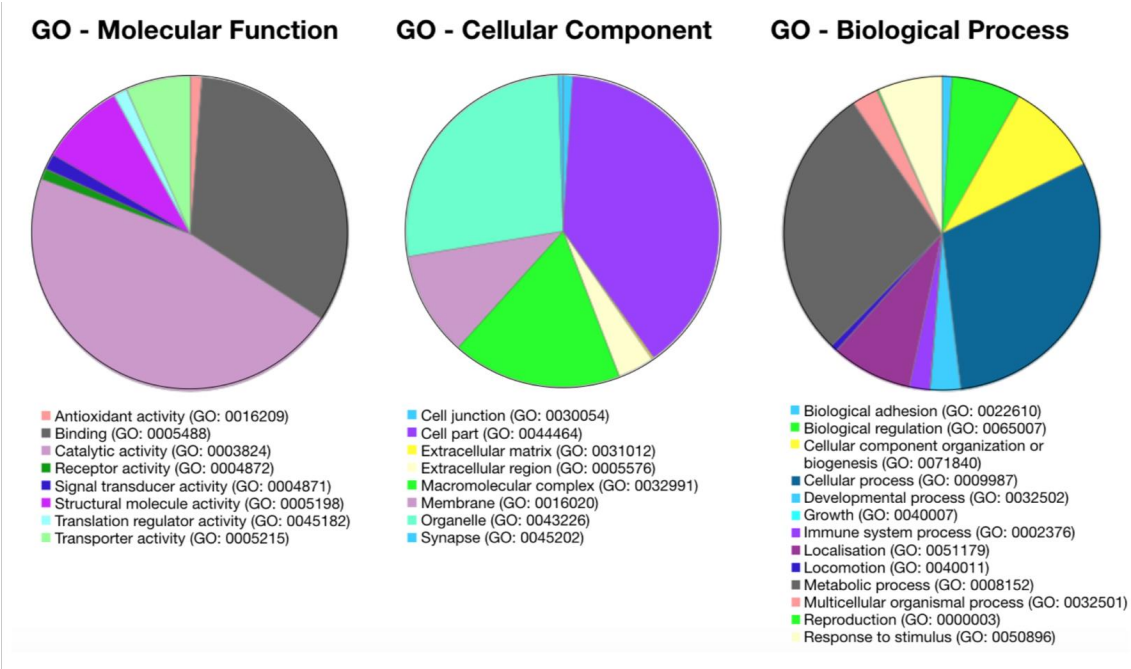

Supplementary Figure 2: GO-Analysis of the 3232 detected protein families (see also Supplementary Table 1A) measured with QExactive (Thermo Scientific) using PANTHER (pantherdb.org).

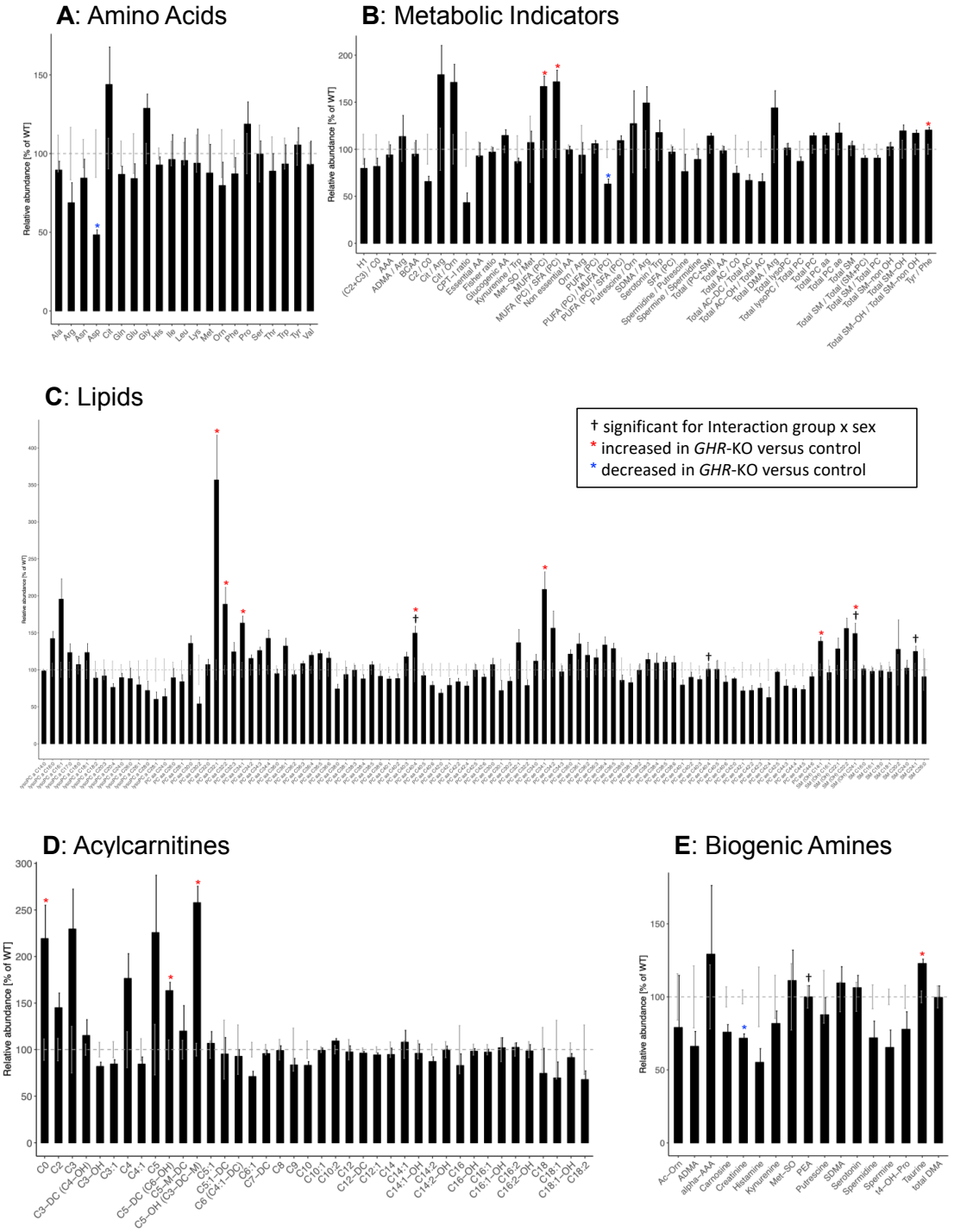

Supplementary Figure 3: Relative abundance changes of metabolites in *GHR*-KO vs. control liver tissue. Graphs show the relative abundances of amino acids (A), metabolic indicators (B), lipids (C), acylcarnitines (D), and biogenic amines (E) determined by targeted metabolomics. The dashed line indicates the mean abundance of the control samples, bars show the mean relative abundance in *GHR*-KO samples. Error bars represent the standard error of the mean (SEM).

6. Paper II

Xenotransplantation. 2021 Mar;28(2):e12664. doi: 10.1111/xen.12664. Epub 2020 Nov 25.

Growth hormone receptor knockout to reduce the size of donor pigs for preclinical xenotransplantation studies

Arne Hinrichs [1,2,*], Evamaria O Riedel [3,*], Nikolai Klymiuk [1,2], Andreas Blutke [4], Elisabeth Kemter [1,2], Matthias Längin [5], Maik Dahlhoff [1], Barbara Keßler [1,2], Mayuko Kurome [1,2], Valeri Zakhartchenko [1,2], Eva-Maria Jemiller [1,2], David Ayares [6], Martin Bidlingmaier [7], Florian Flenkenthaler [3], Martin Hrabě de Angelis [4], Georg J Arnold [3], Bruno Reichart [8], Thomas Fröhlich [3,°], Eckhard Wolf [1,2,3,°]

Affiliations

[1] Department of Veterinary Sciences, Chair for Molecular Animal Breeding and Biotechnology, Gene Center, LMU Munich, Munich, Germany. [2] Center for Innovative Medical Models (CiMM), LMU Munich, Munich, Germany. [3] Laboratory for Functional Genome Analysis (LAFUGA), Gene Center, LMU Munich, Munich, Germany. [4] Institute of Experimental Genetics, Helmholtz Zentrum München, Chair of Experimental Genetics, Technical University of Munich, Neuherberg, Germany. [5] Department of Anaesthesiology, University Hospital, LMU Munich, Munich, Germany. [6] Revivicor Inc., Blacksburg, VA, USA. [7] Medizinische Klinik und Poliklinik IV, Klinikum der Universität München, Munich, Germany. [8] Walter Brendel Center for Experimental Medicine, LMU Munich, Munich, Germany.

* Arne Hinrichs and Evamaria O. Riedel equal first author contribution

° Thomas Fröhlich and Eckhard Wolf equal last author contribution

PMID: 33241624 DOI: 10.1111/xen.12664

Abstract

Background: Many genetically multi-modified donor lines for xenotransplantation have a background of domestic pigs with rapid body and organ growth. The intrinsic growth potential of porcine xeno-organs may impair their long-term function after orthotopic transplantation in non-human primate models. Since growth hormone is a major stimulator of postnatal growth, we deleted its receptor (*GHR*-KO) to reduce the size of donor pigs in one step.

Methods: Heart weight and proteome profile of myocardium were investigated in *GHR*-KO and control pigs. *GHR*-KO mutations were introduced using CRISPR/Cas9 in an α1,3-galactosyltransferase (GGTA1)-deficient background expressing the human cluster of differentiation (hCD46) and human thrombomodulin (hTHBD) to generate quadruple-modified (4GM) pigs.

Results: At age 6 months, *GHR*-KO pigs had a 61% reduced body weight and a 63% reduced heart weight compared with controls. The mean minimal diameter of cardiomyocytes was 28% reduced. A holistic proteome study of myocardium samples from the two groups did not reveal prominent differences. Two 4GM founder sows had low serum insulin-like growth factor 1 (IGF1) levels (24 ± 1 ng/mL) and reached body weights of 70.3 and 73.4 kg at 9 months. Control pigs with IGF1 levels of 228 ± 24 ng/mL reached this weight range three months earlier. The 4GM sows showed normal sexual development and were mated with genetically multi-modified boars. Offspring revealed the expected Mendelian transmission of the genetic modifications and consistent expression of the transgenes.

Conclusion: *GHR*-KO donor pigs can be used at an age beyond the steepest phase of their growth curve, potentially reducing the problem of xeno-organ overgrowth in preclinical studies.

Keywords: gene editing, growth hormone receptor, organ growth, pig.

Received: 21 September 2020 | Revised: 3 November 2020 | Accepted: 9 November 2020
DOI: 10.1111/xen.12664

ORIGINAL ARTICLE

Xenotransplantation WILEY

Growth hormone receptor knockout to reduce the size of donor pigs for preclinical xenotransplantation studies

Arne Hinrichs[1,2] | Evamaria O. Riedel[3] | Nikolai Klymiuk[1,2] | Andreas Blutke[4] | Elisabeth Kemter[1,2] | Matthias Längin[5] | Maik Dahlhoff[1] | Barbara Keßler[1,2] | Mayuko Kurome[1,2] | Valeri Zakhartchenko[1,2] | Eva-Maria Jemiller[1,2] | David Ayares[6] | Martin Bidlingmaier[7] | Florian Flenkenthaler[3] | Martin Hrabě de Angelis[4] | Georg J. Arnold[3] | Bruno Reichart[8] | Thomas Fröhlich[3] | Eckhard Wolf[1,2,3]

[1]Department of Veterinary Sciences, Chair for Molecular Animal Breeding and Biotechnology, Gene Center, LMU Munich, Munich, Germany

[2]Center for Innovative Medical Models (CiMM), LMU Munich, Munich, Germany

[3]Laboratory for Functional Genome Analysis (LAFUGA), Gene Center, LMU Munich, Munich, Germany

[4]Institute of Experimental Genetics, Helmholtz Zentrum München, Chair of Experimental Genetics, Technical University of Munich, Neuherberg, Germany

[5]Department of Anaesthesiology, University Hospital, LMU Munich, Munich, Germany

[6]Revivicor Inc., Blacksburg, VA, USA

[7]Medizinische Klinik und Poliklinik IV, Klinikum der Universität München, Munich, Germany

[8]Walter Brendel Center for Experimental Medicine, LMU Munich, Munich, Germany

Correspondence
Eckhard Wolf, Gene Center, LMU Munich, Feodor-Lynen-Str. 25, D-81377 Munich, Germany.
Email: ewolf@genzentrum.lmu.de

Present address
Nikolai Klymiuk, Professorship for Large Animals Models in Cardiovascular Research, Technical University of Munich, Munich, Germany

Abstract

Background: Many genetically multi-modified donor lines for xenotransplantation have a background of domestic pigs with rapid body and organ growth. The intrinsic growth potential of porcine xeno-organs may impair their long-term function after orthotopic transplantation in non-human primate models. Since growth hormone is a major stimulator of postnatal growth, we deleted its receptor (*GHR*-KO) to reduce the size of donor pigs in one step.

Methods: Heart weight and proteome profile of myocardium were investigated in *GHR*-KO and control pigs. *GHR*-KO mutations were introduced using CRISPR/Cas9 in an α1,3-galactosyltransferase (GGTA1)-deficient background expressing the human cluster of differentiation (hCD46) and human thrombomodulin (hTHBD) to generate quadruple-modified (4GM) pigs.

Results: At age 6 months, *GHR*-KO pigs had a 61% reduced body weight and a 63% reduced heart weight compared with controls. The mean minimal diameter of cardiomyocytes was 28% reduced. A holistic proteome study of myocardium samples from the two groups did not reveal prominent differences. Two 4GM founder sows had low serum insulin-like growth factor 1 (IGF1) levels (24 ± 1 ng/mL) and reached body weights of 70.3 and 73.4 kg at 9 months. Control pigs with IGF1 levels of 228 ± 24 ng/mL reached this weight range three months earlier. The 4GM sows showed normal sexual development and were mated with genetically multi-modified boars. Offspring revealed the expected Mendelian transmission of the genetic modifications and consistent expression of the transgenes.

Arne Hinrichs and Evamaria O. Riedel equal first author contribution.

Thomas Fröhlich and Eckhard Wolf equal last author contribution.

Maik Dahlhoff, Institute of in vivo and in vitro models, University of Veterinary Medicine Vienna, Vienna, Austria

Funding information
Deutsche Forschungsgemeinschaft, Grant/Award Number: HI 2206/2-1 and TRR 127

Conclusion: *GHR*-KO donor pigs can be used at an age beyond the steepest phase of their growth curve, potentially reducing the problem of xeno-organ overgrowth in preclinical studies.

KEYWORDS
gene editing, growth hormone receptor, organ growth, pig

1 | INTRODUCTION

Xenotransplantation of genetically modified pig hearts reached a milestone on the way to clinical trials by consistent long-term survival of orthotopic xenografts in baboons.[1,2] With hearts from α1,3-galactosyltransferase (GGTA1)-deficient pigs expressing the human cluster of differentiation 46 (hCD46) and human thrombomodulin (hTHBD), the recipients survived for up to 195 days. In addition to non-ischemic perfusion preservation of the donor heart and safe immunosuppression of the recipient baboon, post-transplantation growth control of the xenotransplant was essential. This was achieved by lowering the recipient's blood pressure, early weaning of cortisone, and temsirolimus treatment. Discontinuation of mechanistic target of rapamycin (mTOR) inhibition by temsirolimus resulted in immediate growth of the xeno-heart, limiting its function in the small chest of a baboon. The donor animals in these studies had a genetic background of domestic pigs (German Landrace/Large White) and had to be used at juvenile age to fit with the size of the recipient baboons. Continued organ growth has also been observed after allotransplantation of domestic pig kidneys into minipigs[3] or after xenotransplantation into baboons ([3-5]; reviewed in[6]). Pigs (and their organs) grow much faster than non-human primates. To overcome this physiological discrepancy, we sought a way to reduce by gene editing the size of xeno-organ donor pigs in one step.

Inactivation of the growth hormone receptor (*GHR*) gene appeared to be an attractive strategy since GHR-deficient mice are small, but fertile and have a prolonged life span.[7,8] Furthermore, GHR-deficient patients (Laron syndrome) are also small and have reduced risk to suffer from diabetes or malignancies.[9] We therefore generated GHR-deficient (*GHR*-KO) pigs, which exhibit low plasma insulin-like growth factor 1 (IGF1) levels and significantly reduced postnatal body and organ growth, but normal fertility.[10]

The aims of the present study were (a) to quantify effects of *GHR*-KO on cardiac growth parameters including morphometric studies of cardiomyocytes and (b) to screen by holistic label-free proteomics for molecular alterations of myocardium potentially affecting the function of GHR-deficient hearts. Furthermore, *GHR*-KO mutations were introduced into a *GGTA1*-KO, *hCD46/hTHBD* double-transgenic genetic background. The phenotype of two female quadruple-modified (4GM) founder pigs was compared with pigs carrying the *GHR*-KO mutation only. After mating with genetically multi-modified boars, the offspring were analyzed for the inheritance of the genetic modifications and for expression of the transgenes.

Our results suggest *GHR*-KO as a feasible strategy to reduce the size of organ donor pigs for preclinical xenotransplantation studies.

2 | METHODS

2.1 | Animal model and collection of heart muscle samples

All animal procedures were approved by the responsible animal welfare authority (Regierung von Oberbayern; permission ROB-55.2Vet-2532.Vet-02-17-136) and performed according to the German Animal Welfare Act and Directive 2010/63/EU on the protection of animals used for scientific purposes.

Six-month-old *GHR*-KO (4 males and 4 females) and GHR expressing control pigs ($GHR^{+/-}$, $GHR^{+/+}$; 2 males and 2 females per genotype)[10] were euthanized after overnight fasting. Heart muscle samples (left ventricle, right ventricle, ventricular septum) were taken according to a standardized protocol,[11,12] routinely fixed in formalin, and processed for paraffin histology, or shock frozen on dry ice and stored at −80°C.

2.2 | Histological measurements

The mean minimal diameters of cardiomyocytes were determined planimetrically (Videoplan-System, Zeiss-Kontron) in systematically randomly sampled fields of view in HE-stained paraffin sections of myocardium samples of the left ventricle (LV), the right ventricle (RV), and the ventricular septum (S). Measurements were performed in a blinded fashion, that is, the examiner was not aware of the genotype-affiliations of the examined sections. Per case, 318 ± 61 fiber profiles were analyzed.

2.3 | Proteomics

Pressure-assisted lysis and digestion of proteins were performed using a Barocycler 2320 EXT (Pressure BioSciences). For tissue lysis, 2 mg frozen muscle tissue, 20 µL 6 mol/L urea/100 mmol/L NH_4HCO_3 and 1:50 (enzyme:substrate) lysyl endopeptidase (Fujifilm Wako) were added to the microtubes closed with a micro-pestle. Subsequently, 90 cycles of 45 kpsi at 35°C were applied. Proteins were reduced at a final concentration of 4.5 mmol/L dithioerythritol

(DTE)/2 mmol/L tris(2-carboxyethyl)phosphine (TCEP) for 30 minutes at 56°C. Cysteine residues were blocked for 30 minutes in the dark at a final concentration of 8.3 mmol/L iodoacetamide. Samples were diluted to a concentration of 0.8 mol/L urea with 50 mmol/L NH_4HCO_3/10% n-propanol. For protein digestion, 1:50 (enzyme:substrate) porcine trypsin (Promega) was added to the microtubes closed with the microcaps. Subsequently, 90 cycles of 20 kpsi at 35°C were applied.

The LC-MS/MS system comprised an UltiMate™ 3000 RSLCnano chromatography system (Thermo Scientific) connected to a Q Exactive HF-X mass spectrometer (Thermo Scientific). One µg of peptides diluted in 0.1% formic acid (FA) was transferred to a 2-cm trap column (Acclaim® PepMap 100, 75 µm × 2 cm, nanoViper C18, 3 µm, 100 Å, Thermo Scientific) and separated using consecutive linear gradients at a flow rate of 250 nL/min on a 50-cm separation column (PepMap® RSLC, 75 µm × 50 cm, nanoViper C18, 2 µm, 100 Å, Thermo Scientific). The LC gradients were from 3% to 25% solvent B (0.1% FA, 100% acetonitrile (ACN)) in 160 minutes followed by 25% to 40% solvent B in 10 minutes, and 40% to 85% solvent B in 10 minutes. MS acquisition cycles comprised one full MS scan at a resolution of 60 000 and 15 data-dependent higher collision dissociation (HCD) MS/MS scans at a resolution of 15 000 and a collision energy of 28. The dataset was submitted to the ProteomeXchange Consortium via the PRIDE partner repository[13] with the identifier PXD019852.

For label-free quantification (LFQ),[14] data were processed using MaxQuant V1.6.2.10, Perseus V1.6.1.3, and the Sus scrofa subset of the NCBI database (NCBI RefSeq Sus scrofa Annotation Release 106 Sscrofa 11.1). As parameters for identification (false discovery rate < 0.01), we used trypsin as enzyme, a mass tolerance of the precursor of 10 ppm, a MS/MS mass tolerance of 0.02 Da, carbamidomethylation of cysteine as fixed modification and oxidized methionine as variable modifications. In cases where proteins were detected in all replicates of one group, but in no replicate of the other group, the MaxQuant imputation feature was applied to allow statistical evaluation. Hierarchical clustering, 2D principal component analysis, and volcano plot analysis were carried out using the algorithms implemented in Perseus.[15]

2.4 | Generation of *GHR*-KO, *GGTA1*-KO, and *hCD46/hTHBD* double-transgenic (4GM) pigs

Primary kidney cells were isolated from a female *GGTA1*$^{-/-}$, *hCD46/hTHBD* double-transgenic pig (both transgenes hemizygous). This triple-modified background is based on a transgene locus with multiple copies of an *hCD46* minigene,[16] which was crossed on a *GGTA1*$^{-/-}$ genetic background[17]; later an expression cassette for hTHBD under the transcriptional control of a porcine *THBD* regulatory sequence was added.[18] The multicopy *hCD46* cluster was localized by fluorescence *in situ* hybridization (FISH) analysis (Cell Line Genetics) on chromosome 18q11, which was confirmed by targeted locus amplification (TLA) technology (Cergentis). The transgene integration site of *hTHBD* was revealed by nanopore sequencing (Oxford Nanopore Technologies) on chromosome 9, 73.189 Mb (Sscrofa 11.1. reference genome), in the intronic region between exons 20 and 21 of the *VPS50* gene. Triple-modified cells were co-transfected using a Cas9 expression plasmid (CMV-Cas9[19]) and a plasmid transcribing the ttcatgccactggacaGAtgGGG gRNA (PAM underlined), specific for the porcine *GHR* exon 3. Single-cell clones were produced; PCR products from the porcine *GHR* gene were amplified with the primer pair 5′-gcacacttcagatgctacctaa and 5′-cacatgctcaccctcagatac; Sanger sequencing of the PCR product was performed and analyzed for frameshift mutations by bi-directional Sanger sequencing, using the primers 5′-accgctctgaagctgtgacc and 5′-caggagaccagagacctatct. A cell clone carrying a bi-allelic constellation of deleterious mutations was used for somatic cell nuclear transfer (SCNT).[20]

Recipient gilts were synchronized in the estrous cycle by oral administration of 20 mg Altrenogest (Regumate®; MSD Animal Health) per day for 15 days, followed by intramuscular injection of 150 µg Peforelin (Maprelin®; Provet AG) and 750 IU HCG (Ovogest®; MSD Animal Health) after additional 24 and 104 hours, respectively. Embryo transfer was performed laparoscopically into one oviduct.[20] Pregnancy was confirmed by ultrasonographic examination first on day 21 and again 4-6 weeks later.

Genomic DNA was isolated from tail tips of piglets using the Wizard DNA Extraction Kit (Promega). *GHR* mutations were detected by sequencing a *GHR* exon 3 PCR product obtained using primers GHR_Fw 5′-acc gct ctg aag ctg tga cc-3′ and GHR_Rv 5′-cac cct cag ata ctc tca tgc-3′. Based on the detected mutations, an *Xcm*I restriction fragment length polymorphism assay was established, yielding fragments of 203 bp and 441 bp for wild-type *GHR* and a single fragment of 644 bp for the mutated *GHR* sequence.

2.5 | Immunohistochemistry

Tissue samples were fixed in 4% formalin overnight and paraffin-embedded; 3-µm sections were cut and dried. Heat-induced antigen retrieval was performed in Target Retrieval solution (S1699, DAKO) in a boiling water bath for 20 minutes (hCD46, αGal) or in citrate buffer, pH 6.0, in a steamer for 45 minutes (hTHBD). Immunohistochemistry was performed using the following primary antibodies: mouse anti-human CD46 monoclonal antibody (HM2103, Hycult Biotech), mouse anti-human thrombomodulin monoclonal antibody (sc-13164, Santa Cruz), and mouse anti-αGal IgM (Alx 801-090, Alexis). As secondary antibodies, biotinylated AffiniPure goat anti-mouse IgG (115-065-146, Jackson ImmunoResearch) or biotinylated goat anti-mouse IgM (BA-2020, Vector) were used. Immunoreactivity was visualized using the Vectastain® Elite ABC-HRP Kit (Vector) and 3,3′-diaminobenzidine tetrahydrochloride dihydrate (DAB) as chromogen (brown color). Nuclear counterstaining was done with hemalum (blue color).

2.6 | Quantification of serum IGF1 levels

IGF1 concentrations were measured using the iSYS automated chemiluminescent IGF1 assay (Immunodiagnostic Systems) as described previously.[21,22]

2.7 | Statistical analysis

Statistical analyses were performed using R[23] with the qvalue package and SAS (SAS Institute) as well as GraphPad Prism (GraphPad Software). Visualizations were performed using R with the ggplot2[24] and pheatmap packages and GraphPad Prism. Effects of group (*GHR*-KO, control), sex, and the interaction group × sex were evaluated using two-way ANOVA.

3 | RESULTS

3.1 | Body weight, heart weight, and cardiomyocyte diameter

At age 6 months, *GHR*-KO pigs had a 61% reduced body weight (Figure 1A; $P < .0001$) and a 63% reduced heart weight compared with controls (Figure 1B; $P < .0001$). The relative heart weight was not different between the two groups (Figure 1C). The mean minimal diameter of cardiomyocytes was 28% reduced in *GHR*-KO vs control pigs (Figure 1D; $P < .001$). Representative histological sections of myocardium are shown in Figure 1E. None of these parameters was significantly influenced by the animal sex.

3.2 | Proteome findings in myocardium

In total, 1,642 protein groups at a false discovery rate (FDR) < 0.01 could be identified. All detected proteins are listed in Table S1A. As a quality control and to check the reproducibility of the approach, multi-scatterplots of MaxQuant intensity values were generated. Mean Pearson correlation coefficients of >0.94 within group were obtained, demonstrating the reproducibility of the results (Figure S1). $GHR^{+/-}$ and $GHR^{+/+}$ animals were pooled as control group, since neither phenotypical analysis[10] nor proteome profiling of the liver[25] did show significant differences between these genotypes.

When comparing the quantitative proteome profiles of myocardium samples from *GHR*-KO (4 males and 4 females) and control pigs (4 males and 4 females), neither principal component analysis (Figure 2A) nor hierarchical clustering did result in defined clusters (Figure 2B) indicating no major aberration in the myocardium proteome as a consequence of GHR deficiency. Furthermore, statistical analysis of the proteome data using a two-way ANOVA (group × sex) identified no protein groups that were significantly ($P < 0.05$) altered in abundance by group, sex or by the interaction group × sex (Table S1B). However, a less stringent volcano plot analysis of *GHR*-KO vs WT proteomes, where data were analyzed

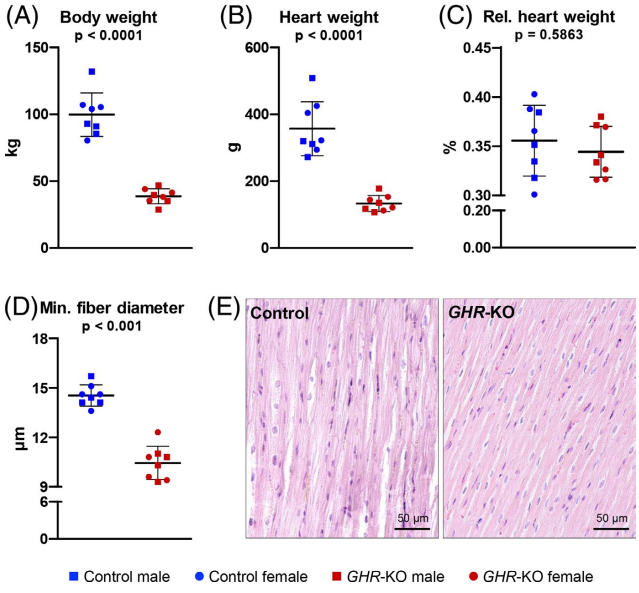

FIGURE 1 Body weights and heart weights of 6-month-old *GHR*-KO pigs (4 males and 4 females) and controls (4 males and 4 females). A, Body weight; B, Heart weight; C, Relative heart weight; D, Mean minimal diameter of cardiomyocytes; E, Representative histological sections of myocardium. *P*-values are from two-way ANOVA for the effect of group (*GHR*-KO, control). Sex and the interaction group × sex had no significant effect

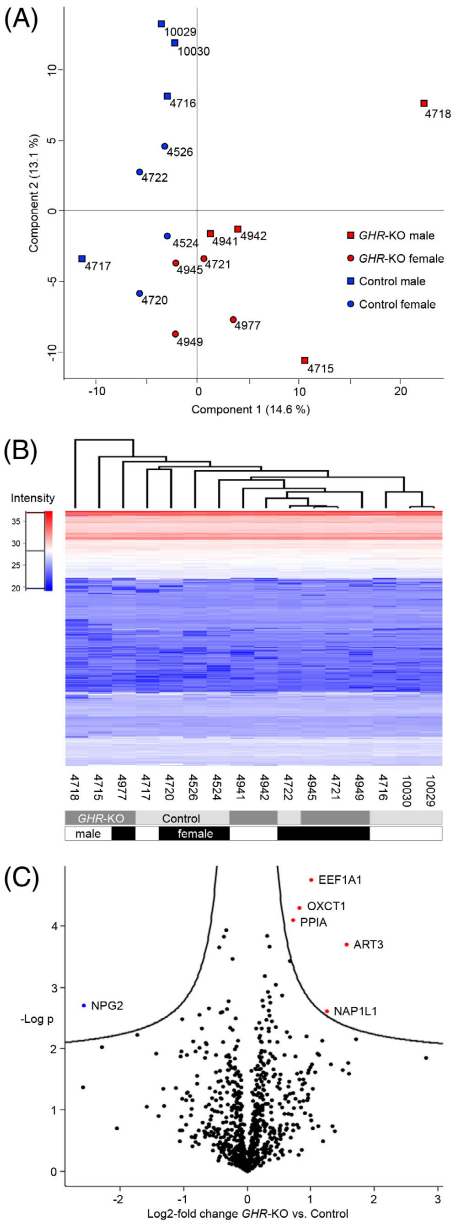

FIGURE 2 Proteomics of myocardium samples from 6-month-old *GHR*-KO pigs and controls. A, Principal component analysis (PCA); B, Heat map; C, Volcano plot. Proteins with significant abundance changes (FDR < 0.05) are labeled: ART3 = ecto-ADP-ribosyltransferase 3; EEF1A1 = elongation factor 1-alpha; NAP1L1 = nucleosome assembly protein 1-like 1; NPG2 = protegrin-2; OXCT13 = oxoacid CoA-transferase 1; PPIA = peptidylprolyl isomerase A. The 4- and 5-digit numbers are individual animal numbers.

without considering the gender, revealed 5 proteins with increased and one protein with reduced abundance in *GHR*-KO vs control myocardium (Figure 2C).

3.3 | *GHR*-KO pigs with a *GGTA1*-KO, *hCD46/hTHBD* double-transgenic background

A *GGTA1*-KO, *hCD46/hTHBD* double-transgenic cell clone with frameshift mutations in both alleles of the *GHR* gene (Figure 3A) was selected for SCNT. The frameshift mutations result in premature stop codons (Figure 3B) and the complete absence of GHR. After transfer of SCNT embryos to recipients, four piglets were born. Two of them died on the first postnatal day; the other two pigs were raised to adulthood without clinical problems (Figure 3C). These exhibited the characteristic phenotype of GHR deficiency and reduced serum IGF1 levels (24 ± 1 ng/mL; mean ± SEM), comparable to *GHR*-KO 1GM pigs (23 ± 5 ng/mL). Serum IGF1 levels of contemporary wild-type pigs were 215 ± 58 ng/mL (Figure 3D). At 9 months, the body weights of the 4GM pigs were 70.3 and 73.4 kg, while wild-type pigs reached this weight range three months earlier. The two 4GM sows showed normal sexual development and were mated with genetically multi-modified boars. The resulting offspring showed the expected Mendelian segregation of the genetic modifications (Figure 3E). Immunohistochemical analysis of myocardium from a $GHR^{+/-}$, $GGTA1^{-/-}$, *hCD46/hTHBD* double-transgenic pig (Figure 3F) and of ear skin samples from the 4GM founder pigs (Figure S2) revealed the absence of αGal epitopes and consistent expression of hCD46 and hTHBD.

4 | DISCUSSION

For a number of reasons, including anatomical and physiological similarities with humans, the possibility of efficient and precise genetic engineering, and maintenance under designated pathogen-free conditions, pigs have become the most likely donors of cells, tissues, and organs for xenotransplantation (reviewed in[26]). Many genetically multi-modified pig lines have been established on the background of domestic pigs, which have been selected for decades to maximize growth rate and feed efficiency. As a consequence, the growth rates of porcine organs do not fit with the requirements of non-human primates used as recipients in preclinical xenotransplantation experiments. Even for humans, organs from domestic pigs may grow too large. One possibility to overcome this problem is the use of minipig lines, which may have other drawbacks, for example, high copy numbers of porcine endogenous retroviruses (PERV)[27] or insufficient organ sizes for adult human recipients. Another possibility is genetic engineering of domestic pigs to reduce their growth rate.

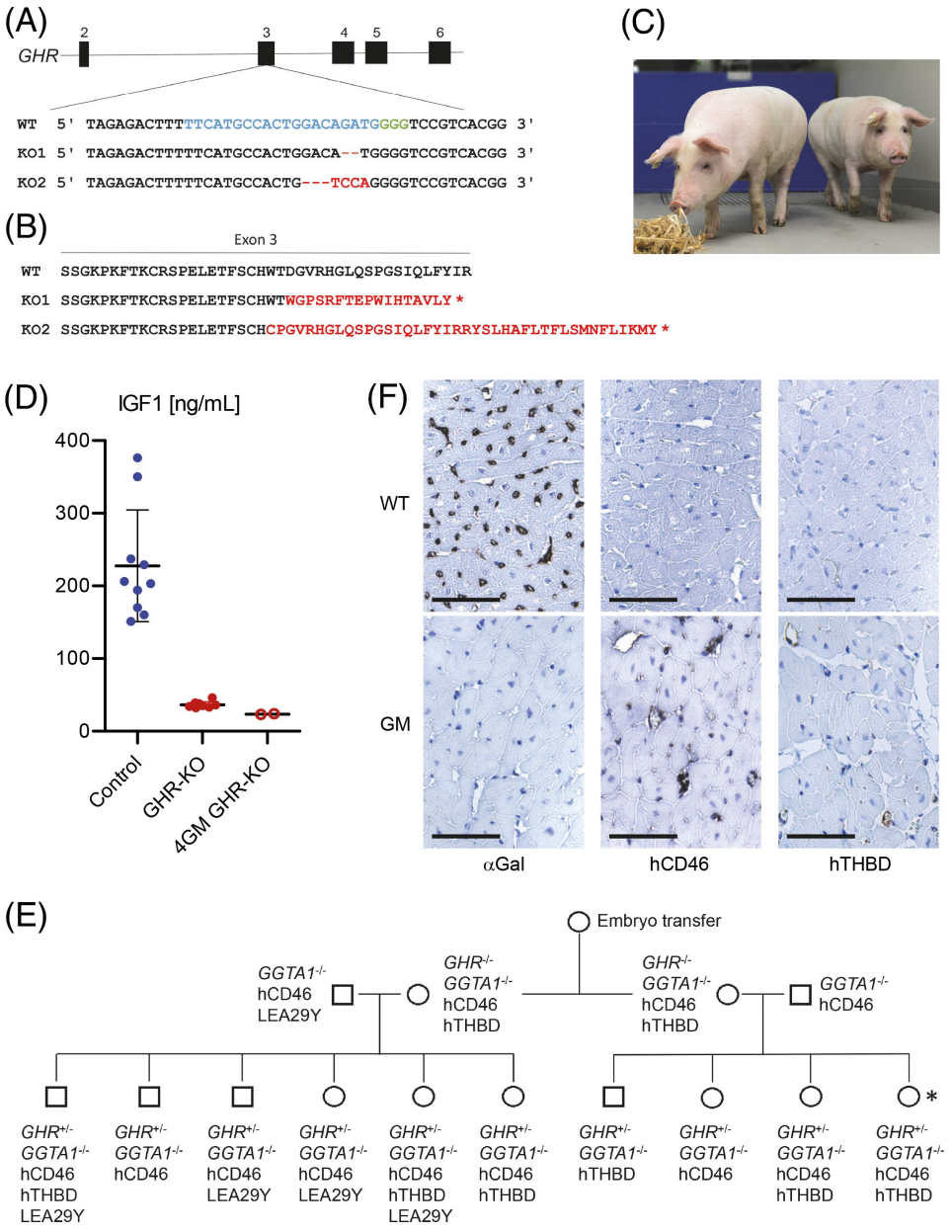
(A)
GHR
2
3
4
5
6
WT 5' TAGAGACTTTTTCATGCCACTGGACAGATGGGGTCCGTCACGG 3'
KO1 5' TAGAGACTTTTTCATGCCACTGGACA--TGGGGTCCGTCACGG 3'
KO2 5' TAGAGACTTTTTCATGCCACTG---TCCAGGGGTCCGTCACGG 3'
(B)
Exon 3
WT SSGKPKFTKCRSPELETFSCHWTDGVRHGLQSPGSIQLFYIR
KO1 SSGKPKFTKCRSPELETFSCHWTWGPSRFTEPWIHTAVLY*
KO2 SSGKPKFTKCRSPELETFSCHCPGVRHGLQSPGSIQLFYIRRYSLHAFLTFLSMNFLIKMY*
(C)
(D)
IGF1 [ng/mL]
400
300
200
100
0
Control
GHR-KO
4GM GHR-KO
(F)
WT
GM
αGal
hCD46
hTHBD
(E)
Embryo transfer
GGTA1-/-
hCD46
LEA29Y
GHR-/-
GGTA1-/-
hCD46
hTHBD
GHR-/-
GGTA1-/-
hCD46
hTHBD
GGTA1-/-
hCD46
GHR+/-
GGTA1-/-
hCD46
hTHBD
LEA29Y
GHR+/-
GGTA1-/-
hCD46
GHR+/-
GGTA1-/-
hCD46
LEA29Y
GHR+/-
GGTA1-/-
hCD46
LEA29Y
GHR+/-
GGTA1-/-
hCD46
hTHBD
LEA29Y
GHR+/-
GGTA1-/-
hCD46
hTHBD
GHR+/-
GGTA1-/-
hTHBD
GHR+/-
GGTA1-/-
hCD46
GHR+/-
GGTA1-/-
hCD46
hTHBD
GHR+/-
GGTA1-/-
hCD46
hTHBD
*

FIGURE 3 *GHR*-KO pigs with a *GGTA1*-KO, *hCD46/hTHBD* double-transgenic background (4GM). A, Frameshift mutations introduced in exon 3 of the *GHR* gene. B, Premature stop codons (*) resulting from the frameshift mutations. C, Female 4GM founder pigs. D, Serum IGF1 concentrations. E, Pedigrees resulting from mating of the 4GM founder sows with genetically multi-modified boars. Transgenic animals with *hTHBD*[18] and *LEA29Y*[47] are hemizygous, those with hCD46 are hemizygous (founder generation) or either hemi- or homozygous (offspring). F, Immunohistochemical staining of αGal, hCD46 and hTHBD in myocardium samples from a $GHR^{+/-}$, *GGTA1*-KO, *hCD46/hTHBD* double-transgenic pig (GM; labeled with an asterisk in panel E) and a wild-type control (WT). Bars = 50 μm

Growth hormone is the major stimulator of postnatal body and organ growth. Excess GH with juvenile or adult onset causes gigantism or acromegaly, respectively (reviewed in[28]), whereas deficiency of GH or its receptor results in reduced body and organ growth (reviewed in[29]). To reduce the size of organ donor pigs, we decided to inactivate the *GHR* gene since the consequences of this condition have been extensively studied in systemic and tissue-specific *Ghr* knockout mice (reviewed in[30,31]) and in GHR-deficient patients (Laron syndrome) (reviewed in[29,32]).

To characterize the consequences of GHR deficiency in pigs, we introduced frameshift mutations in exon 3 of the porcine *GHR* gene using CRISPR/Cas9.[10] *GHR*-KO pigs resemble the phenotype of human Laron syndrome, including low IGF1 levels, reduced postnatal body and organ growth, an increased proportion of body fat, but no pathological alterations of the blood lipid levels. Moreover, *GHR*-KO pigs are fertile.[10] Significantly reduced body and heart weights of *GHR*-KO pigs were confirmed in a different set of animals in the present study. In addition, the mean minimal diameter of cardiomyocytes was determined, revealing significantly reduced values for *GHR*-KO pigs, which explain—at least in part—their smaller heart size and weight.

A holistic proteome analysis of myocardium samples was performed to screen for prominent molecular changes potentially caused by GHR deficiency. In contrast to liver samples from the same set of animals, where multiple proteome differences between *GHR*-KO and control pigs were revealed,[25] the myocardial proteome profiles did not clearly cluster according to group or sex. Furthermore, two-way ANOVA did not identify proteins whose abundance was significantly affected by group, sex, or the interaction group × sex. However, a less stringent *t* test based volcano plot analysis revealed 6 proteins with significant abundance differences between myocardium samples from *GHR*-KO vs control pigs.

Increased in abundance were the enzymes ecto-ADP-ribosyltransferase 3 (ART3, reviewed in[33]), 3-oxoacid CoA-transferase 1 (OXCT1, reviewed in[34]) and peptidylprolyl isomerase A (PPIA, reviewed in[35]) as well as elongation factor 1-alpha (EEF1A1, reviewed in[36]) and nucleosome assembly protein 1-like 1 (NAP1L1, reviewed in[37]). Exclusively protegrin-2 (NPG2), a leukocyte-derived peptide with antimicrobial activity,[38] was found to be significantly decreased in *GHR-KO* myocardium. However, none of these proteins is specifically expressed in the myocardium or directly involved in heart contraction. Moreover, none of these proteins is known to be directly regulated by or involved in GH/IGF1 pathways in the heart.

In contrast to the subtle proteome changes in myocardium, there were prominent differences between liver samples of *GHR*-KO and control pigs (same set of animals).[25] Specifically, GHR deficiency resulted in an increased abundance of enzymes involved in amino acid degradation, in the urea cycle, and in the tricarboxylic acid cycle. Additional analyses of acylcarnitine profiles provided evidence for reduced mitochondrial import of fatty acids for beta-oxidation. Moreover, the abundances of several proteins functionally linked to non-alcoholic fatty liver disease (fetuin B, retinol-binding protein 4, and several mitochondrial proteins) were increased. In addition, distinct changes in the methionine and glutathione metabolic pathways were noted. These findings underline the central role of GH to regulate multiple metabolic pathways in the liver (reviewed in[39,40]).

IGF1 is involved in multiple processes in the heart, including contractility, metabolism, hypertrophy, autophagy, senescence, and apoptosis. Moreover, low IGF1 levels are associated with an increased risk of cardiovascular disease (reviewed in[41]). A holistic proteome study of myocardium from GHR-deficient individuals with low IGF1 levels has to our knowledge not been performed. Our proteomics data did not provide evidence for substantial molecular changes in the myocardium of *GHR*-KO pigs, which would indicate developmental disturbances or functional abnormalities of the heart. However, the animals were only 6 months old, and it will be important to monitor cardiac function of older *GHR*-KO pigs in the future. Notably, a cardiac-specific inducible knockout of *Ghr* in 4-month-old mice did not affect heart function, as revealed by baseline and post-dobutamine stress test echocardiography and by longitudinal blood pressure measurements.[42] Patients with Laron syndrome were shown to have reduced cardiac dimensions and output but normal left ventricular (LV) ejection fraction at rest and LV contractile reserve following stress.[43]

In our previous orthotopic xenotransplantation studies in baboons, we used donor pigs in the body weight range of 10-34 kg.[44] *GHR*-intact landrace hybrid pigs are in this weight range for less than 2 months (age 41-95 days), whereas *GHR*-KO pigs stay within this weight range for more than 3 months (age 81-181 days)[10] (Figure S3).

To generate small organ donor pigs, we introduced by CRISPR/Cas9 frameshift mutations in female *GGTA1*-KO, *hCD46/hTHBD* double-transgenic cells and used them for SCNT. The two resulting founder pigs with four genetic modifications (4GM) were phenotypically similar to *GHR*-KO 1GM pigs, for example, in postnatal growth rate and serum IGF1 levels. Both sows became sexually mature and were mated with genetically multi-modified boars. Genotyping of the offspring demonstrated the expected Mendelian segregation of the genetic modifications. One of the offspring was subjected to necropsy to evaluate the absence of αGal epitopes and the expression of hCD46 and hTHBD in heart and skin samples. The expression patterns of both transgenes were consistent with those reported for *GGTA1*-KO, *hCD46/hTHBD* double-transgenic pigs without *GHR*-KO.[1]

An open question is what will happen to a GHR-deficient organ if it is xenotransplanted into a host with normal IGF1 levels. Observations in liver-specific *Igf1* knockout mice suggest that local IGF1 levels (that would be low in a *GHR*-KO organ) are more important for organ growth than circulating IGF1, which is mainly derived from the liver.[45]

5 | CONCLUSION

In summary, *GHR*-KO appears to be a feasible approach to reduce the size of xeno-organ donor pig lines in one step without apparent deleterious effects on health and fertility. In addition to preclinical xenotransplantation experiments into non-human primates, this strategy may also be important to provide xeno-hearts for pediatric patients suffering from early onset dilated cardiomyopathy or severe congenital cardiac malformations (reviewed in[46]). A clear advantage of *GHR*-KO pigs is that the donors can be used at an older age when they have already passed the steepest phase of their growth curve.

ACKNOWLEDGMENTS

This study was supported by the Deutsche Forschungsgemeinschaft (TRR127, HI 2206/2-1). Oxford nanopore sequencing was performed by Stefan Krebs, Andreas Hauser, and Helmut Blum, Laboratory for Functional Genome Analysis (LAFUGA), Gene Center, LMU Munich. The authors gratefully acknowledge excellent technical support by Christina Blechinger, Christian Eckardt, Christian Erdle, Tuna Güngör, Sylvia Hering, Harald Paul, and Tatjana Schröter. Open access funding enabled and organized by Projekt DEAL.

CONFLICT OF INTEREST

David Ayares is chief executive officer and chief scientific officer of Revivicor Inc The other authors have no conflicts of interest to disclose.

ORCID

Arne Hinrichs https://orcid.org/0000-0003-3022-5983
Evamaria O. Riedel https://orcid.org/0000-0003-2259-9221
Nikolai Klymiuk https://orcid.org/0000-0003-3532-1659
Andreas Blutke https://orcid.org/0000-0001-7824-2681
Elisabeth Kemter https://orcid.org/0000-0001-7785-7502
Matthias Längin https://orcid.org/0000-0003-0996-4941
Maik Dahlhoff https://orcid.org/0000-0001-9189-7631
Barbara Keßler https://orcid.org/0000-0001-7036-238X
Mayuko Kurome https://orcid.org/0000-0002-2725-8613
Valeri Zakhartchenko https://orcid.org/0000-0002-5974-9759
David Ayares https://orcid.org/0000-0002-4638-3321
Martin Bidlingmaier https://orcid.org/0000-0002-4681-6668
Florian Flenkenthaler https://orcid.org/0000-0003-2964-9236
Martin Hrabě de Angelis https://orcid.org/0000-0002-7898-2353
Georg J. Arnold https://orcid.org/0000-0002-2716-0229
Bruno Reichart https://orcid.org/0000-0003-2859-3664
Thomas Fröhlich https://orcid.org/0000-0002-4709-3211
Eckhard Wolf https://orcid.org/0000-0002-0430-9510

REFERENCES

1. Längin M, Mayr T, Reichart B, et al. Consistent success in life-supporting porcine cardiac xenotransplantation. *Nature*. 2018;564(7736):430-433.
2. Reichart B, Längin M, Radan J, et al. Pig-to-non-human primate heart transplantation: The final step toward clinical xenotransplantation? *J Heart Lung Transplant*. 2020;39(8):751-757.
3. Tanabe T, Watanabe H, Shah JA, et al. Role of intrinsic (graft) versus extrinsic (host) factors in the growth of transplanted organs following allogeneic and xenogeneic transplantation. *Am J Transplant*. 2017;17(7):1778-1790.
4. Iwase H, Liu H, Wijkstrom M, et al. Pig kidney graft survival in a baboon for 136 days: longest life-supporting organ graft survival to date. *Xenotransplantation*. 2015;22(4):302-309.
5. Iwase H, Hara H, Ezzelarab M, et al. Immunological and physiological observations in baboons with life-supporting genetically engineered pig kidney grafts. *Xenotransplantation*. 2017;24(2):e12293.
6. Iwase H, Cooper DK. Growth hormone receptor knockout: relevance to xenotransplantation. *Xenotransplantation*. 2020; e12652 (accepted).
7. Zhou Y, Xu BC, Maheshwari HG, et al. A mammalian model for Laron syndrome produced by targeted disruption of the mouse growth hormone receptor/binding protein gene (the Laron mouse). *Proc Natl Acad Sci U S A*. 1997;94(24):13215-13220.
8. Coschigano KT, Clemmons D, Bellush LL, Kopchick JJ. Assessment of growth parameters and life span of GHR/BP gene-disrupted mice. *Endocrinology*. 2000;141(7):2608-2613.
9. Guevara-Aguirre J, Balasubramanian P, Guevara-Aguirre M, et al. Growth hormone receptor deficiency is associated with a major reduction in pro-aging signaling, cancer, and diabetes in humans. *Sci Transl Med*. 2011;3(70):70ra13.
10. Hinrichs A, Kessler B, Kurome M, et al. Growth hormone receptor-deficient pigs resemble the pathophysiology of human Laron syndrome and reveal altered activation of signaling cascades in the liver. *Mol Metab*. 2018;11:113-128.
11. Albl B, Haesner S, Braun-Reichhart C, et al. Tissue sampling guides for porcine biomedical models. *Toxicol Pathol*. 2016;44(3):414-420.
12. Blutke A, Renner S, Flenkenthaler F, et al. The munich MIDY pig biobank - a unique resource for studying organ crosstalk in diabetes. *Mol Metab*. 2017;6(8):931-940.
13. Perez-Riverol Y, Csordas A, Bai J, et al. The PRIDE database and related tools and resources in 2019: improving support for quantification data. *Nucleic Acids Res*. 2019;47(D1):D442-d450.
14. Cox J, Hein MY, Luber CA, Paron I, Nagaraj N, Mann M. Accurate proteome-wide label-free quantification by delayed normalization and maximal peptide ratio extraction, termed MaxLFQ. *Mol Cell Proteomics*. 2014;13(9):2513-2526.
15. Tyanova S, Temu T, Sinitcyn P, et al. The Perseus computational platform for comprehensive analysis of (prote)omics data. *Nat Methods*. 2016;13(9):731-740.
16. Loveland BE, Milland J, Kyriakou P, et al. Characterization of a CD46 transgenic pig and protection of transgenic kidneys against hyperacute rejection in non-immunosuppressed baboons. *Xenotransplantation*. 2004;11(2):171-183.
17. Phelps CJ, Koike C, Vaught TD, et al. Production of alpha 1,3-galactosyltransferase-deficient pigs. *Science*. 2003;299(5605):411-414.
18. Wuensch A, Baehr A, Bongoni AK, et al. Regulatory sequences of the porcine THBD gene facilitate endothelial-specific expression of bioactive human thrombomodulin in single- and multitransgenic pigs. *Transplantation*. 2014;97(2):138-147.
19. Mali P, Yang L, Esvelt KM, et al. RNA-guided human genome engineering via Cas9. *Science*. 2013;339(6121):823-826.
20. Kurome M, Kessler B, Wuensch A, Nagashima H, Wolf E. Nuclear transfer and transgenesis in the pig. *Methods Mol Biol*. 2015;1222:37-59.

21. Bidlingmaier M, Friedrich N, Emeny RT, et al. Reference intervals for insulin-like growth factor-1 (igf-i) from birth to senescence: results from a multicenter study using a new automated chemiluminescence IGF-I immunoassay conforming to recent international recommendations. *J Clin Endocrinol Metab*. 2014;99(5):1712-1721.
22. Hofmann I, Kemter E, Theobalt N, et al. Linkage between growth retardation and pituitary cell morphology in a dystrophin-deficient pig model of Duchenne muscular dystrophy. *Growth Horm IGF Res*. 2020;51:6-16.
23. Team RC. *R: A language and environment for statistical computing*. Vienna, Austria: R foundation for statistical computing. 2013.
24. Wickham H. *ggplot2: elegant graphics for data analysis*. New York: Springer; 2016.
25. Riedel EO, Hinrichs A, Kemter E, et al. Functional changes of the liver in the absence of growth hormone (GH) action - Proteomic and metabolomic insights from a GH receptor deficient pig model. *Mol Metab*. 2020;36:100978.
26. Kemter E, Schnieke A, Fischer K, Cowan PJ, Wolf E. Xeno-organ donor pigs with multiple genetic modifications - the more the better? *Curr Opin Genet Dev*. 2020;64:60-65.
27. Semaan M, Rotem A, Barkai U, Bornstein S, Denner J. Screening pigs for xenotransplantation: prevalence and expression of porcine endogenous retroviruses in *Göttingen minipigs*. *Xenotransplantation*. 2013;20(3):148-156.
28. Beckers A, Petrossians P, Hanson J, Daly AF. The causes and consequences of pituitary gigantism. *Nat Rev Endocrinol*. 2018;14(12):705-720.
29. Aguiar-Oliveira MH, Bartke A. Growth hormone deficiency: health and longevity. *Endocr Rev*. 2019;40(2):575-601.
30. List EO, Duran-Ortiz S, Kopchick JJ. Effects of tissue-specific GH receptor knockouts in mice. *Mol Cell Endocrinol*. 2020;515:110919.
31. Basu R, Qian Y, Kopchick JJ. Mechanisms in Endocrinology: lessons from growth hormone receptor gene-disrupted mice: are there benefits of endocrine defects? *Eur J Endocrinol*. 2018;178(5):R155-r181.
32. Laron Z. Lessons from 50 years of study of Laron syndrome. *Endocr Pract*. 2015;21(12):1395-1402.
33. Grahnert A, Grahnert A, Klein C, Schilling E, Wehrhahn J, Hauschildt S. Review: NAD+: a modulator of immune functions. *Innate Immun*. 2011;17(2):212-233.
34. Fukao T, Mitchell G, Sass JO, Hori T, Orii K, Aoyama Y. Ketone body metabolism and its defects. *J Inherit Metab Dis*. 2014;37(4):541-551.
35. Rostam MA, Piva TJ, Rezaei HB, et al. Peptidyl-prolyl isomerases: functionality and potential therapeutic targets in cardiovascular disease. *Clin Exp Pharmacol Physiol*. 2015;42(2):117-124.
36. Sasikumar AN, Perez WB, Kinzy TG. The many roles of the eukaryotic elongation factor 1 complex. *Wiley Interdiscip Rev RNA*. 2012;3(4):543-555.
37. Attia M, Rachez C, Avner P, Rogner UC. Nucleosome assembly proteins and their interacting proteins in neuronal differentiation. *Arch Biochem Biophys*. 2013;534(1–2):20-26.
38. Harwig SS, Swiderek KM, Lee TD, Lehrer RI. Determination of disulphide bridges in PG-2, an antimicrobial peptide from porcine leukocytes. *J Pept Sci*. 1995;1(3):207-215.
39. Vijayakumar A, Yakar S, Leroith D. The intricate role of growth hormone in metabolism. *Front Endocrinol (Lausanne)*. 2011;2:32.
40. Vijayakumar A, Novosyadlyy R, Wu Y, Yakar S, LeRoith D. Biological effects of growth hormone on carbohydrate and lipid metabolism. *Growth Horm IGF Res*. 2010;20(1):1-7.
41. Troncoso R, Ibarra C, Vicencio JM, Jaimovich E, Lavandero S. New insights into IGF-1 signaling in the heart. *Trends Endocrinol Metab*. 2014;25(3):128-137.
42. Jara A, Liu X, Sim D, et al. Cardiac-specific disruption of GH receptor alters glucose homeostasis while maintaining normal cardiac performance in adult male mice. *Endocrinology*. 2016;157(5):1929-1941.
43. Feinberg MS, Scheinowitz M, Laron Z. Echocardiographic dimensions and function in adults with primary growth hormone resistance (Laron syndrome). *Am J Cardiol*. 2000;85(2):209-213.
44. Längin M, Konrad M, Reichart B, et al. Hemodynamic evaluation of anesthetized baboons and piglets by transpulmonary thermodilution: Normal values and interspecies differences with respect to xenotransplantation. *Xenotransplantation*. 2020;27(5):e12576.
45. Yakar S, Liu JL, Stannard B, et al. Normal growth and development in the absence of hepatic insulin-like growth factor I. *Proc Natl Acad Sci U S A*. 1999;96(13):7324-7329.
46. Reichart B, Längin M, Denner J, Schwinzer R, Cowan PJ, Wolf E. Pathways to clinical cardiac xenotransplantation. *Transplantation*. 2020. (accepted for publication).
47. Klymiuk N, van Buerck L, Bahr A, et al. Xenografted islet cell clusters from INSLEA29Y transgenic pigs rescue diabetes and prevent immune rejection in humanized mice. *Diabetes*. 2012;61(6):1527-1532.

SUPPORTING INFORMATION

Additional supporting information may be found online in the Supporting Information section.

How to cite this article: Hinrichs A, Riedel EO, Klymiuk N, et al. Growth hormone receptor knockout to reduce the size of donor pigs for preclinical xenotransplantation studies. *Xenotransplantation*. 2020;00:e12664. https://doi.org/10.1111/xen.12664

6.1 Supplementary data

Supplementary data to this article can be found online at *https://onlinelibrary.wiley.com/doi/10.1111/xen.12664*.

The supplementary data to this article consists of:

Supplementary Figure S1

Supplementary Figure S2

Supplementary Figure S3

Supplementary Table S1

Due to the size of the Supplementary Table, only the Supplementary Figures are included in this version. The Supplementary Table can be accessed via the link above.

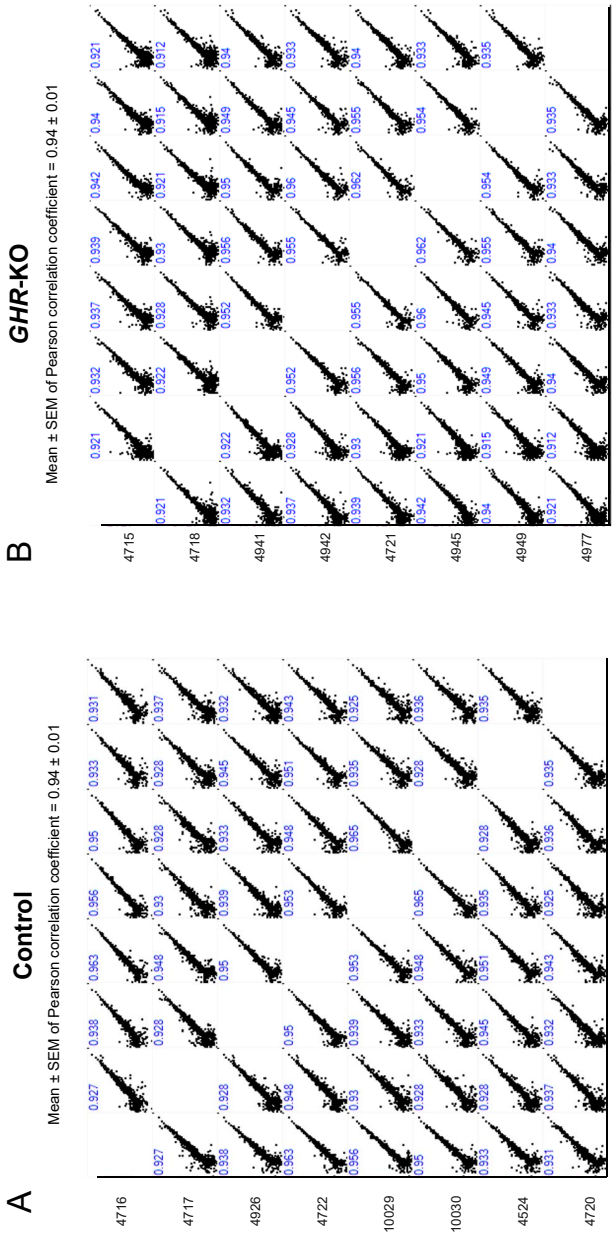

Supplementary Figure 1. Multi-scatterplots of MaxQuant intensity values were generated. The blue number represents the Pearson correlation coefficient for each sample pair. Average Pearson correlation coefficients of > 0.94 within control (A) and GHR-KO (B) proteomes were obtained, demonstrating the reproducibility of the results. The 4- and 5-digit numbers are individual animal numbers. Single dots represent the quantified proteins.

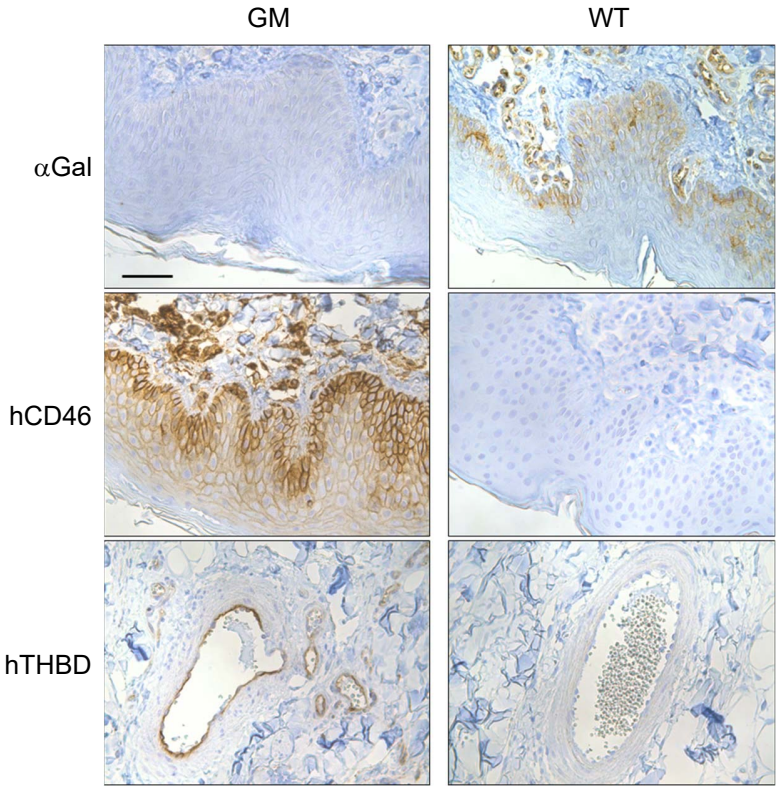

Supplementary Figure 2. Immunohistochemical staining of αGal, hCD46 and hTHBD in skin samples from a *GHR*-KO, *GGTA1*-KO, *hCD46/hTHBD* double-transgenic (4GM) founder pig (GM) and a wild-type control (WT). Bar = 50 µm.

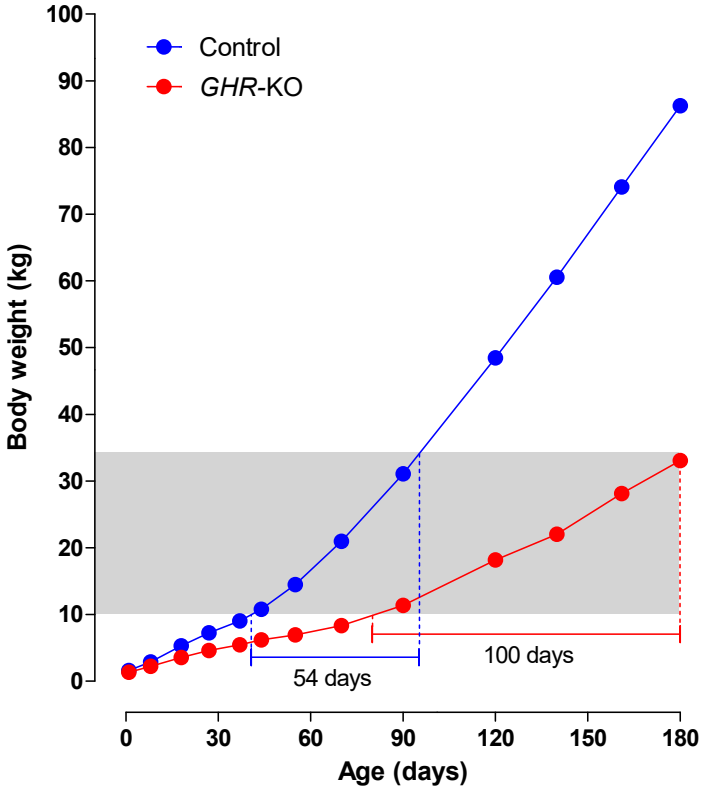

Supplementary Figure 3. Body weight gain of *GHR*-KO pigs (n = 12) compared to *GHR*-intact control pigs (n = 25). The graph shows least squares means (LSMs) estimated for the two genotypes, taking the effect of sex into account (modified from reference 10). The weight range of donor pigs used for orthotopic cardiac xenotransplantation into baboons is shown as grey area. The age span of animals within this weight range is shown under the growth curves.

7. References

Backeljauw, P.F., Kuntze, J., Frane, J., Calikoglu, A.S., and Chernausek, S.D. (2013). Adult and near-adult height in patients with severe insulin-like growth factor-I deficiency after long-term therapy with recombinant human insulin-like growth factor-I. Horm Res Paediatr *80*, 47-56.

Baker, J., Liu, J.P., Robertson, E.J., and Efstratiadis, A. (1993). Role of insulin-like growth factors in embryonic and postnatal growth. Cell *75*, 73-82.

Beckers, A., Petrossians, P., Hanson, J., and Daly, A.F. (2018). The causes and consequences of pituitary gigantism. Nat Rev Endocrinol *14*, 705-720.

Bindea, G., Galon, J., and Mlecnik, B. (2013). CluePedia Cytoscape plugin: pathway insights using integrated experimental and in silico data. Bioinformatics *29*, 661-663.

Bindea, G., Mlecnik, B., Hackl, H., Charoentong, P., Tosolini, M., Kirilovsky, A., Fridman, W.H., Pagès, F., Trajanoski, Z., and Galon, J. (2009). ClueGO: a Cytoscape plug-in to decipher functionally grouped gene ontology and pathway annotation networks. Bioinformatics *25*, 1091-1093.

Brooks, A.J., and Waters, M.J. (2010). The growth hormone receptor: mechanism of activation and clinical implications. Nat Rev Endocrinol *6*, 515-525.

Brooks, A.J., Wooh, J.W., Tunny, K.A., and Waters, M.J. (2008). Growth hormone receptor; mechanism of action. Int J Biochem Cell Biol *40*, 1984-1989.

Chernausek, S.D., Backeljauw, P.F., Frane, J., Kuntze, J., and Underwood, L.E. (2007). Long-term treatment with recombinant insulin-like growth factor (IGF)-I in children with severe IGF-I deficiency due to growth hormone insensitivity. The Journal of clinical endocrinology and metabolism *92*, 902-910.

Chisalita, S.I., and Arnqvist, H.J. (2005). Expression and function of receptors for insulin-like growth factor-I and insulin in human coronary artery smooth muscle cells. Diabetologia *48*, 2155-2161.

Cohick, W.S., and Clemmons, D.R. (1993). The insulin-like growth factors. Annu Rev Physiol *55*, 131-153.

Cox, J., Hein, M.Y., Luber, C.A., Paron, I., Nagaraj, N., and Mann, M. (2014). Accurate proteome-wide label-free quantification by delayed normalization and maximal peptide ratio extraction, termed MaxLFQ. Mol Cell Proteomics *13*, 2513-2526.

Cox, J., and Mann, M. (2011). Quantitative, high-resolution proteomics for data-driven systems biology. Annu Rev Biochem *80*, 273-299.

Cruz-Topete, D., and Kopchick, J.J. (2011). Cardiac Function in GHR—/ Mice. In Laron Syndrome - From Man to Mouse, Z. Laron, and J.J. Kopchick, eds., pp. 473-479.

Cui, D., Li, F., Li, Q., Li, J., Zhao, Y., Hu, X., Zhang, R., and Li, N. (2015). Generation of a miniature pig disease model for human Laron syndrome. Scientific reports *5*, 15603.

De Ponti, F.F., and Scott, C.L. (2021). In matters of the heart, (cellular) communication is key. Immunity *54*, 1906-1908.

Eurotransplant (2021). Annual Report 2020.

Feinberg, M.S., Scheinowitz, M., and Laron, Z. (2000). Echocardiographic dimensions and function in adults with primary growth hormone resistance (Laron syndrome). Am J Cardiol *85*, 209-213.

Gärke, C., Ytournel, F., Sharifi, A.R., Pimentel, E.C., Ludwig, A., and Simianer, H. (2014). Footprints of recent selection and variability in breed composition in the Göttingen Minipig genome. Anim Genet *45*, 381-391.

Goerlich, C.E., Griffith, B., Hanna, P., Hong, S.N., Ayares, D., Singh, A.K., and Mohiuddin, M.M. (2021). The growth of xenotransplanted hearts can be reduced with growth hormone receptor knockout pig donors. J Thorac Cardiovasc Surg.

Guevara-Aguirre, J., Balasubramanian, P., Guevara-Aguirre, M., Wei, M., Madia, F., Cheng, C.W., Hwang, D., Martin-Montalvo, A., Saavedra, J., Ingles, S.*, et al.* (2011). Growth hormone

receptor deficiency is associated with a major reduction in pro-aging signaling, cancer, and diabetes in humans. Science translational medicine *3*, 70ra13.

Guevara-Aguirre, J., Rosenbloom, A.L., Fielder, P.J., Diamond, F.B., Jr., and Rosenfeld, R.G. (1993). Growth hormone receptor deficiency in Ecuador: clinical and biochemical phenotype in two populations. The Journal of clinical endocrinology and metabolism *76*, 417-423.

Hinrichs, A., Kessler, B., Kurome, M., Blutke, A., Kemter, E., Bernau, M., Scholz, A.M., Rathkolb, B., Renner, S., Bultmann, S.*, et al.* (2018). Growth hormone receptor-deficient pigs resemble the pathophysiology of human Laron syndrome and reveal altered activation of signaling cascades in the liver. Molecular Metabolism.

Hinrichs, A., Riedel, E.O., Klymiuk, N., Blutke, A., Kemter, E., Längin, M., Dahlhoff, M., Keßler, B., Kurome, M., Zakhartchenko, V.*, et al.* (2021). Growth hormone receptor knockout to reduce the size of donor pigs for preclinical xenotransplantation studies. Xenotransplantation *28*, e12664.

Honda, Y., Takahashi, K., Takahashi, S., Azumi, K., Irie, M., Sakuma, M., Tsushima, T., and Shizume, K. (1969). Growth hormone secretion during nocturnal sleep in normal subjects. The Journal of clinical endocrinology and metabolism *29*, 20-29.

Huang da, W., Sherman, B.T., and Lempicki, R.A. (2009). Systematic and integrative analysis of large gene lists using DAVID bioinformatics resources. Nat Protoc *4*, 44-57.

Iwase, H., Ball, S., Adams, K., Eyestone, W., Walters, A., and Cooper, D.K.C. (2021). Growth hormone receptor knockout: Relevance to xenotransplantation. Xenotransplantation *28*, e12652.

Iwase, H., Hara, H., Ezzelarab, M., Li, T., Zhang, Z., Gao, B., Liu, H., Long, C., Wang, Y., Cassano, A.*, et al.* (2017). Immunological and physiological observations in baboons with life-supporting genetically engineered pig kidney grafts. Xenotransplantation *24*.

Iwase, H., Liu, H., Wijkstrom, M., Zhou, H., Singh, J., Hara, H., Ezzelarab, M., Long, C., Klein, E., Wagner, R.*, et al.* (2015). Pig kidney graft survival in a baboon for 136 days: longest life-supporting organ graft survival to date. Xenotransplantation *22*, 302-309.

Jansson, J.O., Eden, S., and Isaksson, O. (1985). Sexual dimorphism in the control of growth hormone secretion. Endocrine reviews *6*, 128-150.

Jara, A., Liu, X., Sim, D., Benner, C.M., Duran-Ortiz, S., Qian, Y., List, E.O., Berryman, D.E., Kim, J.K., and Kopchick, J.J. (2016). Cardiac-Specific Disruption of GH Receptor Alters Glucose Homeostasis While Maintaining Normal Cardiac Performance in Adult Male Mice. Endocrinology *157*, 1929-1941.

Jolliffe, I.T., and Cadima, J. (2016). Principal component analysis: a review and recent developments. Philos Trans A Math Phys Eng Sci *374*, 20150202.

Kemter, E., Schnieke, A., Fischer, K., Cowan, P.J., and Wolf, E. (2020). Xeno-organ donor pigs with multiple genetic modifications - the more the better? Curr Opin Genet Dev *64*, 60-65.

Längin, M., Mayr, T., Reichart, B., Michel, S., Buchholz, S., Guethoff, S., Dashkevich, A., Baehr, A., Egerer, S., Bauer, A.*, et al.* (2018). Consistent success in life-supporting porcine cardiac xenotransplantation. Nature *564*, 430-433.

Laron, Z. (2004). Laron syndrome (primary growth hormone resistance or insensitivity): the personal experience 1958-2003. The Journal of clinical endocrinology and metabolism *89*, 1031-1044.

Laron, Z. (2011a). IGF-I Treatment of Patients with Laron Syndrome. In Laron Syndrome - From Man to Mouse, Z. Laron, and J.J. Kopchick, eds., pp. 343-380.

Laron, Z. (2011b). Nonalcoholic Fatty Liver Disease (NAFLD) in Patients with Laron syndrome. In Laron Syndrome – From man to mouse Lessons from Clinical and Experimental Experience, Z. Laron, and J.J. Kopchick, eds., pp. 143-147.

Laron, Z., Ginsberg, S., and Webb, M. (2008). Nonalcoholic fatty liver in patients with Laron syndrome and GH gene deletion - preliminary report. Growth hormone & IGF research : official journal of the Growth Hormone Research Society and the International IGF Research Society *18*, 434-438.

Laron, Z., and Karmon, T. (2011). Liver Enzymes in patients with Laron Syndrome. In Laron Syndrome – From man to mouse Lessons from Clinical and Experimental Experience, Z. Laron, and J.J. Kopchick, eds., pp. 273-281.

Laron, Z., and Kauli, R. (2011). Head Shape, Size, and Growth of Untreared Patients with Laron Syndrome. In Laron Syndrome - From Man to Mouse, Z. Laron, and J.J. Kopchick, eds., pp. 91-100.

Laron, Z., Kauli, R., Lapkina, L., and Werner, H. (2017). IGF-I deficiency, longevity and cancer protection of patients with Laron syndrome. Mutation research Reviews in mutation research *772*, 123-133.

Laron, Z., Pertzelan, A., and Karp, M. (1968). Pituitary dwarfism with high serum levels of growth hormone. Isr J Med Sci *4*, 883-894.

Laustsen, P.G., Russell, S.J., Cui, L., Entingh-Pearsall, A., Holzenberger, M., Liao, R., and Kahn, C.R. (2007). Essential role of insulin and insulin-like growth factor 1 receptor signaling in cardiac development and function. Mol Cell Biol *27*, 1649-1664.

Li, F., Li, Y., Liu, H., Zhang, X., Liu, C., Tian, K., Bolund, L., Dou, H., Yang, W., Yang, H.*, et al.* (2015). Transgenic Wuzhishan minipigs designed to express a dominant-negative porcine growth hormone receptor display small stature and a perturbed insulin/IGF-1 pathway. Transgenic research *24*, 1029-1042.

List, E.O., Sackmann-Sala, L., Berryman, D.E., Funk, K., Kelder, B., Gosney, E.S., Okada, S., Ding, J., Cruz-Topete, D., and Kopchick, J.J. (2011). Endocrine parameters and phenotypes of the growth hormone receptor gene disrupted (GHR-/-) mouse. Endocrine reviews *32*, 356-386.

Lund, L.H., Khush, K.K., Cherikh, W.S., Goldfarb, S., Kucheryavaya, A.Y., Levvey, B.J., Meiser, B., Rossano, J.W., Chambers, D.C., Yusen, R.D.*, et al.* (2017). The Registry of the International Society for Heart and Lung Transplantation: Thirty-fourth Adult Heart Transplantation Report-2017; Focus Theme: Allograft ischemic time. J Heart Lung Transplant *36*, 1037-1046.

Mallick, P., and Kuster, B. (2010). Proteomics: a pragmatic perspective. Nature biotechnology *28*, 695-709.

Montessuit, C., Palma, T., Viglino, C., Pellieux, C., and Lerch, R. (2006). Effects of insulin-like growth factor-I on the maturation of metabolism in neonatal rat cardiomyocytes. Pflugers Arch *452*, 380-386.

Ong, S.E., and Mann, M. (2005). Mass spectrometry-based proteomics turns quantitative. Nat Chem Biol *1*, 252-262.

Perkins, D.N., Pappin, D.J., Creasy, D.M., and Cottrell, J.S. (1999). Probability-based protein identification by searching sequence databases using mass spectrometry data. Electrophoresis *20*, 3551-3567.

Ranke, M.B., and Wit, J.M. (2018). Growth hormone - past, present and future. Nat Rev Endocrinol *14*, 285-300.

Riedel, E.O., Hinrichs, A., Kemter, E., Dahlhoff, M., Backman, M., Rathkolb, B., Prehn, C., Adamski, J., Renner, S., Blutke, A.*, et al.* (2020). Functional changes of the liver in the absence of growth hormone (GH) action - Proteomic and metabolomic insights from a GH receptor deficient pig model. Mol Metab, 100978.

Ringnér, M. (2008). What is principal component analysis? Nature biotechnology *26*, 303-304.

Rosenbloom, A.L., and Guevara-Aguirre, J. (1998). Lessons from the genetics of laron syndrome. Trends Endocrinol Metab *9*, 276-283.

Rosenfeld, R.G., Rosenbloom, A.L., and Guevara-Aguirre, J. (1994). Growth Hormone (GH) Insensitivity Due to Primary GH Receptor Deficiency. Endocrine reviews *15*, 369-390.

Rossano, J.W., Cherikh, W.S., Chambers, D.C., Goldfarb, S., Khush, K., Kucheryavaya, A.Y., Levvey, B.J., Lund, L.H., Meiser, B., Yusen, R.D.*, et al.* (2017). The Registry of the International Society for Heart and Lung Transplantation: Twentieth Pediatric Heart Transplantation Report-2017; Focus Theme: Allograft ischemic time. J Heart Lung Transplant *36*, 1060-1069.

Santini, M.P., Tsao, L., Monassier, L., Theodoropoulos, C., Carter, J., Lara-Pezzi, E., Slonimsky, E., Salimova, E., Delafontaine, P., Song, Y.H.*, et al.* (2007). Enhancing repair of the mammalian heart. Circ Res *100*, 1732-1740.

Scheinowitz, M., Feinberg, M.S., Shechter, M., Laron, Z., and Kauli, R. (2011). Cardiovascular Aspects in Laron Syndrome Patients. In Laron Syndrome - From Man to Mouse, Z. Laron, and J.J. Kopchick, eds., pp. 293-305.

Shannon, P., Markiel, A., Ozier, O., Baliga, N.S., Wang, J.T., Ramage, D., Amin, N., Schwikowski, B., and Ideker, T. (2003). Cytoscape: a software environment for integrated models of biomolecular interaction networks. Genome Res *13*, 2498-2504.

Shevah, O., and Laron, Z. (2007). Patients with congenital deficiency of IGF-I seem protected from the development of malignancies: a preliminary report. Growth hormone & IGF research : official journal of the Growth Hormone Research Society and the International IGF Research Society *17*, 54-57.

Shevah, O., and Laron, Z. (2011). Genetic Aspects. In Laron Syndrome - From Man to Mouse, Z. Laron, and J.J. Kopchick, eds., pp. 29-52.

Steuerman, R., Shevah, O., and Laron, Z. (2011). Congenital IGF1 deficiency tends to confer protection against post-natal development of malignancies. European journal of endocrinology *164*, 485-489.

Subramanian, A., Tamayo, P., Mootha, V.K., Mukherjee, S., Ebert, B.L., Gillette, M.A., Paulovich, A., Pomeroy, S.L., Golub, T.R., Lander, E.S.*, et al.* (2005). Gene set enrichment analysis: a knowledge-based approach for interpreting genome-wide expression profiles. Proc Natl Acad Sci U S A *102*, 15545-15550.

Symonds, M.E., Sebert, S.P., Hyatt, M.A., and Budge, H. (2009). Nutritional programming of the metabolic syndrome. Nat Rev Endocrinol *5*, 604-610.

Takahashi, Y. (2017). The Role of Growth Hormone and Insulin-Like Growth Factor-I in the Liver. Int J Mol Sci *18*.

Tanabe, T., Watanabe, H., Shah, J.A., Sahara, H., Shimizu, A., Nomura, S., Asfour, A., Danton, M., Boyd, L., Dardenne Meyers, A.*, et al.* (2017). Role of Intrinsic (Graft) Versus Extrinsic (Host) Factors in the Growth of Transplanted Organs Following Allogeneic and Xenogeneic Transplantation. Am J Transplant *17*, 1778-1790.

Team, R.C. (2022). R: A language and environment for statistical computing. In R Foundation for Statistical Computing (Vienna, Austria).

Tyanova, S., Temu, T., Sinitcyn, P., Carlson, A., Hein, M.Y., Geiger, T., Mann, M., and Cox, J. (2016). The Perseus computational platform for comprehensive analysis of (prote)omics data. Nature methods *13*, 731-740.

Vijayakumar, A., Novosyadlyy, R., Wu, Y., Yakar, S., and LeRoith, D. (2010). Biological effects of growth hormone on carbohydrate and lipid metabolism. Growth hormone & IGF research : official journal of the Growth Hormone Research Society and the International IGF Research Society *20*, 1-7.

Vijayakumar, A., Yakar, S., and Leroith, D. (2011). The intricate role of growth hormone in metabolism. Front Endocrinol (Lausanne) *2*, 32.

Vilar, L., Vilar, C.F., Lyra, R., Lyra, R., and Naves, L.A. (2017). Acromegaly: clinical features at diagnosis. Pituitary *20*, 22-32.

Walther, T.C., and Mann, M. (2010). Mass spectrometry-based proteomics in cell biology. J Cell Biol *190*, 491-500.

Wong, N.R., Mohan, J., Kopecky, B.J., Guo, S., Du, L., Leid, J., Feng, G., Lokshina, I., Dmytrenko, O., Luehmann, H.*, et al.* (2021). Resident cardiac macrophages mediate adaptive myocardial remodeling. Immunity *54*, 2072-2088.e2077.

Yakar, S., Liu, J.L., Stannard, B., Butler, A., Accili, D., Sauer, B., and LeRoith, D. (1999). Normal growth and development in the absence of hepatic insulin-like growth factor I. Proc Natl Acad Sci U S A *96*, 7324-7329.

Yu, H., Long, W., Zhang, X., Xu, K., Guo, J., Zhao, H., Li, H., Qing, Y., Pan, W., Jia, B.*, et al.* (2018). Generation of GHR-modified pigs as Laron syndrome models via a dual-sgRNAs/Cas9 system and somatic cell nuclear transfer. Journal of translational medicine *16*, 41.

Zaman, R., Hamidzada, H., Kantores, C., Wong, A., Dick, S.A., Wang, Y., Momen, A., Aronoff, L., Lin, J., Razani, B.*, et al.* (2021). Selective loss of resident macrophage-derived insulin-like growth factor-1 abolishes adaptive cardiac growth to stress. Immunity *54*, 2057-2071 e2056.

Zhou, Y., Xu, B.C., Maheshwari, H.G., He, L., Reed, M., Lozykowski, M., Okada, S., Cataldo, L., Coschigamo, K., Wagner, T.E.*, et al.* (1997). A mammalian model for Laron syndrome produced by targeted disruption of the mouse growth hormone receptor/binding protein gene (the Laron mouse). Proc Natl Acad Sci U S A *94*, 13215-13220.

8. Acknowledgements

I want to thank everybody from the research unit Proteomics (Fröhlich Lab) from the Laboratory for Functional Genome Analysis (LAFUGA) at the Gene Center of the Ludwig Maximilians-Universität (LMU) Munich, especially Dr. Thomas Fröhlich, Dr. Georg J. Arnold and Dr. Florian Flenkenthaler. I also want to thank everyone from the research unit Model Organisms (Wolf Lab) from the LAFUGA at the Gene Center Munich and the Center for Innovative Medical Models (CiMM) at the Chair for Molecular Animal Breeding and Biotechnology of the Ludwig-Maximilians-Universität Munich, especially to mention Prof. Dr. Eckhard Wolf and Dr. Arne Hinrichs. My thanks also go to Prof. Dr. Jochen Schopohl and Dr. Martin Bidlingmaier at the Department for Endocrinology from the Medical Clinic and Polyclinic IV of the Ludwig Maximilians-Universität Munich. I thank you all very much for receiving me, for the kind atmosphere, the support and helpful guidance and productive collaboration.

Especially I want to express my gratitude to Prof. Dr. Eckhard Wolf, Dr. Thomas Fröhlich and Dr. Georg J. Arnold for their invaluable support on a professional as well as a personal level.

Last but not least, I want to thank my family for their patience and encouragement.

The papers included in this thesis are published with the permission of Molecular Metabolism by Elsevier and Xenotransplantation by John Wiley & Sons. Open access funding for the paper in Xenotransplantation is enabled and organized by Projekt DEAL.